EXPLOSIBILITY OF MICRON- AND NANO-SIZE TITANIUM POWDERS

by

SIMON BOILARD

Submitted in partial fulfilment of the requirements
for the degree of Master of Applied Science

at

Dalhousie University
Halifax, Nova Scotia
February 2013

DALHOUSIE UNIVERSITY

DEPARTMENT OF PROCESS ENGINEERING AND APPLIED SCIENCE

The undersigned hereby certify that they have read and recommend to the Faculty of Graduate Studies for acceptance a thesis entitled "Explosibility of Micron- and Nano-Size Titanium Powders" by Simon Boilard in partial fulfilment of the requirements for the degree of Master of Applied Science.

Dated: February 15, 2013

Supervisor:

_____

Readers:

_____

_____

_____

_____

DALHOUSIE UNIVERSITY

DATE: February 15, 2013

AUTHOR: Simon Boilard

TITLE: Explosibility of Micron- and Nano-Size Titanium Powders

DEPARTMENT OR SCHOOL: Department of Process Engineering and Applied
                                                        Science

DEGREE: M.A.Sc.   CONVOCATION: May   YEAR: 2013

_____
Signature of Author

TABLE OF CONTENTS

LIST OF TABLES

LIST OF FIGURES

x

ABSTRACT

The current research is aimed at investigating the explosion behaviour of hazardous materials in relation to particle size. The materials of study are titanium powders having size distributions in both the micron- and nano-size ranges with nominal size distributions: -100 mesh, -325 mesh, ≤ 20 μm, 150 nm, 60-80 nm, and 40-60 nm. The explosibility parameters investigated explosion severity and explosion likelihood for both size ranges of titanium. Tests include, maximum explosion pressure (P_{max}), maximum rate of pressure rise ($(dP/dt)_{max}$), minimum explosible concentration (MEC), minimum ignition energy (MIE), minimum ignition temperature (MIT) and dust inerting using nano-titanium dioxide. ASTM protocols were followed using standard dust explosibility test equipment (Siwek 20-L explosion chamber, MIKE 3 apparatus, and BAM oven). The explosion behaviour of the micron-size titanium has been characterized to provide a baseline study for the nano-size testing, however, nano-titanium dust explosion research presented major experimental challenges using the 20-L explosion chamber.

LIST OF ABBREVIATIONS AND SYMBOLS USED

$(dP/dt)_{max}$	Maximum rate of pressure rise of a material
$(dP/dt)_m$	Rate of pressure rise of a single concentration trial
$(dP/dt)'_{max}$	Pseudo maximum rate of pressure rise for nano-titanium
$(dP/dt)'_m$	Rate of pressure rise for a single nano-titanium concentration trial
KSEP332	Siwek 20-L chamber control unit
KSEP 6.0f	Siwek 20-L chamber software
MEC	Minimum explosible concentration
MIE	Minimum ignition energy
MIKE 3.3	MIKE 3 apparatus software
MIT	Minimum ignition temperature
NFPA	National Fire Protection Agency
P_d	Rise in pressure due to dispersion of dust in the 20-L chamber
P_{max}	Maximum explosion pressure of a material
P_m	Overpressure of a single concentration trial
P'_{max}	Pseudo maximum explosion pressure of a nano-titanium
P'_m	Pseudo overpressure of a single nano-titanium concentration trial
SEM	Scanning electron micrograph
TTIP	Titanium Tetraisopropoxide
WEE	Wired Electric Explosion
XRD	X-ray diffraction
ϕ	Equivalence Ratio

ACKNOWLEDGEMENTS

CHAPTER 1: INTRODUCTION

Dust explosions are industrial events that have occurred in many types of processing plants. Dust explosions are similar to gas explosions but are not recognized as such due to the solid fuel and circumstances required for the events to occur.[1] Past industrial dust explosions have precipitated the need for further research in this area in order to better understand the explosion likelihood and severity of these events. Until recently, the materials given the most attention are dust powders found in many industrial processes. These include metals, pharmaceuticals, and coal powders of micron sized-particles. With modern industrial processes and technological advancements, new dust powders can present different hazards and challenges. Nano-technology has allowed the creation of smaller, 'non-traditional' dust such as nano-powders. Smaller particles can also generate increasingly hazardous and more severe explosions that have not been previously experienced or tested.

The purpose of this work is to determine the explosion severity and likelihood of micron- and nano-sized titanium powders by using standardized dust explosion equipment. During this process, methodologies were developed to avoid newly observed hazards involving nano-particles. These include additional safety equipment, handling procedures, and equipment procedures to ensure consistent results as well as operator safety. This thesis explains dust explosions and discusses the significance of experimental work with nano-materials. Materials, equipment, results, and challenges are also reviewed. These results demonstrate that dust explosions at the nano-scale are significant and should be further explored to better understand and prevent future industrial incidents.

1.1   Dust Explosion Background

The U.S. National Fire Protection Agency (NFPA) describes a combustible dust as a powder having a particle size of less than 420 µm that can pass through a 40 mesh screen

and can present a fire or explosion hazard when dispersed in air with an ignition source. [2] If a combustible dust cloud is suspended in air and an ignition source is present, an explosion can occur. A dust explosion can be most easily explained by an analogy involving a wooden log. A log will burn very slowly releasing heat produced over an extended period of time. Cutting the log into several pieces causes the wood to burn much faster, releasing more heat at a faster rate. These small wood pieces can be further divided into particles and then into dust, suspended in air. Combustion of the wood dust in air occurs so quickly that an explosion is created.[3] Applying this analogy, it would be expected that nano-particles should create dust explosions that are much more severe than micron-size particles.

1.1.1 Dust Explosion Requirements

To further understand the basic principles of dust explosions, the safety concept of the fire triangle must also be understood. The fire triangle, seen in Figure 1.1a, is composed of three components. All three of these components are required for a fire to be present: a fuel, an oxidant and an ignition source; removing one of these conditions eliminates the possibility of a fire. The fire triangle is also used to understand the concept of dust explosions, seen in Figure 1.1b. Two more requirements are added to the fuel side of the triangle: particle size and concentration.[4] These factors have a significant effect on the combustion and the amount of fuel present. Along with the fire triangle requirements, a dust explosion must possess four unique requirements as listed by Amyotte and Eckhoff:[1]

i)   The dust/fuel must be combustible.
ii)   The dust must be airborne.
iii)   The particle size distribution must be capable of propagating a flame front when dispersed in air.
iv)   The dust concentration must be within the explosible range.
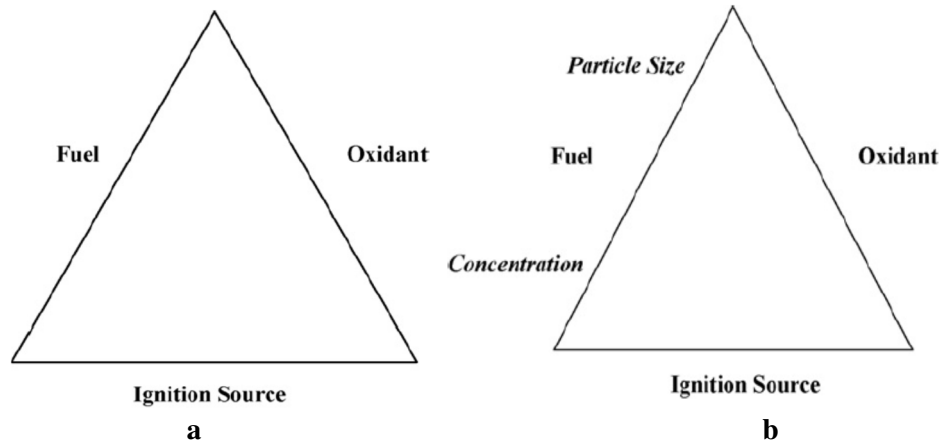
Figure 1.1   Fire triangle for dust explosions

An explosion can be similarly represented by the explosion pentagon. The pentagon, seen in Figure 1.2, describes the five requirements for an explosion. Criteria from the fire triangle (fuel, oxidant, and ignition source) now include mixing and confinement in order to complete the pentagon.[5] Dust (fuel) must be dispersed and mixed in air to achieve an ignitable concentration. If the fuel/air mixture is within a confined area and an ignition source is present then a dust explosion can occur.[1]
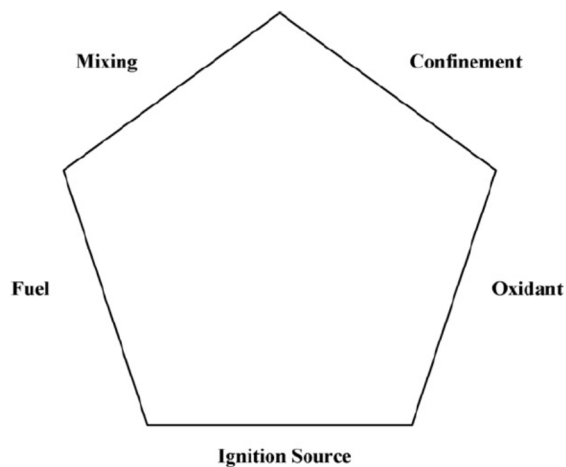
Figure 1.2   Explosion pentagon

The fire triangle and explosion pentagon still hold for nano-dust explosions but the concentration, particle size and mixing requirements could provide increased severity and likelihood of an explosion. These are explained in sections 6.1 and 6.2.

1.1.2   Fuel Types

The type of fuel plays a very strong role in the explosion severity and likelihood of a dust explosion. The composition of the material dictates the combustion process that takes place. Materials such as organics (grains, sugar, linen and coal), synthetic organics (polyethylene, plastics and pesticides), and metals (aluminum, titanium, magnesium, zinc and iron) all combust and oxidize very quickly to create an explosion. Organic materials combust to create carbon dioxide and water while metals react to form their corresponding oxides (Al_2O_3, TiO_2, MgO, ZnO, Fe_2O_3). As a result, materials that are completely oxidized cannot generate dust explosions.[3]

1.1.3   Particle Size

As previously stated, particle size affects the ignition of a dust cloud. The size, distribution, and shape of the particles affect the amount of exposed surface. Surface area affects the reactivity of the dust; higher surface area exposes more reactant to participate in the combustion process. Powders with a high surface area typically generate explosions with higher severity and likelihood.

Di Benedetto et al.[6] explain how this phenomenon occurs. First, the particles are heated by an ignition source or surrounding flame front. The particles then melt and devolatilize. Once vapor is formed, it reacts and combusts as a gas in the explosion. Therefore, smaller particles take much less time to melt and vaporize, increasing their reactivity.[6]

The degree of dispersion also greatly affects the ignition and severity of a dust explosion. In well dispersed dust clouds, the individual particles are separate and therefore react separately. As dispersion decreases, the particles are closer together and clump or agglomerate. Agglomeration of dust particles can increase the effective particle size thus decreasing the reactivity and severity of an explosion. When particle sizes are in the low micron range (10 µm), explosion severity has been shown to reach a quasi-plateau.[3] This plateau effect is investigated as the particle size decreases into the nano-region. This thesis determines the trend of explosion severity as particle size decreases.

1.1.4   Concentration

Dust explosions require solid material to fuel an explosion. As previously explained, the concentration of the dust cloud is an important factor. The concentration must be within the explosible range for an ignition to occur. Similar to a gas explosion, dust explosions have upper and lower explosion limits. However, the flammable concentration range of a gas explosion is very narrow when compared to a dust explosion. Figure 1.3 shows the difference in flammable concentration for methane gas compared to solid dust fuels, polyethylene and coal. Methane's explosion limits are between 35 g/m^3 and 120 g/m^3. Dust explosion limits can be as low as 50 g/m^3 for the lower explosible limit (minimum explosible concentration); however, the upper explosible limit can reach concentrations well over 3000 g/m^3.[7]
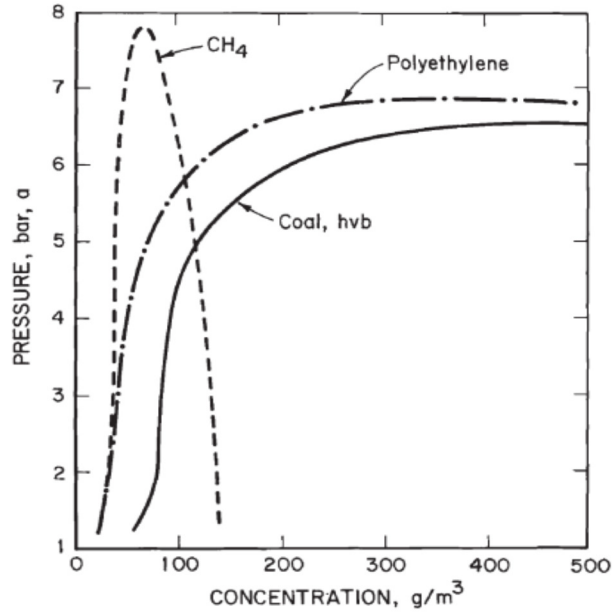
Figure 1.3   Lower and upper explosion limits of a gas and dust[7]

To put the concentration of a dust cloud in perspective, a dust layer 1 mm thick on a surface has a bulk density of 500 kg/m^3. However, this dust, if disturbed, can create a dust cloud. If a disturbance causes the dust to become airborne, an ignitable concentration can be reached. The 1 mm thick, 500 kg/m^3 bulk density sample can create a dust cloud 5 m high with a concentration of 100 g/m^3 or 1 m high dust cloud with a concentration of 500 g/m^3. This is depicted in Figure 1.4.[3] In this situation, dust explosion hazards can be unexpected. Although a hazard does not seem to be present, a quick disturbance can cause a very hazardous environment.
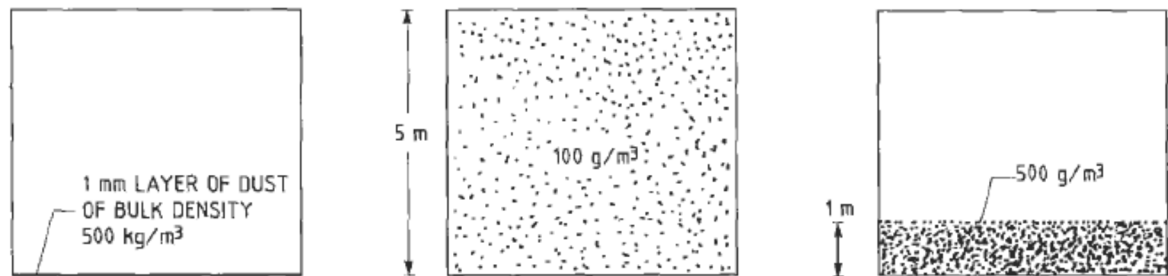
Figure 1.4   Concentration variation with dispersion[3]

1.2   Dust Explosion Causes

A dust explosion can be caused by many types of ignition sources described below. An ignition source (explained in section 1.2.1) is the cause of a primary explosion. However, a secondary explosion can be created by the interaction of the primary explosion with additional fuel. These causes are further explained throughout this section.

1.2.1   Ignition Sources

Dust explosions cannot be initiated unless all five requirements of the explosion pentagon are met, one of the requirements being an ignition source. An ignition source must have sufficient energy in order to cause the dust to ignite. Common ignition sources are:[3]

- Smouldering or burning dust
- An open flame
- Hot surfaces
- Heat from a mechanical impact
- Electrical discharges

1.2.2   Primary Explosions

Dust explosions of the primary type are caused directly by an ignition source. These explosions commonly occur within process equipment (mills, mixers, grinders, dryers, etc.) where the dust ignition is the primary event.[3] Once the ignition occurs, an explosion can propagate.[1]

1.2.3 Secondary explosions

Secondary explosions occur outside of the equipment in the process area and are fueled by dust deposits being disturbed by a primary explosion. This event is depicted in Figure 1.5.[8] Dust deposits can be found on the floor, work surfaces or in obscure areas such as above duct work. The pressure blast occurring from the primary event entrains the dust in a cloud. If the primary event contains enough energy, the newly formed dust cloud may ignite and cause a secondary explosion.[1]
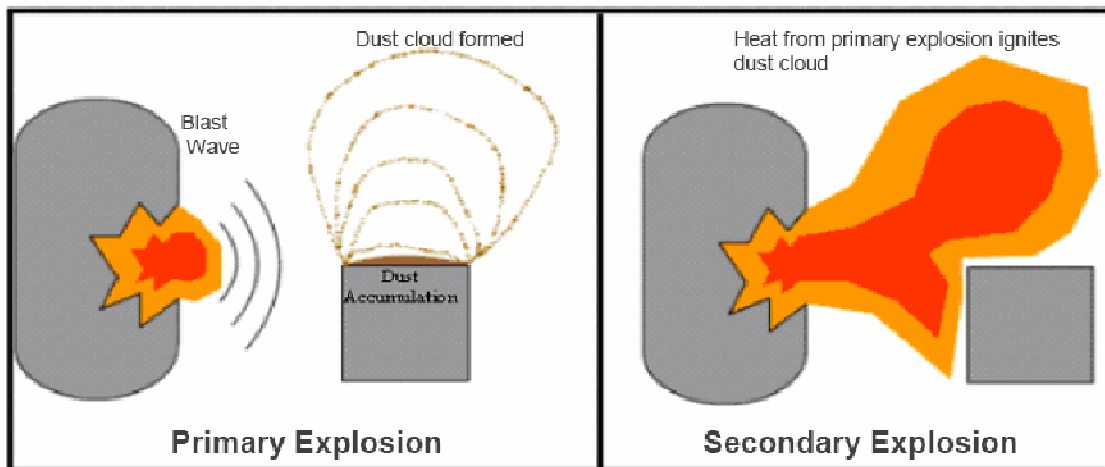
Figure 1.5   Secondary explosion igntion caused by a primary explosion[8]

1.3   Dust Explosion Prevention

Five requirements must be met for dust explosions to occur (ignition source, oxidant, fuel, confinement, and mixing), as explained earlier with the fire triangle and the explosion pentagon. Controlling or preventing one of these requirements inhibits the possibility of an event. For example, an explosion cannot occur if fuel is not present. If removing the fuel is not possible, then eliminating possible ignition sources or confinement removes or reduces the potential of an occurrence. A loss prevention approach known as the hierarchy of controls explains the details and steps needed to

eliminate the possibility of industrial accidents. The hierarchy of controls is divided into levels with the latter levels being less effective:[1]

- Inherent Safety
- Engineered Safety - Passive
- Engineered Safety - Active
- Procedural Safety

1.3.1 Inherent Safety

The concept of inherent safety is further divided into four categories: minimization, substitution, moderation, and simplification. This concept was first proposed by Trevor Kletz in 1978 in the Jubilee Lecture to the Society of Chemical Industry in Widnes, UK.[9] The idea is to eliminate all risks that pose a potential hazard. Kletz's seminar paper was entitled "What you don't have can't leak."[9] Amyotte restated this phrase as "what you don't have can't explode", in reference to dust explosions. [10]

Minimization is a key aspect of reducing the risk involved with dust explosions. It is essential to minimize the amount of combustible dust that could be available in an explosion. The amount of fuel available for an explosion can be eliminated or significantly reduced by performing proper housekeeping practices.[1, 10]

Substitution involves replacing a hazardous material or work procedure with one that is safer. Two examples are: to use an explosion proof vacuum cleaner instead of sweeping dust, or to substitute a combustible dust with a non-explosible powder.[1,10]

Moderation involves reducing the potential severity of an explosion. This includes increasing the particle size of a powder to reduce potential ignition, changing the composition of the dust by admixing inert dust, or controlling the effects of a process

upset by spacing out equipment. Moderation typically does not prevent an incident from occurring, but instead reduces the effects if such an event should exist.[1,10]

Simplification is a method of keeping processes, equipment and information simple. For example, a WHIMIS label indicating a flammable substance can direct the user to a clearly written MSDS where the hazards are properly explained. Another example of simplification is a process vessel. Adding extra strength to a vessel increases the tolerance level and enables the vessel to handle process upsets. This helps to contain the event within the vessel and eliminates the risk of an explosion.[1,10]

1.3.2 Passive Engineered Safety

Engineered safety is classified as either passive or active. Add on devices that do not require mechanical activation are considered passive. These devices perform their function independently; for example, explosion vents remain closed until an event occurs and are opened by the pressure wave of the explosion. Passive engineered safety devices should be used once the principles of inherent safety have been applied.[1]

1.3.3 Active Engineered Safety

Engineered safety devices that require mechanical activation are referred to as active devices. These devices require the detection of a problem and mechanical activation to perform their function. Active engineered devices are therefore less reliable than passive devices. The active device must be properly maintained and tested to limit the possibility of failure. Examples of active devices include dust explosion suppression systems or mechanical block valves, both of which require detection and mechanical movement.[1]

1.3.4 Procedural Safety

The final step in the hierarchy of controls is procedural safety. Individuals are responsible for following procedures but the potential for human error makes procedural safety the least reliable of the controls. At this stage, the personnel become critical in the success of the procedural safety system. Examples of these procedures include permits-to-work and hot-work permits. [1]

1.4   **Nano-Particles**

Much of the previously described work on the background, causes, and prevention of dust explosions were first researched and developed for micron-sized dust powders. The knowledge and application for micron-powder explosion prevention should be transferred and applied to nano-powders. Micron particles are in the order of magnitude of 10^{-6} m while nano-particles are in the order of 10^{-9} m.

1.4.1 Nano-Background

The principles of the fire triangle and the explosion pentagon do not change with regard to nano-powders. All components still apply; however, a significant change occurs within the fuel requirement. Nano-particle sizes are much smaller than micron particles, and as a result, the surface area of the dust is increased. As explained in section 1.1.3, as surface area increases, additional combustible material becomes exposed, causing the combustion process to occur more rapidly. This phenomenon helps to explain the potential increase in likelihood and severity of a nano-powder explosion.

Although nano-particles have a higher surface area, the particles are small enough to be affected by agglomeration forces, causing a larger effective particle size. The process of

particle agglomeration may, in fact, limit the increase in explosion severity and likelihood of nano-powders.

1.4.2 Nano-Safety

With a potential increase in severity and likelihood, it is important to consider the hierarchy of controls for nano-powders. Morose[11] developed five principles, *design for a safer nanotechnology*, known as SAFER. These design principles, seen in Table 1.1, are nano-specific but have a direct relation to inherent safety as explained by Amyotte.[12]

Table 1.1 Relationship between design for safer nanotechnology and inherent safety[12]

Safer Nanotechnology Design	Inherently Safer Design
Size, surface and structure	Moderation
Alternative materials	Substitution
Functionalization	Moderation
Encapsulation	Moderation
Reduce the quantity	Minimization

Morose mainly discusses the SAFER design principles in relation to exposure and health effect. However, the design principles are directly related to nano-dust explosions. Morose states that the size, surface and structure of a nano-particle can be slightly changed to provide a less hazardous material. For example, a gold nano-particle of 2 nm will melt at 650 K but a 6 nm particle will melt at 1150 K. This is directly related to the likelihood of an ignition. Although gold does not ignite, different combustible material may have similar properties. Changing the size, surface, or structure of a particle may help to control or prevent the ignition of a nano-particle cloud.[11]

An 'alternative material' is closely linked to inherent safety (substitution). Using an alternative material that is less harmful reduces the potential risk involved with the

previous hazardous material. Chemicals involved in nano-powder production may also be an issue and substituting chemicals with one that is less harmful reduces potential hazards and risks involved in production.[11]

Functionalization is related to the synthesis of the nano-particle. Adding an additional molecule or atom to the particle may reduce or eliminate the hazard while maintaining the functional properties of the particle.[11] This principle may work for biological effects; however, an explosion may be difficult to completely prevent. Functionalization may only serve to reduce the explosion severity.

Encapsulation is another method of reducing the particle effects and risk. This principle involves enclosing the nano-particle within another material.[11] For example, a method of synthesising titanium nano-particles, explained in section 2.1, is through chemical vapour and sodium chloride encapsulation.[13] Pure nano-titanium is coated with sodium chloride, allowing the salt covering to moderate or even prevent an explosion from occurring.

Reducing the quantity of nano-powder is a direct form of minimization. Decreasing the amount of material present avoids or minimizes the severity of an explosion. Steps should be taken to reduce the amount of nano-particles handled within a processing plant.

It is evident that there are many hazards involved with nano-materials, whether the hazards are health or explosion related. It is important to know at which stages the material is most hazardous within its lifecycle. There are various stages within a product's lifecycle where particle emission and dispersion generate a risk of ignition. These stages include particle production, product manufacturing and product disposal. At each stage, handling of the dust creates risk and the potential for an incident. It is therefore important to follow the hierarchy of controls and utilize the SAFER design principles discussed earlier in order to minimize industrial accidents.

1.4.3   Nano-Titanium

Titanium is the main material of focus for the remainder of this thesis; therefore, it is necessary to discuss the lifecycle of titanium products. According to *The Project on Emerging Nanotechnologies*, titanium and titanium dioxide are the third most widely used nano-materials with 59 products in use as of March 2011.[14] Titanium and titanium dioxide nano-particles are very valuable due to their strength, light weight, UV protection and anti-microbial properties. These unique properties have led to the improvement of older products and also to the production of more recent technologies. Products commercially available today include:[14]

- Hair straighteners /Curling irons – Added strength and reduced weight.
- Filters (fridge and vacuum) – Titanium filters capture and eliminate bacterial odours.
- Anti-microbial coatings – Titanium dioxide provide a surface with anti-bacterial, anti-mould and anti-fungal properties that prevent growth.
- Sunscreens – Titanium dioxide provides milder and longer lasting protection against UV rays.
- Tennis Rackets – Titanium adds strength and reduces weight.
- Fishing Rods– Titanium adds strength to graphite rods while retaining flexibility.

Many products make use of nano-titanium for its unique functional properties. Throughout the stages of nano-titanium production, product manufacturing and disposal, nano-titanium generates dust explosion hazards which must be understood.

1.5   Thesis Objectives

Throughout this thesis, the explosibility parameters of severity (maximum pressure, P_{max}, and maximum rate of pressure rise, $(dP/dt)_{max}$) and the parameters of explosion likelihood (minimum explosible concentration, MEC, minimum ignition energy, MIE, and minimum ignition temperature, MIT) are studied for micron- and nano-titanium.

Six titanium samples (-100 mesh, -325 mesh, ≤20 µm, 150 nm, 60-80 nm, and 40-60 nm) were investigated with standard dust explosion equipment (Siwek 20-L explosion chamber, MIKE 3 apparatus, and BAM oven) to determine whether the explosibility and likelihood of titanium increases as the particle size decreases into the nano-range and whether nano-titanium dust explosion testing is possible with traditional dust explosion equipment. Tests with nano-titanium dioxide were also performed to determine whether nano-titanium dust explosions can be inerted.

CHAPTER 2: LITERATURE REVIEW

This chapter describes information found in the literature that is relevant to titanium and nano-dust explosions. The production of nano-titanium, titanium incidents and nano-dust explosion research are all explained in detail within this chapter.

2.1   Production of Titanium Nano-Powders

There are many methods used today for the production of nano-particles. The methods of focus for this thesis are the specific processes used to create nano-titanium. Processes include wire electric explosion, chemical vapour, and sol-gel, all of which are further explained in this section. These techniques are classified as either a "top-down" or a "bottom up" method.[15] The "top-down" method involves taking a bulk sample of the metal and reducing the size to achieve nano-sized particles. This process makes use of either mechanical crushing in a mill or the wired explosion process.[15] The "bottom-up" method involves the chemical synthesis of a sample to create nano-particles. Many processes incorporate the "bottom-up" method and the desired products are dependent on the type of process used. The sol-gel and the chemical vapour processes are considered "bottom-up" methods.[15]

2.1.1   Sol-Gel

Titanium dioxide can be formed using the sol-gel process. This process is used to create nano-oxide particles along with other nano-materials including: aerogel, dense coatings, ceramic fibres, and dense ceramics.[15,16] Nano-titanium dioxide is synthesised from titanium tetrachloride ($TiCl_4$) used in the Kroll process for titanium processing.[17] Equation 2.1 shows the reaction of bulk titanium dioxide with chlorine gas to form titanium tetrachloride. Titanium tetrachloride is then reacted with isopropanol (rubbing alcohol) to form titanium tetraisopropoxide, TTIP, ($Ti\{OCH(CH_3)_2\}_4$) seen in Equation

2.2. TTIP is the titanium precursor for the sol gel process. TTIP is then mixed with an amine, ratio 1:2, and water. The water reacts with TTIP to create TiO_2 while the amine solution forms the shape of the particle based on the pH of the solution, seen in Equation 2.3. If the pH is approximately 11, a spherical structure is formed. If the pH is lower than 9, an ellipsoidal shape is formed. The solution is then heated (100 - 140 °C) for several days and the resulting product is nano-titanium dioxide.[16,18]

$$TiO_2(bulk) + 2Cl_2 + C \rightarrow TiCl_4 + CO/CO_2 \tag{2.1}$$

$$TiCl_4 + 4C_3H_8O \rightarrow Ti(OCH(CH_3)_2)_4 + 4HCl \tag{2.2}$$

$$Ti(OCH(CH_3)_2)_4 + 2H_2O \rightarrow 4C_3H_8O + TiO_2(nano) \tag{2.3}$$
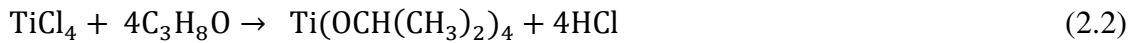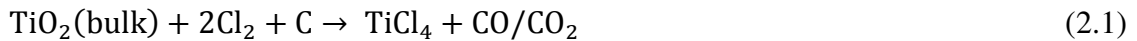
2.1.2 Chemical Vapour

Nano-titanium can be produced using a chemical vapour method.[13] Titanium is created in a vapour form and is then further condensed to form nano-sized particles. The starting material for this process is the same as the sol-gel method. Titanium tetrachloride ($TiCl_4$) is used in conjunction with sodium and ethanol. $TiCl_4$ is heated to 110 °C on a hot plate and the sodium chunks are placed in a quartz tube oven at 300 °C. At these temperatures, the sodium and titanium tetrachloride are vaporized. Argon gas is used to carry the $TiCl_4$ through the quartz tube oven, where the sodium reacts with $TiCl_4$ according to Equation 2.4. The resulting titanium particles are very small due to the vapour reaction and are encapsulated in a sodium chloride coating. The product is then diluted in an ethanol bath and the ethanol is vaporized to produce the final product.[13]

$$Na + TiCl_4 \rightarrow 4NaCl + Ti \tag{2.4}$$

2.1.3   Wire Electric Explosion

Wire electric explosion (WEE) technique is a method of creating titanium nano-powder from a bulk titanium sample.[19,20,21] WEE uses a high density current ($>10^{10}$ A/m^2) to cause the destruction of a metallic wire through an explosion. The process is started by increasing the electrical current to heat up the wire through resistance. The temperature of the wire continues to increase until it liquefies. During this process, the wire expands and the steep increase in resistance causes the wire to ignite and explode.[19] The resulting particles formed are between 10 and 100 nm in size. This process happens very quickly and the explosion time is 10^{-5} to 10^{-8} s. In this short time frame, the temperature reaches 10^4 K, pressures increases to $\sim10^9$ Pa and the velocity of the products reach 1-5 km/s.[20]

The following conditions can affect the resulting titanium product and its characteristics: the amount of current sent through the wire, the length and diameter of the wire, and the atmosphere of the explosion. These properties determine the composition of the titanium produced and the resulting size of the powder.[20] Using argon or helium for the explosion atmosphere creates pure titanium metal powders. The use of nitrogen creates titanium nitride and oxygen forms titanium dioxide. The approximate diameter and length of the wire should be 0.2 - 0.5 mm and 50 - 120 mm, respectively in order for the process to be effective.[21] The various particle sizes are accomplished by changing the initial current that is supplied to the wire. The nano-titanium used in this thesis was created using this WEE method.

2.2   Titanium Incidents

Like many metal powders, titanium has flammable and explosive properties. Many industrial incidents have occurred within the past 5 to 10 years resulting in severe workplace injuries and, in some cases, fatalities. These traumatic events can be prevented with the proper knowledge and use of safety measures. In these industrial events, titanium shavings and powders ignited causing an explosion and a subsequent fire. When

considering nano-titanium, no industrial cases have been reported but lab incidents have occurred with this highly flammable metal as the cause.

2.2.1 Early Titanium Incidents

Titanium processing started in the early 1950s and involved melting titanium metal in a vessel containing copper cooling water pipes. To melt the titanium, the temperature must have exceeded 1635 ºC. Copper, on the other hand, melts at 1100 ºC. Therefore, if the cooling water was lost, the copper pipes would melt. The melting of the copper pipes allowed water to mix with molten titanium, creating hydrogen gas. Molten titanium reacts strongly with water and strips the oxygen from a water molecule creating flammable hydrogen gas. Equation 2.5 shows the chemistry involved with the reaction. Fifty cases of titanium reactor explosions have been documented with the most recent being in 1999.[22]

$$Ti + 2H_2O \rightarrow TiO_2 + 2H_2 \tag{2.5}$$

2.2.2 Wichita, Kansas

A fire was started in a metal storage building in Wichita, Kansas, on July 30, 2005 and caused fireballs to rise 15 m in the air. Once the firefighters arrived on the scene, they realised that 82,000 kg of titanium shavings had been ignited to cause the fire. Fortunately, knowing titanium was the source of the blaze, firefighters did not extinguish the fire using water and were forced to let the building burn. Extinguishing the fire with water would have caused flammable hydrogen gas to be released and the possibility of a hydrogen explosion. No serious injuries were caused by this explosion.[23]

2.2.3   Los Angeles, California

Similar to the Wichita explosion, a fire erupted at a metal recycling plant in Los Angeles where titanium was ignited on July 13, 2010.[24] When firefighters responded to the scene, water was used to extinguish the flame. Within 12 min, the firefighters were forced to retreat due to the deteriorating conditions and the increased flames. After 40 min, a large explosion sent debris and pieces of titanium into the air. Seven firefighters were injured during the explosion with a second explosion occurring 2 hr later. Large amounts of water intensified the flame and caused flammable hydrogen gas build-up. The total damages were estimated at 5 million dollars.[25,26]

2.2.4   New Cumberland, West Virginia

On December 9, 2010, a large explosion and fire occurred at a titanium and zirconium processing plant in West Virginia. This accident is currently being investigated by the US Chemical Safety Board. It is suspected that the spontaneous explosion and fire may have been caused by titanium dust. This incident resulted in three fatalities.[27]

2.2.5   Nano-Titanium Flash Fires

The cases described all previously dealt with bulk and micron titanium and it has become evident that micron titanium is very dangerous. The reactivity of nano-titanium increases due to the very small particle size. Throughout this thesis, precautions were taken before the completion of any experimental work, taking into account the explosibility of this metal. Reaction tests were performed under the surveillance of the Dalhousie Safety Office in order to assess the spontaneous ignitability of nano-titanium samples. Initially, nano-titanium was exposed to air with no spontaneous reaction occurring. Small amounts of water and acid were then added to the nano-particles, still with no reaction noted. Following the completion of the reaction safety testing, explosion research testing began.

Although preventative precautions were taken, an incident still occurred even with the small amounts of titanium (<100 g).

Nano-titanium powder was packaged in individual 100 g bags and handled in a glove bag under nitrogen gas during the experiments. If any nano-titanium particles were remaining after the experiments, the left over powder was placed in a re-sealable plastic bag within the nitrogen glove bag. In this particular case, an experiment was performed, titanium dust was stored and no testing was done for a two-week period. Upon re-opening of the bag (not under nitrogen due to handling difficulties) the titanium spontaneously ignited. The period of time that the nano-titanium was exposed to air (two weeks prior) allowed moisture to enter the bag and react with the titanium. Similarly to the incident of water reacting with molten titanium, nano-titanium reacts with moisture in the air to create hydrogen gas. Opening the bag created static electricity which caused the hydrogen ignition followed by the combustion of nano-titanium. Hydrogen has a very low minimum ignition energy, approximately 0.017 mJ, which may have influenced the ignition.[28]

A similar incident occurred to an individual working with nano-titanium at the University of Wisconsin-Madison. The nano-titanium spontaneously ignited when the researcher was using a spatula to remove 2 g of powder. It is suspected that the ignition was caused by static charge or chemical contamination of the spatula.[29]

2.3   Previous Nano Dust Explosion Research

Dust explosion research involving nano-materials has been limited, but some research groups have performed tests with various materials to better understand the properties of nano-sized powders. At the nano-scale, properties of substances are altered and begin to exhibit physical (added strength) and chemical (increased reactivity, fluorescence and conduction) changes. The physical and chemical properties that pertain to bulk samples no longer apply to nano-particles. The unique surface properties of nano-sized particles

take precedence. For example, titanium and zinc are solid metals that, once under 100 nm in size, become transparent due to their specialized surface properties.[30]

Discussions relating to dust explosions with decreasing particle sizes and the effects of size on the explosion severity have been a major topic in the past decade. Severity is indicated by the maximum explosion pressure (P_{max}) and the maximum rate of pressure rise (($dP/dt)_{max}$). The trend has been for the severity to increase as the particle size decrease; however, as the particles reach a smaller micron-size, severity approaches a quasi-plateau and ceases to increase. This quasi-plateau may be caused by particle agglomeration, reaction mechanisms, or a combination of both. Particle agglomeration causes an increase in the effective size of the dust, decreasing the explosion severity.

A reaction mechanism is the method in which a dust is combusted during an explosion. This can be further explained by an example involving coal that initiates an explosion with a maximum severity occurring with a particle size of approximately 50 µm. Smaller, micron-sized coal particles do not further increase the severity. As explained in section 1.1.3, the particles must undergo heating, melting, devolatilization and a gas phase reaction for the particles to react. Once coal dust particles reach low micron-sizes, the steps of heating, melting and vaporization of the particles occur very quickly; however, the gas phase reaction step occurs much slower. As a result, the gas phase reaction is the rate determining step. If a nano-coal dust explosion were to occur, the severity of the explosion is not expected to increase because the rate limiting step is the vapour combustion.[30, 31] Similar processes exist for metal dusts where the burning mechanisms as well as the process of agglomeration may limit the explosion potential as the particle size decreases from the micron to the nano-range.

Research with nano-dust explosions has received more attention in recent years. Holbrow et al.[32], with the UK Health and Safety Executive, performed dust explosion tests using different types of nano-materials including metals (aluminum, zinc, copper and iron) and carbon nanotubes. Experiments were performed in a specially designed 2-L explosion chamber. The results demonstrated weak explosions with copper and iron: P_{max}

of 1.2 bar(g) and 2.9 bar(g) and $(dP/dt)_{max}$ of 10 bar/s and 68 bar/s, respectively. Zinc results showed a more severe explosion with a P_{max} of 5.6 bar(g) and $(dP/dt)_{max}$ of 377 bar/s. Two different nano-aluminum particle sizes were tested, 210 nm and 100 nm. The results illustrated a P_{max} of 12.5 bar(g) and 11.2 bar(g) and a $(dP/dt)_{max}$ of 1677 bar/s and 2000 bar/s, respectively.[32]

Explosions performed using a Siwek 20-L explosion chamber with various nano-particle materials were also investigated by Vignes et al.[33] Materials tested included carbon black, multi-walled carbon nanotubes and aluminum. No previous titanium dust explosion results could be found for maximum pressure (P_{max}) and maximum rate of pressure rise ($(dP/dt)_{max}$). The results for the nano-aluminum dust explosions are further discussed within this section due to the similarity between aluminum and titanium metals.

Using the nano-aluminum (100 nm and 200 nm) results from Vignes et al.[33], Dufaud et al.[34] compared the nano-aluminum explosions to micron-size aluminum explosions in a 20-L explosion chamber. The results indicated a maximum explosion pressure, P_{max}, of 8.2 bar(g) and 9.5 bar(g) while the maximum rate of pressure rise, $(dP/dt)_{max}$, was 1340 bar/s and 2420 bar/s for the 100 nm and 200 nm samples, respectively. At the micron-scale, 3 µm and 7 µm aluminium gave a P_{max} of 9.8 bar(g) and 9.1 bar(g) and $(dP/dt)_{max}$ of 2090 bar/s and 1460 bar/s, respectively. Explosion severity was limited by the size of the particles with the peak severity occurring at approximately 1 µm. Dust explosions initiated with smaller aluminum particles would cause a decreased explosion severity. This decrease in severity is caused partly by the oxidation of the nano-aluminum samples and is also due to the degree of agglomeration.[34]

Likewise, Wu et al.[35] performed nano-dust explosions in a 20-L chamber using aluminum with average particle sizes of 35 nm and 100 nm, resulting in a P_{max} of 7.3 bar(g) and 12.5 bar(g), and $(dP/dt)_{max}$ of 1286 bar/s and 1090 bar/s, respectively. These results can be compared to larger micron-aluminum powder data obtained from Eckhoff.[3] For a mean particle size of 22 µm, P_{max} was 12.5 bar(g) and $(dP/dt)_{max}$ was 1474 bar/s within a

20-L chamber.[3] Again, agglomeration affects the severity of the explosion and decreases the maximum pressure and maximum rate of pressure rise.[35]

Wu et al.[36] also tested the minimum ignition energy (MIE) of micron- and nano-titanium. As the particle size was decreased from 45 µm to 3 µm, the MIE dropped from 21.9 mJ to <1 mJ. For three nano-titanium sizes (35 nm, 75 nm and 100 nm), the MIE was lower than 1 mJ.[36] An energy of 1 mJ is the lowest value generated with the MIKE 3 and is therefore the limitation of the equipment used by Wu et al.[36] However, 3 µm titanium has been seen to ignite at 0.012 mJ by Randeberg et al.[37]

Consistent results using materials such as iron and titanium have been difficult to obtain using the Siwek 20-L chamber. Wu et al.[38] performed tests with nano-aluminum, nano-iron, and nano-titanium and dispersed them according to procedures described in section 4.2.1. The Siwek 20-L chamber traditionally uses air to disperse dust from the external reservoir into the explosion chamber. With air, nano-aluminum was properly dispersed from the external dispersion reservoir to create a homogenous dust cloud. However, nano-titanium and nano-iron did not create a homogenous dust cloud. When the dust was dispersed, an explosion occurred within the external reservoir. Friction or electrostatic sparking between the dust and the metal reservoir container caused the nano-iron and nano-titanium to ignite. It was found that dispersion with nitrogen gas instead of air can prevent nano-titanium and nano-iron from exploding within the dispersion reservoir.[38] This is the approach that was taken for the experimental work performed in this thesis.

CHAPTER 3: APPARATUS

This section describes the explosion apparatus used to determine the explosion severity and likelihood parameters of micron- and nano-titanium dust. The pieces of equipment include the Siwek 20-L chamber, the MIKE 3 apparatus, and the BAM oven.

3.1   Siwek 20-L Chamber

The Siwek 20-L chamber, manufactured by Kühner A.G. of Switzerland, is used to determine various explosion parameters including: maximum pressure (P_{max}), maximum rate of pressure rise ($(dP/dt)_{max}$) and minimum explosible concentration (MEC). The 20-L chamber is regarded as the industry standard for dust explosion testing. This apparatus incorporates five pieces (explosion chamber, external dispersion reservoir, ignition system, pressure measuring system and a control system) that work to disperse, ignite, and record the properties of the dust explosion.[39] Figures 3.1 and 3.2 illustrate the parts and design of the 20-L chamber.

1. Pressure Gauge
2. Solenoid Valve
3. Dust Storage Chamber
4. Vacuum Pump
5. Exhaust Valve
6. Vacuum Valve
7. Pressure Transducer
8. Rebound Nozzle
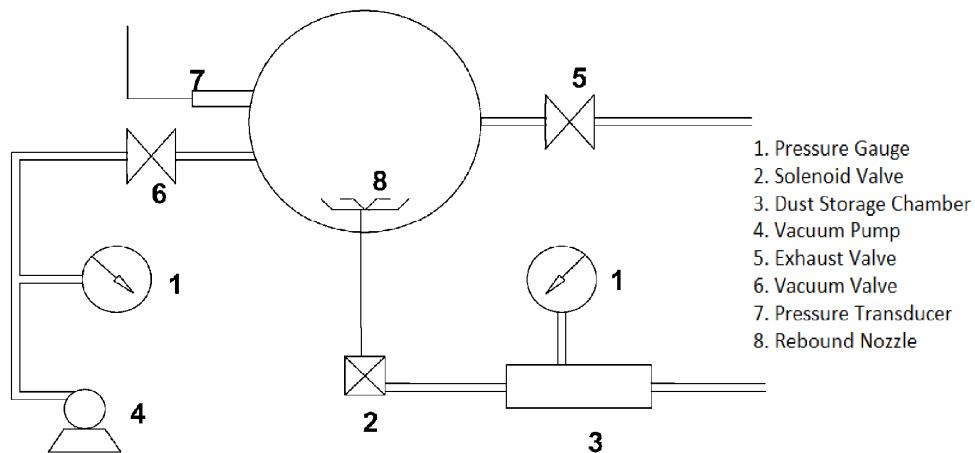
Figure 3.1   Sequematic of the Siwek 20-L chamber
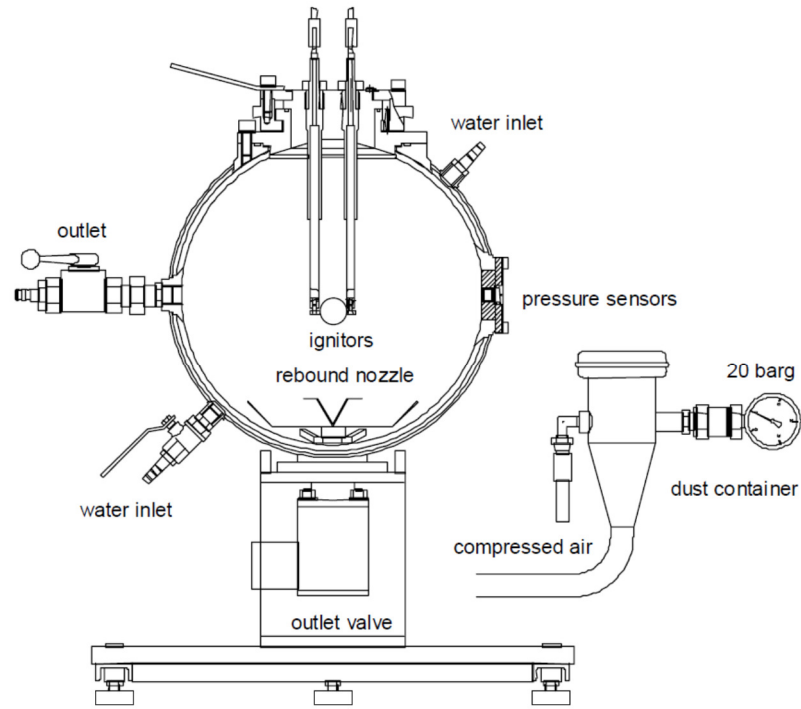
Figure 3.2   Siwek 20-L chamber[39]

3.1.1   Explosion Chamber

The explosion chamber consists of a stainless steel, hollow sphere with a total volume of 20-L. Around the outside of the sphere is a cooling jacket. Cooling water can be sent through this jacket to keep the inside vessel at a constant temperature between explosions. The operating temperature of the vessel should be approximately 20 °C, or room temperature.[39]

At the top of the 20-L chamber is a 94-mm opening where the bayonet ring is located. The bayonet ring seals the top of the sphere when in use. Two ignitor posts are located through the bayonet ring and hold the pyrotechnic ignitors during a test. These ignitors cause the explosion and are described in detail in section 3.1.3. Between tests, the bayonet ring can be removed to enable access to the 20-L chamber for cleaning and to mount new ignitors.

Located at the bottom of the 20-L chamber is a solenoid valve that separates the explosion chamber from the external dispersion reservoir. The dispersion reservoir is a 0.6-L chamber that holds the dust during the dispersion sequence.

The 20-L chamber also contains a 30-mm flange that is located on the side of the chamber. This flange holds two pressure transducers that measure the pressure changes caused by the explosion. Two valves are also located on the side of the sphere. One is connected to a suction system to generate a vacuum within the chamber while the other is used for venting combustion products.

3.1.2   Dispersion System

The dispersion of the dust in the 20-L chamber occurs through the external dispersion reservoir, the solenoid valve and the rebound nozzle. Dust is placed in the dispersion reservoir and compressed gas acts as the dust carrier. During the dispersion sequence, the dust is placed in the dispersion reservoir and a compressed gas fills the remaining space within chamber. The solenoid valve is then activated to allow the compressed gas and dust mixture to enter the 20-L chamber. Once through the valve, the mixture passes through a rebound nozzle. The high velocity mixture hits the top of the nozzle and is forced back down to rebound against the bottom of the valve. The nozzle is designed to allow turbulent mixing effects and fills the entire 20-L chamber with a uniform dust cloud.

3.1.3   Ignition System

Ignition of the dust cloud is achieved by pyrotechnic ignitors. An electrical current is sent through the ignitor post and ignites the 5-kJ Sobbe ignitor. The ignitors are composed of 40% zirconium, 30% barium nitrate and 30% barium peroxide.[39] The number of ignitors is dependent on the test. P_{max} and $(dP/dt)_{max}$ testing is performed with two 5-kJ ignitors

while MEC testing is performed using one 5-kJ ignitor. Ignition of the dust cloud occurs 60 ms after the dispersion sequence.

3.1.4   Pressure Measuring System

The 20-L chamber uses two Kistler piezoelectric pressure transducers to measure the rate of pressure rise caused by the explosion. The pressure transducer works by the deformation of a quartz crystal. The pressure wave causes the deformation of the crystal and this deformation is directly proportional to the pressure differences throughout the explosion. The pressure transducers can only measure changes in pressure and not in static pressure.[39]

3.1.5   Control System

The 20-L chamber utilizes a fully automated system that controls the dispersion and the ignition of the dust. A control unit, KSEP 332, manufactured by Kühner, connects all compressed gas and electrical components together. KSEP 332 allows the equipment to create a uniform dust cloud and a subsequent explosion at the proper time. This unit controls the release of compressed gas and the sequencing of the solenoid valve with the ignitors. The Kühner software, KSEP 6.0f, relays information to KSEP 332 relating to the explosion and also initiates the dust dispersion and explosion process.

3.2   MIKE 3 Apparatus

The MIKE 3 apparatus is manufactured by Kühner and is a modified Hartman tube used to measure the dust's minimum ignition energy (MIE).[40] The MIKE 3 consists of a glass tube, electrodes and dispersion cup. Figure 3.3 shows the MIKE 3 in more detail. A

thorough description of the dispersion, ignition and control systems is given in subsequent sections.

moving electrode	door lock
compressed air for ME	high-voltage electrode
compressed air for purging	dispersion pressure (7 bar overpressure)
on/off switch	keys for: inlet valve
	ME / outlet valve

Front

air connection:
7 bar overpressure
air filter

connection for the PC
(RS 232)

for pneumatic cylinders:
pressure indicator

pressure regulator (5 bar)

power supply
(100-240V / 50-60 Hz)

Back
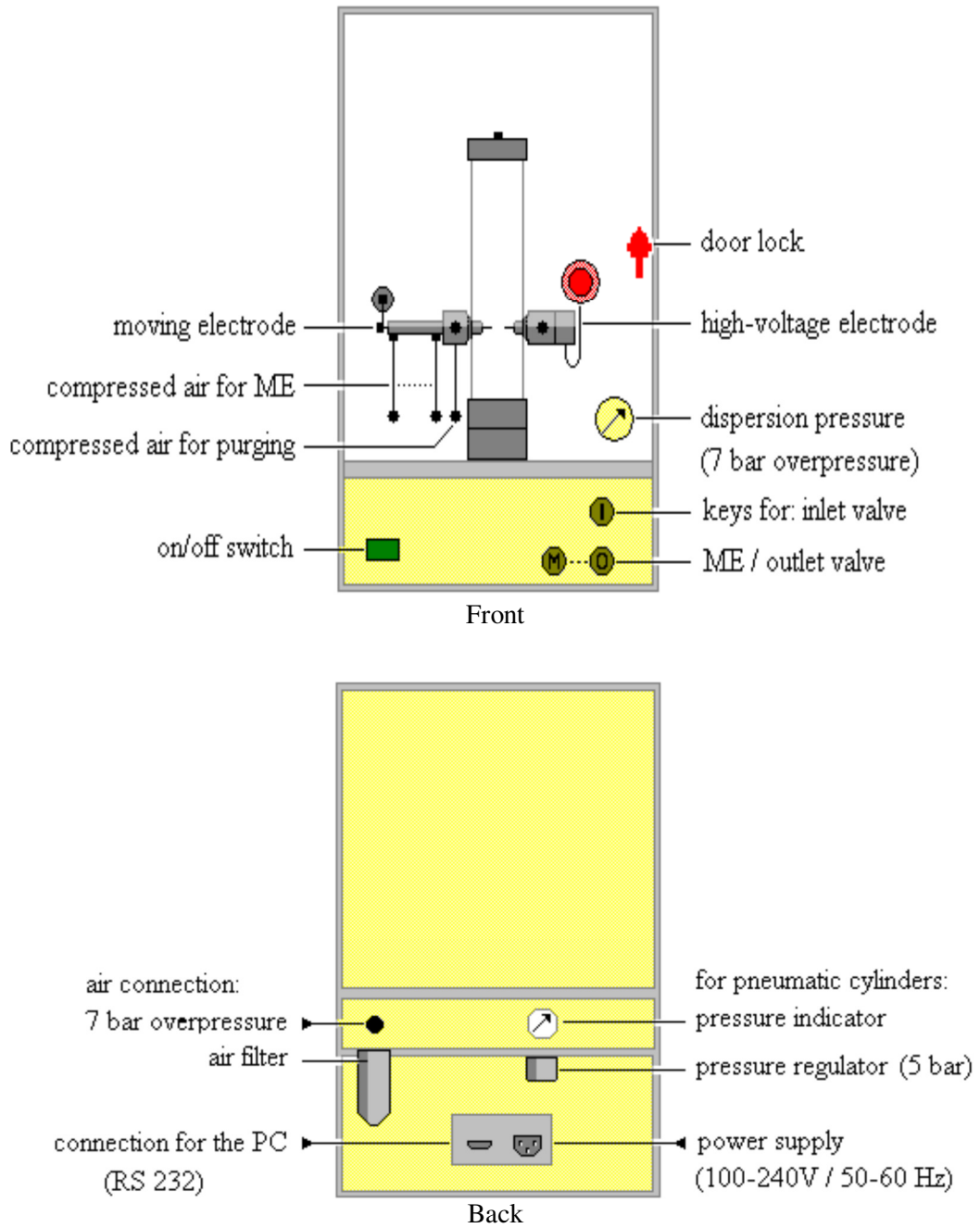
Figure 3.3   Sequematic of the MIKE 3 Apparatus[40]

3.2.1 Dispersion System

The MIKE 3 apparatus uses compressed air for many different actions. The air pressure is used at 5 bar(g) for the ignition system and 7 bar(g) for dust dispersion. Dust is first placed in the dispersion cup around a mushroom cap nozzle, located beneath the glass tube. The mushroom cap forces the high velocity air down to disperse the dust into a homogenous cloud within the glass tube. Once a cloud is formed, the electrode generates a spark to ignite the dust.

3.2.2 Ignition System

The ignition of a dust cloud in the MIKE 3 is accomplished using a spark with an energy amount that is predetermined by the operator. Energy values for the MIKE 3 are: 1000 mJ, 300 mJ, 100 mJ, 30 mJ, 10 mJ, 3 mJ, and 1 mJ. Different energy values are used to determine the lowest possible energy at which a dust ignites. The energy values are obtained using a variety of pneumatic, high-voltage switches that use capacitors to create the specified amount of energy. Each energy setting is controlled through switches that complete different circuits for the specified energy level. When the circuit is closed, the energy is discharged through the electrode. The high-voltage electrode releases the energy across a 6-mm gap causing the spark. The receiving electrode is grounded, dissipating the remaining charge.

The time delay of the ignition can also be altered and is the difference between the dust dispersion and the spark ignition. The regular settings are 60 ms, 90 ms, 120 ms, 150 ms and 180 ms. These different time delays allow the dust to ignite with different turbulence levels and can affect the MIE.

Inductance can also be varied by choosing either 0 mH or 1 mH of inductance and serves to change the duration of the spark. Higher inductance releases the same amount of energy but the energy is dissipated over a longer period of time.

3.2.3   Control System

The MIKE 3 apparatus controls the dispersion of the dust and ignition sequence through an automated system. The software, MIKE 3.3, is provided by Kühner and works in conjunction with the control system. Manual initiation is required by the operator to start the process. The system then controls the pressurization of the pneumatic switches and finishes with the generation of the spark. The software ensures the correct spark energy, time delay and inductance; however, the software cannot determine whether an ignition has occurred. A visual check is required by the operator to inform the computer if an ignition was achieved.

3.3   BAM Oven

The BAM oven is used to determine the minimum hot-surface temperature of a dust. The purpose of this test is to find the lowest temperature at which the dust will ignite. It consists of a manual dispersion system and a heater. Figure 3.4 shows an outline of the equipment and the subsequent sections describe the individual parts in greater detail.

3.3.1   Dispersion System

There are three main parts to the dispersion system for the BAM oven: a rubber bulb, a nozzle and a deflecting surface. The dust is placed in the nozzle and dispersed into the oven through the use of the rubber bulb. Injecting the dust creates a dust cloud and is ignited by the deflecting surface or walls of the oven. The BAM oven walls and the deflecting surface are at specified temperatures recorded by the user.

3.3.2 Ignition System

The BAM oven is used to create a dust cloud within a hot environment to determine at which temperature the dust cloud will ignite. To create the hot surface, the test chamber is surrounded by a 1500 W heater enabling the BAM oven walls to reach temperatures up to 600°C. The temperature in the heater can be altered by an external controller and the temperature is measured through 2 thermocouples with an accuracy of +/- 1 °C.[41]
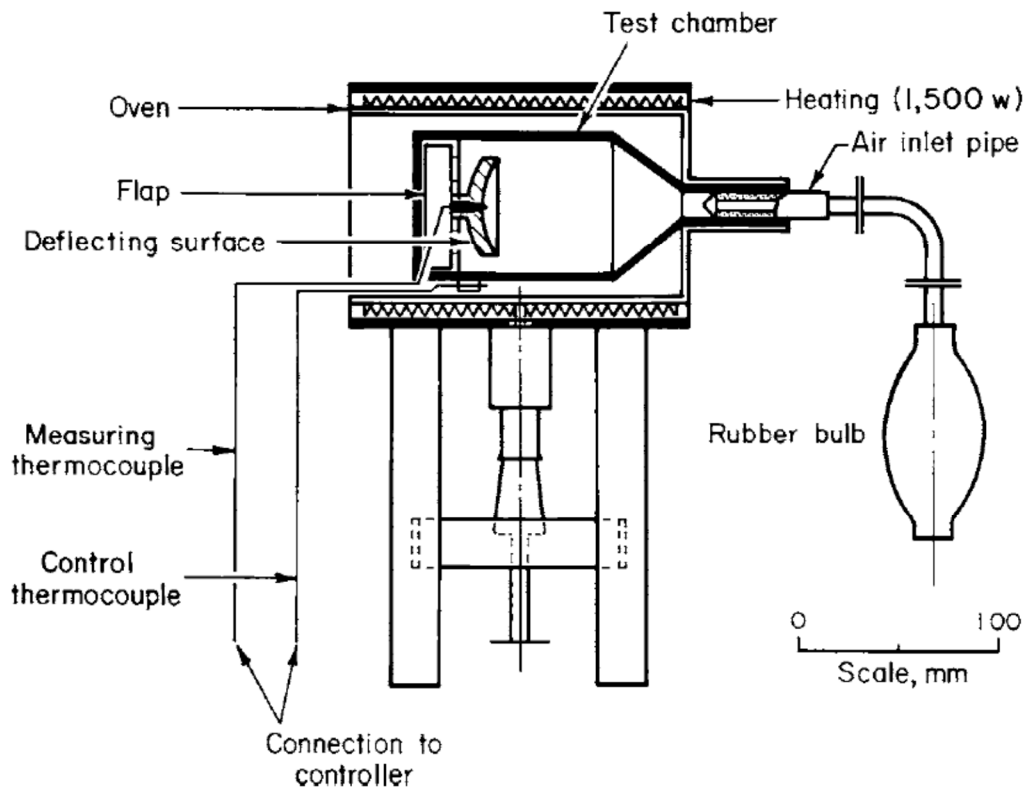
Figure 3.4   Sequematic of the BAM oven[41]

CHAPTER 4: EXPERIMENTAL

This chapter gives a description of the materials used and the procedures followed during the experimental work. Micron- and nano-titanium samples are described and characterized by using a Malvern particle size analyser, a sieve analysis and through SEM micrographs. The procedures for the equipment described in chapter 3 are further explained and clarified in this chapter.

4.1   Materials

Titanium was chosen as the topic of interest for this research due to its unique reactivity and the availability of existing data on dust explosibility at the micron-scale. Six sample sizes were selected: -100 mesh (<150 µm), -325 mesh (<45 µm), ≤20 µm, 150 nm, 60-80 nm, and 40-60 nm. Particle size distributions were determined to characterize the micron-size titanium. The powder manufacturer's (American Elements) literature states that the two smaller micron-titanium samples are nominally ≤20 µm and <45 µm (-325 mesh) – but are sized differently; a single-point BET surface area analysis is used to determine the size of the ≤20 µm titanium while a sieve analysis is used to analyze the -325 mesh titanium. According to American Elements, the BET surface area analysis measures the average unagglomerated particle size; however, a traditional sieve analysis measures the particle size distribution of agglomerated particles. The sieve analysis that was performed specifically on titanium is shown in Table 4.1.

A Malvern particle size analyser (based on laser diffraction) was also performed (Appendix A). The results demonstrated larger than expected particle size due to the granular shape and agglomeration effects of the titanium powder. Laser diffraction assumes that the particles are spherical in shape and that no agglomeration has occurred. The laser reads across the wetted sample of powder but the irregular shape of the titanium particle may orientate in a lengthwise direction, increasing the expected particle size. Agglomerates of small titanium fragments are read as one particle.

According to the sieve and the Malvern analysis, the ≤20 µm and the -325 mesh titanium samples are similar in agglomerated size. American Elements states that the -325 mesh titanium sample can be smaller than the specified mesh size. The size of the -325 titanium particles may actually be the same size or smaller than the ≤20 µm titanium sample. Unfortunately, it is not possible to determine the exact particle size due to the irregularity of the micron-titanium samples. Particle sizes of the nano-titanium samples were taken as documented by the manufacturer, Skyspring Nanomaterials Inc., and no further size analysis was performed.

Table 4.1   Sieve analysis of micron-size titanium powders

		Wt. % Retained		
Sieve Size	Micron Size	≤20 µm	-325 mesh	-100 mesh
+325	>45 µm	0.98	0.00	91.88
-325+400	45-38 µm	10.55	6.45	5.06
-400+450	38-32 µm	5.96	4.50	0.38
-450+500	32-25 µm	23.54	23.03	1.72
-500	<25 µm	58.98	66.02	0.96

A scanning electron micrograph (SEM) of the ≤20 µm titanium sample is shown in Figure 4.1. Individual particles of titanium are not spherical but have a granular shape. Agglomerates are seen in Figure 4.1b for the ≤20 µm titanium. Two types of agglomerates are present; the larger titanium particles are covered by smaller titanium 'bits', and the medium-sized particles are joined to form a larger agglomerate. Figure 4.2 shows the 150 nm sample. While the individual particles are much smaller, agglomerates are still present. The nano-agglomerates varied in composition between approximately 50 particles and thousands of particles. Additional SEM micrographs can be seen in Appendix B for all titanium samples.
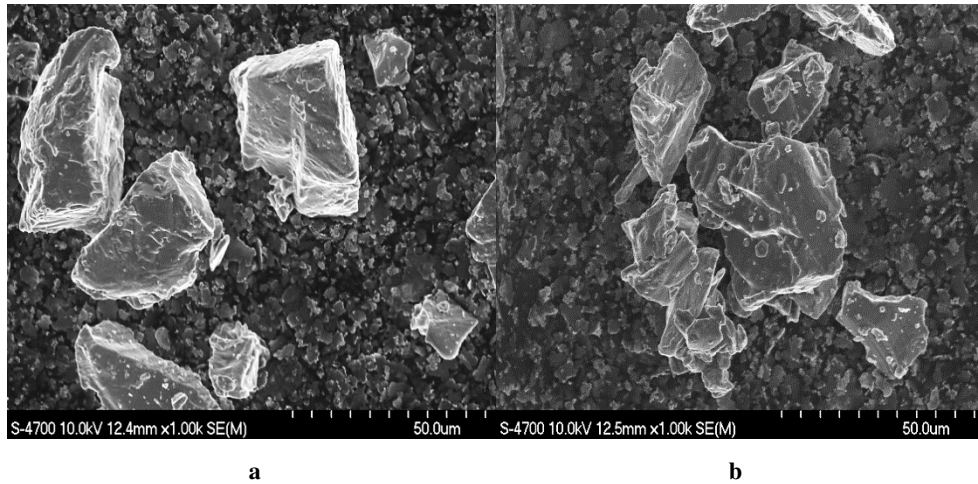
Figure 4.1 Scanning electron micrographs of ≤20 µm titanium powder
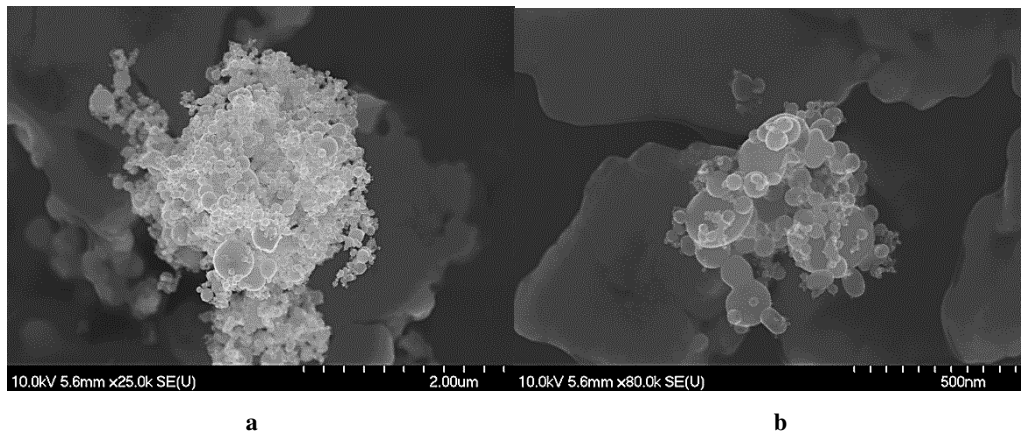
Figure 4.2 Scanning electron micrographs of 150 nm titanium powder

4.2   Procedures

The following section describes the procedures used for testing the micron- and nano-titanium samples. Each sample is tested using the applicable ASTM methods, seen in Table 4.2, ensuring that the tests are precise and reliable. The standardized dust explosion equipment described in chapter 3 is used for micron- and nano-titanium dust explosion testing.

Table 4.2   ASTM Methods

ASTM Designation	Method Title	Experiment
E1226-10	Standard Test Method for Explosibility of Dust Clouds[42]	P_{max}, K_{st}
E2019-07	Standard Test Method for Minimum Ignition Energy of a Dust Cloud in Air[43]	MIE
E1515-07	Standard Test Method for Minimum Explosible Concentration of Combustible Dusts[44]	MEC
E1491-06	Standard Test Method for Minimum Autoignition Temperature of Dust Clouds[41]	MIT

4.2.1   Siwek 20-L chamber

Micron- and nano-titanium powders are tested for P_{max}, $(dP/dt)_{max}$ and MEC using the Siwek 20-L chamber. The testing procedures are slightly different for the nano-titanium dispersion and ignition due to material sensitivity. This section explains the procedures and the corresponding explosion curves from a 20-L chamber explosion test.

4.2.1.1 Micron-Procedures

Once all protective equipment is applied, the experimental work begins. First, the Siwek 20-L chamber is inspected and cleaned if necessary. The rebound nozzle is placed in the bottom of the vessel and screwed into position. Next, the ignitors are removed from their packaging and the excess wiring is cut. The wire is then stripped of its covering to expose the copper wire. Two 5-kJ ignitors are used for a P_{max} / $(dP/dt)_{max}$ test and one 5-kJ ignitor is used for a MEC test. The ignitors are secured to the ignitor posts and the top is placed on the Siwek 20-L chamber.

The air bottle is opened and regulated to the appropriate pressure. This allows the compressed air to be released into the external dispersion reservoir at 20 bar(g). Test

checks may be required to ensure proper regulator position. Once this setting is correct, dust is weighed and placed in the dispersion reservoir.

After correct placement of the dust and ignitors, all valves are closed except the vacuum valve (Figure 3.1, item 6). The vacuum reduces the pressure in the 20-L chamber to 0.4 bar(a). As soon as the vacuum pressure is correct, the parameters are entered into the computer software. These parameters include the test series number, dust concentration (g/m^3), time delay (ms) and ignition energy (10-kJ for P_{max} / $(dP/dt)_{max}$ and 5-kJ for MEC). Once this information is entered, the operator initiates the test and the automated system starts the explosion sequence. The manuals given by Kühner provide the testing and cleaning procedures.[39,45,46]

After the explosion process is initiated, compressed air fills the dispersion reservoir until the pressure reaches 20 bar(g). The solenoid valve (Figure 3.1, item 2), located between the dispersion reservoir and the 20-L chamber, is opened. The 20 bar(g) air/dust mixture enters the 0.4 bar(a) evacuated chamber. This allows the pressurized air and dust mixture to enter the 20-L chamber via the rebound nozzle and to properly disperse the dust into a cloud. Once the air/dust mixture enters the 20-L chamber, the resulting pressures within the 20-L chamber are at 1 atm. Sixty ms after the dust dispersion process begins, the ignitors fire and the dust cloud ignites. Pressure within the 20-L chamber resulting from the ignition of the dust cloud is recorded as a pressure trace curve seen in Figure 4.3. The X shows the maximum pressure (P_m) and Δ shows the maximum rate of pressure rise $(dP/dt)_m$ for this particular explosion.
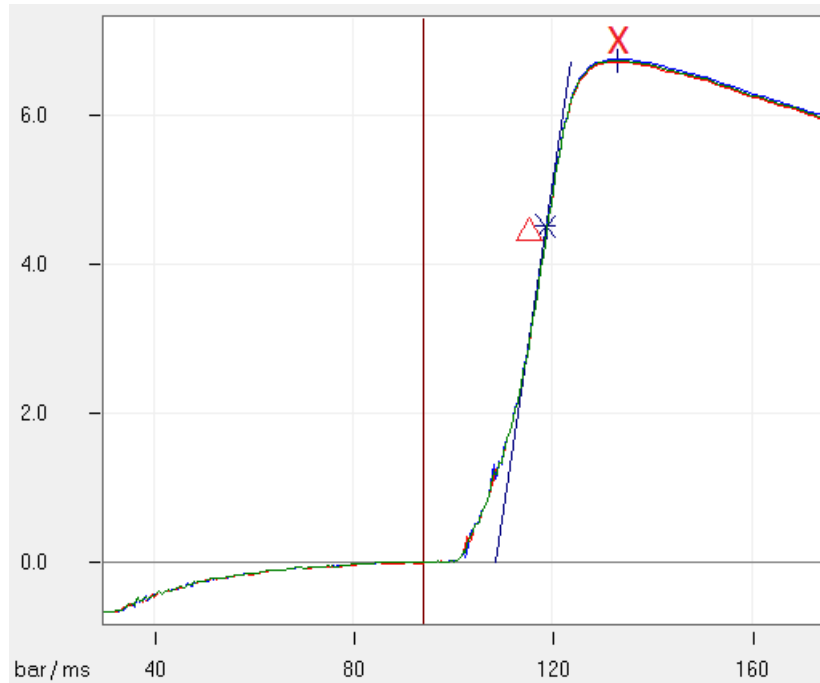
Figure 4.3   Explosion curve for micron-titanium powder

This procedure is repeated for different concentrations of dust until P_{max} and $(dP/dt)_{max}$ are recorded. Normally, multiple series are performed to ensure the reliability of the test. An initial series is done for all micron samples over a range of concentrations to find the maximum explosion severity. A subsequent series is then performed to validate the data, therefore, two explosion tests are carried out to test the maximum pressure and rate of pressure rise.

Using the -325 mesh titanium sample as an example, testing began at concentrations of 250 g/m^3. The concentration is increased by 250 g/m^3 increments until the maximum pressure and the maximum rate of pressure rise are determined. Once the maximum explosion severity is established, a second series is performed, shown through a testing matrix. The testing matrix used for the -325 mesh titanium can be seen in Table 4.3. The maximum pressure is between 1500 g/m^3 and 1750 g/m^3 and the maximum rate of pressure rise is between 1750 g/m^3 and 2000 g/m^3. Concentrations must be tested above and below the maximum pressure and maximum rate of pressure rise. For the -325 mesh

titanium sample, concentrations between 1250 g/m^3 and 2250 g/m^3 are performed twice each. A similar matrix is used for the -100 mesh and $\leq$20 μm titanium samples.

Table 4.3   Testing Matrix for -325 Mesh Titanium

Series	Concentration [g/m^3]										
1	250	500	750	1000	1250	1500	1750	2000	2250	2500	2750
2					1250	1500	1750	2000	2250		

The minimum explosible concentration (MEC) is tested by using similar procedures as the P_{max} and $(dP/dt)_{max}$ testing except one 5-kJ ignitor is used instead of two. The purpose of this test is to determine the lowest concentration of material that does not explode. ASTM E1515-07, sets the explosion limit as 1 bar(g),[44] therefore, if the dust can create a maximum explosion pressure greater than or equal to 1 bar(g), that specific concentration is considered explosible. Maximum explosion pressures below 1 bar(g) are not considered an explosion.

Concentrations of dust are much lower during an MEC test and normally start around 100 g/m^3. If 100 g/m^3 ignites, then the concentration is lowered to 90 g/m^3 and then to 80 g/m^3. The concentration is continuously dropped by 10 g/m^3 until a concentration is found at which the maximum pressure does not exceed 1 bar(g). This test is performed twice to ensure that no explosion occurs.

4.2.1.2 Nano-Procedures

The nano-titanium 20-L chamber explosion procedures are similar to the micron-procedures but some additional equipment is required. First, the nano-titanium is placed in a glovebag containing nitrogen. The nitrogen acts as an inert gas and prevents any oxidation of the nano-titanium or any unwanted hydrogen formation. Oxidation of the nano-titanium is minimized by using a glovebag. Nano-titanium is produced, packaged and stored within an inert environment. The only oxidation potential of the nano-titanium

occurs while transferring the nano-titanium from the glovebag to the 20-L chamber which results in a few seconds of exposure. Within the glovebag, the nano-titanium bag is opened, handled and weighed.

Handling of nano-titanium requires additional protective equipment. This equipment is outlined in section 6.4.4. The experimental work begins by ensuring that the Siwek 20-L chamber is cleaned. The rebound nozzle is placed in the vessel and into position. Nano-titanium does not require an ignitor for an explosion to occur. The very fine nano-powder is sensitive to static or frictional sparking and causes an ignition while dispersing into the 20-L chamber, therefore, no ignitors were used for any P_{max} and $(dP/dt)_{max}$ testing.

According to Wu et al.[38] dispersion of nano-titanium powder using air causes an explosion within the external dispersion reservoir. To solve this problem, nitrogen is used to disperse the nano-titanium into the 20-L chamber. In order to keep atmospheric conditions during the explosion, additional oxygen is added to the 20-L chamber.

First, the compressed nitrogen is opened and regulated to the appropriate pressure, 20 bar(g). Test checks may be required to ensure proper regulator position and the vacuum within the 20-L chamber is reduced to 0.25 bar(a). Additional oxygen increases the pressure to 0.4 bar(a). Because the dust is dispersed with nitrogen, oxygen is added to the 20-L chamber prior to dust dispersion to ensure that the resulting mixture after dispersion is atmospheric conditions.

Once equipment is ready, initial parameters are entered into the computer software. The pre-weighed nano-titanium is then taken from the glovebag and is placed in the dispersion reservoir and the test begins.

After the operator initiates the dispersion process, compressed nitrogen fills the external dispersion reservoir until the pressure reaches 20 bar(g). The solenoid valve opens and the nitrogen/dust mixture enters the 0.4 bar(a) evacuated chamber. Normally, the mixture creates a uniform dust cloud and the nitrogen and oxygen produce atmospheric

conditions. Unfortunately, this did not occur with the nano-titanium samples. While the dust is dispersed, the nano-titanium ignites and causes an explosion as soon as the dust encounters oxygen gas. This sudden explosion during the dispersion process is referred to as the pre-ignition of the nano-titanium. The resulting pressure change is recorded as a pressure trace curve seen in Figure 4.4. Here, the X represents the pseudo maximum pressure (P'_m) and Δ is the pseudo maximum rate of pressure rise $(dP/dt)'_m$ for this particular explosion. The term 'pseudo' is used to describe the maximum pressure and maximum rate of pressure rise for the nano-titanium explosions. Since the explosion is not occurring at the proper conditions (time or proper dispersion), the results are different than the micron-titanium. The nano-titanium curve is further discussed in section 6.1.2
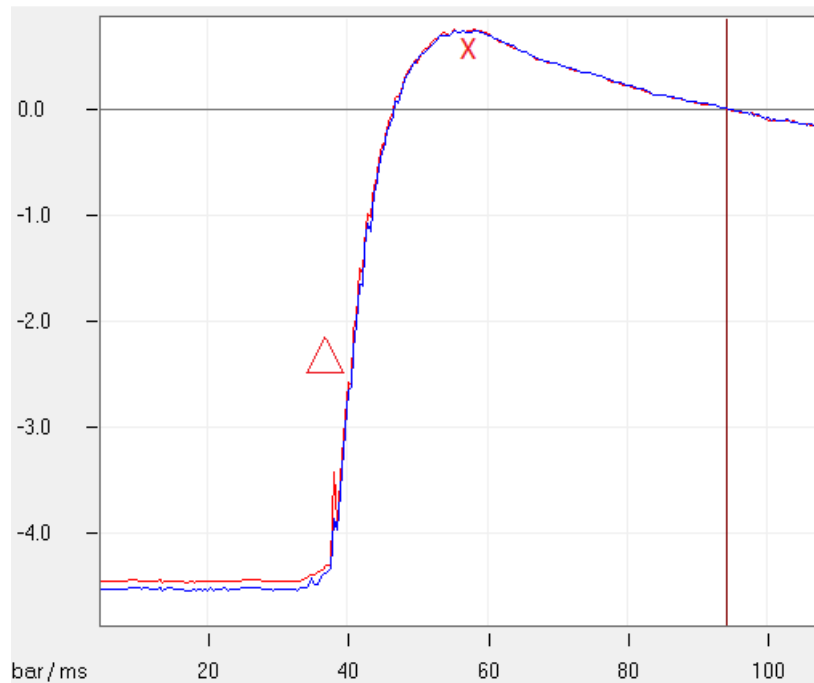
Figure 4.4   Explosion curve for nano-titanium powder

The nano-explosion curves are different than the typical micron explosion curves. The Kühner software, KSEP 6.0f, requires a curve shape seen in Figure 4.3 to determine the maximum pressure and the maximum rate of pressure rise. The nano-titanium explosion, seen in Figure 4.4, does not occur at the expected time and the software assumes errors.

Figure 4.5a shows typical results from KSEP 6.0f for the micron titanium while Figure 4.5b shows the results obtained for the nano-titanium explosion. Figure 4.4 clearly illustrates an explosion but the maximum pressure and maximum rate of pressure rise are not automatically calculated. All the nano-titanium files are exported onto Microsoft Excel and a manual calculation is done to determine the pseudo maximum pressure and pseudo maximum rate of pressure rise of the nano-titanium dust explosions.

	1	2	1,2	✋
Pex	6.7	6.8	6.7	
Pm	6.9	7.0	6.9	
dP/dt	440	448	444	
Pd	.65	.65	.65	
td	35	34	34	
tv	60	60	60	
t1	39	38	39	
	<1>	<2>	result	

a

	1	2	1,2	✋
Pex	.0	.0	.0	
Pm	.0	.0	.0	
dP/dt	0	0	614	
Pd	4.28	4.39	4.34	
td	35	35	35	
tv	60	60	60	
t1	0	0	0	
	<1>	<2>	result	

b
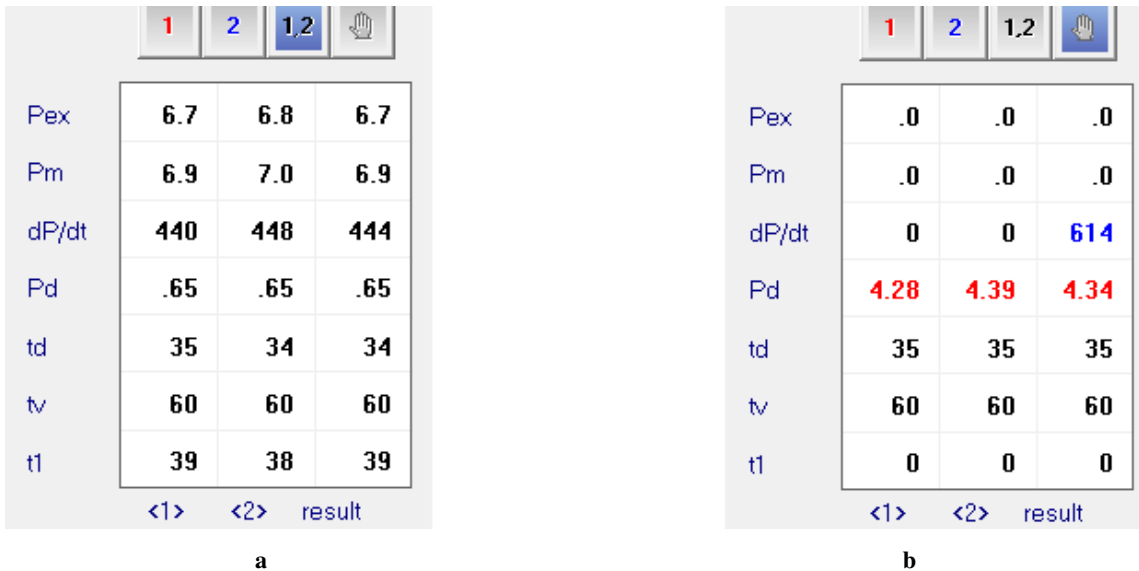
Figure 4.5 Kühner software results for micron-titanium (a) and nano-titnium (b)

The nano-procedures are repeated for various concentrations of nano-titanium until P'_{max} and $(dP/dt)'_{max}$ are found. A similar approach to the micron-titanium procedures is used for the nano-titanium. A testing matrix for the nano-titanium is followed. The first test series determines P'_{max} and $(dP/dt)'_{max}$ and the second series serves to validate the results. The 150 nm explosion matrix can be seen in Table 4.4. A similar matrix was used for the 60-80 nm and the 40-60 nm particle sizes.

Table 4.4   Testing Matrix for 150 nm Titanium

Series	Concentration [g/m³]								
1	60	80	100	125	250	500	750	1000	1250
2			100	125	250	500	750	1000	

The minimum explosible concentration (MEC) tests have similar nano-procedures to the P'_{max} and $(dP/dt)'_{max}$ testing. A 5-kJ ignitor is used for dust concentrations where the pre-ignition is not expected to occur (5-kJ ignitor is used for concentrations of approximately 20-40 g/m³).

The explosion limit set for MEC testing is changed for the nano-titanium explosion tests. Normally, the explosion limit is 1 bar(g) but the explosion limit is raised to 1.6 bar(g) for the nano-sizes to encompass the overlapping of the dust dispersion and the explosion. The additional 0.6 bar(g) is to account for the rise in pressure caused by the compressed nitrogen in the dispersion reservoir. Consequently, if the dust creates a maximum pressure of 1.6 bar(g) or higher, it is considered an explosion. Maximum explosion pressures below 1.6 bar(g) are not considered an explosion.

A different testing approach is taken for the nano-titanium MEC in comparison to the micron-titanium MEC testing. Concentrations of nano-titanium start at 20 g/m³ and rise until the MEC is found. These tests are performed in this manner to prevent higher than expected dust loading at the lower concentrations. No explosions were recorded at the lower concentrations (20-30 g/m³), therefore, the nano-titanium dust was removed from the 20-L chamber upon test completion. Even though the explosion chamber is cleaned, some nano-titanium particles may still remain within the apparatus.

Nano-titanium dust inerting procedures are similar to the nano-MEC procedure except nano-titanium dioxide is admixed with nano-titanium. The purpose is to find the percentage of TiO_2 that works to completely suppress an explosion. For complete explosion suppression, the maximum pressure cannot exceed the 1 bar(g) explosion limit.

An explosion limit of 1 bar(g) (not 1.6 bar(g)) is set because the addition of nano-titanium dioxide prevents the pre-ignition of the nano-titanium. Nano-titanium dust concentration was maintained at 125 g/m^3 while the percentage of titanium dioxide was increased from 0 % to 100 %.

4.2.2   MIKE 3 Apparatus

The MIKE 3 apparatus is used to determine the MIE of a powder. The first step when using the MIKE 3 apparatus is to regulate the amount of compressed air entering the dispersion reservoir. The pressure of compressed air must be set at 7.0 bar(g) according to the pressure gauge located on the front face of the machine. Secondly, the electrode spacing must be checked. The space between the electrodes must be 6 mm and is measured by using an insulated glass rod. The various components of the MIKE 3 apparatus can be seen in Figure 3.3.

The next step of MIE testing is to weigh the sample size. The MIKE 3 apparatus measures the mass of the material instead of the materials concentration. The amount of a material to be tested ranges from 300 mg to 3600 mg. Once the material is placed in the dispersion cup, the operator must then enter the mass of the sample (mg), energy (mJ), delay time (ms), and inductance (mH). The operator then initiates the testing sequence using MIKE 3.3 software. The dispersion and ignition sequence are automated to create a dust cloud, generate a spark and create the dust explosion. A visual inspection of the glass tube is required to determine if an explosion has occurred. An explosion occurs when a flame propagates more than 6 cm from the electrodes. If no ignition occurs, the operator chooses 'no' within the MIKE 3.3 software and more trials are required. After three consecutive, non-ignitable trials, the dust sample must be changed. A total of ten consecutive non-ignitions must occur for that specific concentration and energy to be considered non-ignitable. If an ignition occurs, the operator choses 'yes' and the test is completed for that ignition energy and concentration. The following test is performed at the same concentration but at a lower energy level.

Experimental testing using the MIKE 3 apparatus is performed to determine the effects of particle size on MIE for titanium powders. The MIE is determined for each sample using the same procedures for the micron- and nano-titanium. No experimental equipment or procedures are changed for the nano-titanium using the MIKE 3 apparatus; however, nano-titanium is handled and weighed in a glove bag under nitrogen before being used for testing.

Figure 4.6 shows a plot created by the ignition and non-ignition results from the MIKE 3 apparatus. The solid squares show the points where an ignition occurred while the hollow squares represent non-ignition points. Overall, points below the minimum ignition point (Figure 4.6 test numbers 4 and 6) prove that no ignition can occur at those recorded concentrations and energy levels. It is also important to recognize the upper and lower limit at which the dust cloud becomes too lean or too rich for a spark ignition to occur. Here, points 7 and 8 show that no ignition occurs at 10 mJ of energy for samples of 600 mg and 1500 mg. According to Figure 4.6, the MIE of this sample would be 3 – 10 mJ.
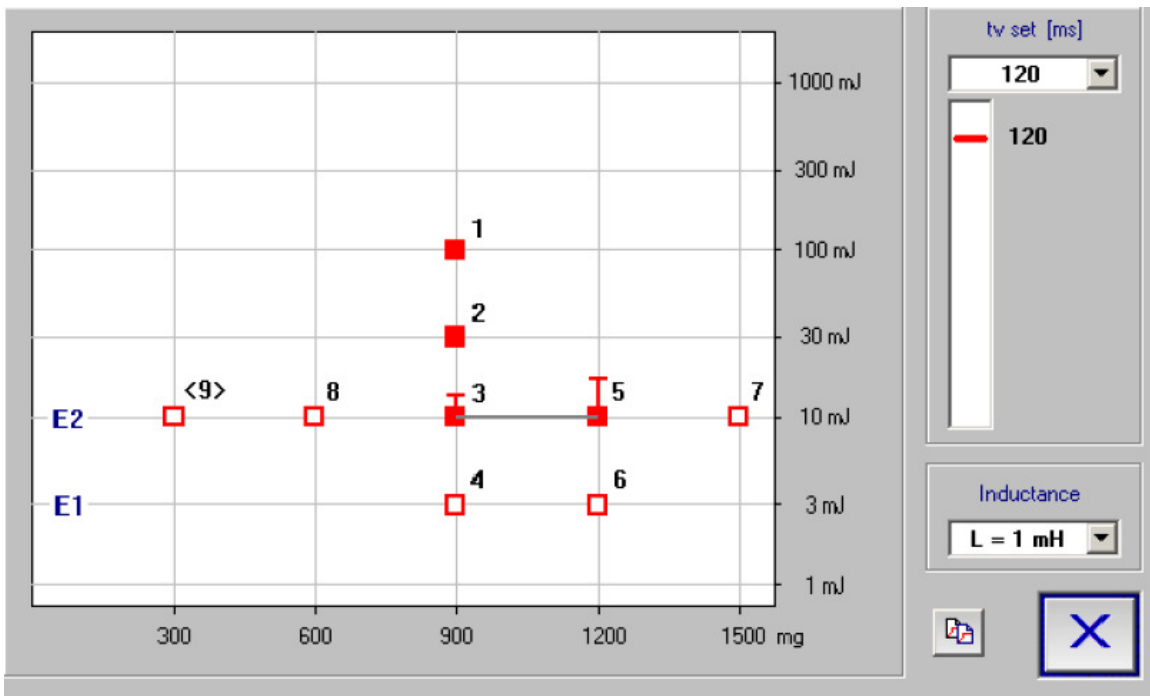
Figure 4.6   MIE data plot[40]

Once the testing is complete and the MIE has been found, the time delay is altered. The time delay is the difference in time between the dust dispersion and the spark generation and is usually set to 120 ms. The time delays chosen are 90, 120, and 150 ms. When changing the time delay, only points of non-ignition are tested, therefore, referring to Figure 4.6, points 4, 6, 7 and 8 would be tested with 90 and 150 ms time delay.

Next, the inductance is changed. The MIKE 3 apparatus offers two settings for inductance, 0 mH or 1 mH. Inductance determines the spark duration, therefore, adding inductance causes the ignition energy to be released over a longer period of time. This normally increases the probability of an ignition. For the micron- and nano-titanium, inductance did not make a significant difference in MIE.

The MIE results are seen in section 5.2. For the micron-titanium MIE, tests are done using both inductance settings and all three time delays. For the nano-titanium MIE, only the 0 mH inductance and 1 mJ settings were used. This is the most sensitive setting the MIKE 3 apparatus can generate. No time delays were varied for the Nano-titanium due to the ignition at all concentrations using only one time delay (120 ms). For nano-titanium, concentrations above 900 mg were not attempted due to the severity of the explosion within the glass tube.

4.2.3 BAM Oven

The BAM oven is used to determine the MIT of a powder sample. Experimental testing using the BAM oven compares the effects of particle size on ignition temperature. Once the BAM oven is ready for testing, it is heated to 590 ºC for the micron titanium and to 300 ºC for the nano-titanium. When the proper starting temperature is reached, 1 ml of dust is measured and placed in the dispersion nozzle. The nozzle is then connected to the rubber bulb. Finally, the nozzle is placed in the oven inlet and the rubber bulb is squeezed to disperse the dust. Figure 3.4 demonstrates the configuration of the equipment.

Upon dispersion of the dust, a flame or explosion must be seen within five seconds of dispersion to be considered an ignition. If a flame is seen, the temperature is recorded and reduced by 10 ºC and then tested at the lower temperature.[41] The temperature is reduced until a non-ignition point occurs. The non-ignition point is then further tested with 0.5 ml and 2 ml of dust. If an explosion occurs, the temperature is reduced. If both volumes result in a non-ignition point, the MIT is recorded as the last ignition temperature.

CHAPTER 5: RESULTS

In this chapter the results for the explosion severity, explosion likelihood and dust inerting of nano-titanium are illustrated in graphical and tabular form. The complete numerical data can be found in Appendix C. Discussions of the results are found in chapter 6; explosion severity in section 6.1, explosion likelihood in section 6.2 and dust inerting in section 6.3.

5.1   Explosion Severity

The explosion severity, P_m and $(dP/dt)_m$, for the micron- and nano-titanium samples are shown graphically in Figures 5.1 to 5.12. The effect of explosion severity between the micron-sizes and between the nano-sizes can both be seen as a function of concentration. It must be noted that the results for the explosion severity between micron- and nano-titanium cannot be directly compared as the explosions occur at different times during the dispersion sequence, at different locations within the equipment, and with different turbulence levels. The nano-titanium sample results are considered as a pseudo maximum pressure (P'_m) and a pseudo maximum rate of pressure rise ($(dP/dt)'_m$). Nano-titanium is very sensitive and the explosion is initiated prematurely upon dispersion. This is referred to as the pre-ignition of the nano-titanium. The pre-ignition phenomenon is discussed in greater detail in section 6.1.2. The full tabulated results of P_{max} and $(dP/dt)_{max}$ can be seen in Table 5.1 and P'_{max} and $(dP/dt)'_{max}$ can be seen in Table 5.2.
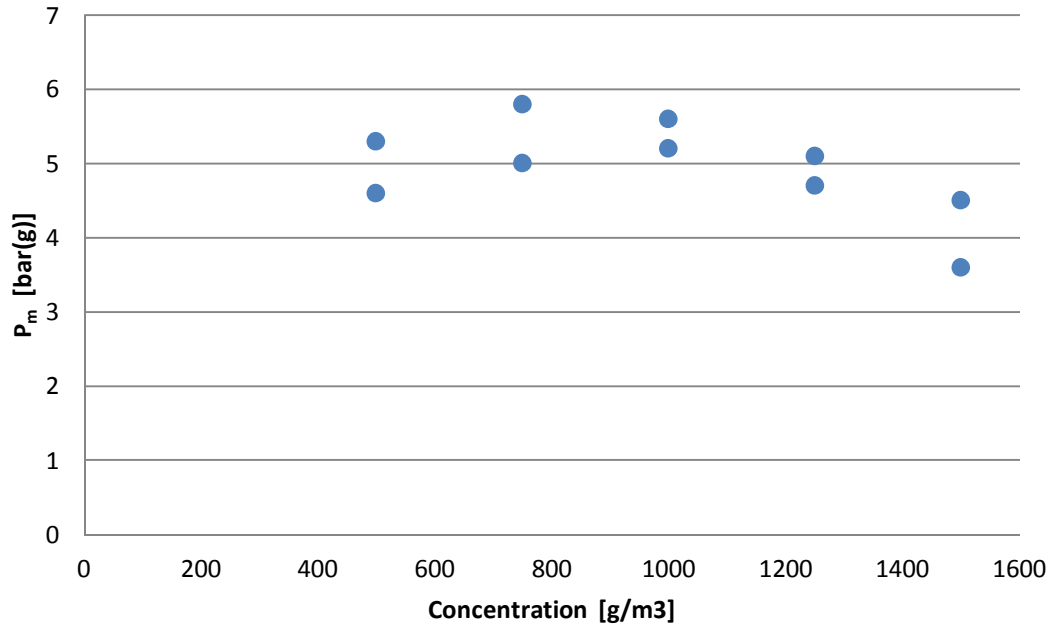
Figure 5.1   Effect of concentration on maximum pressure for -100 mesh titanium
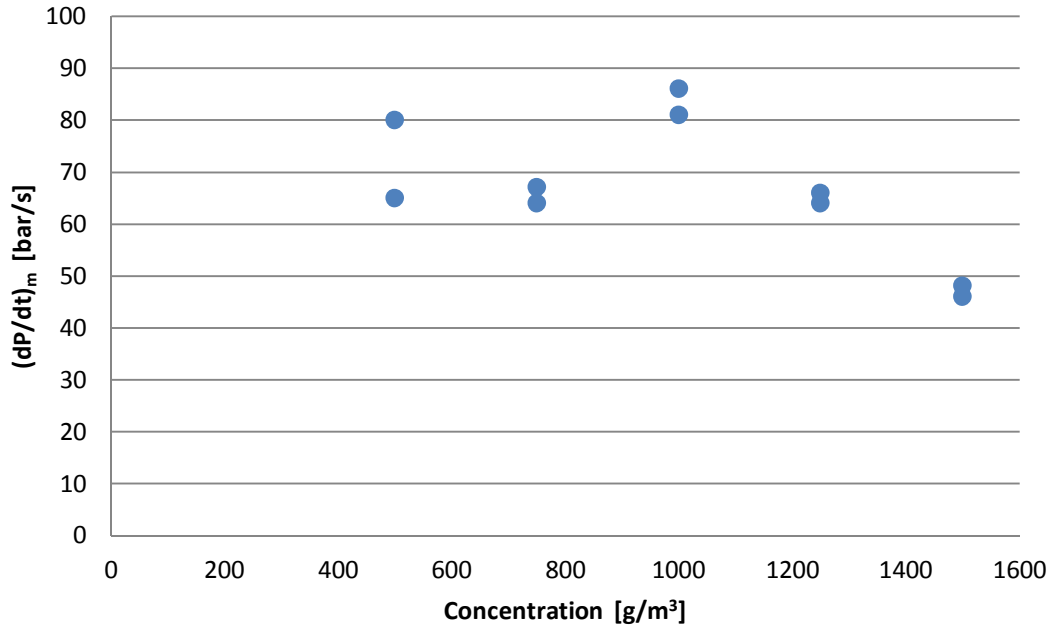
Figure 5.2   Effect of concentration on maximum rate of pressure rise for -100 mesh titanium
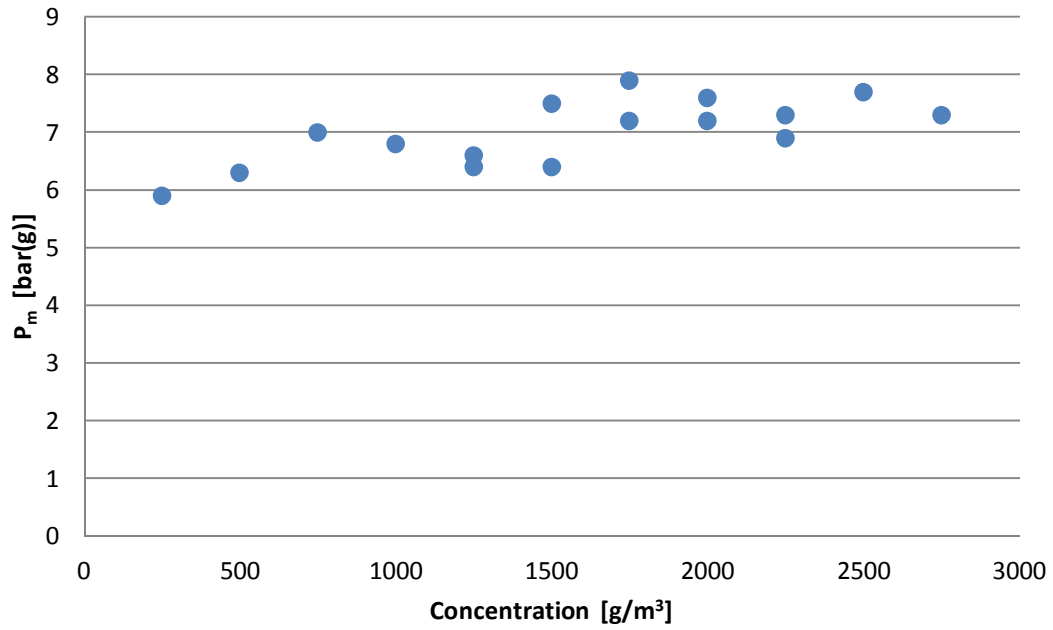
Figure 5.3   Effect of concentration on maximum pressure for -325 mesh titanium
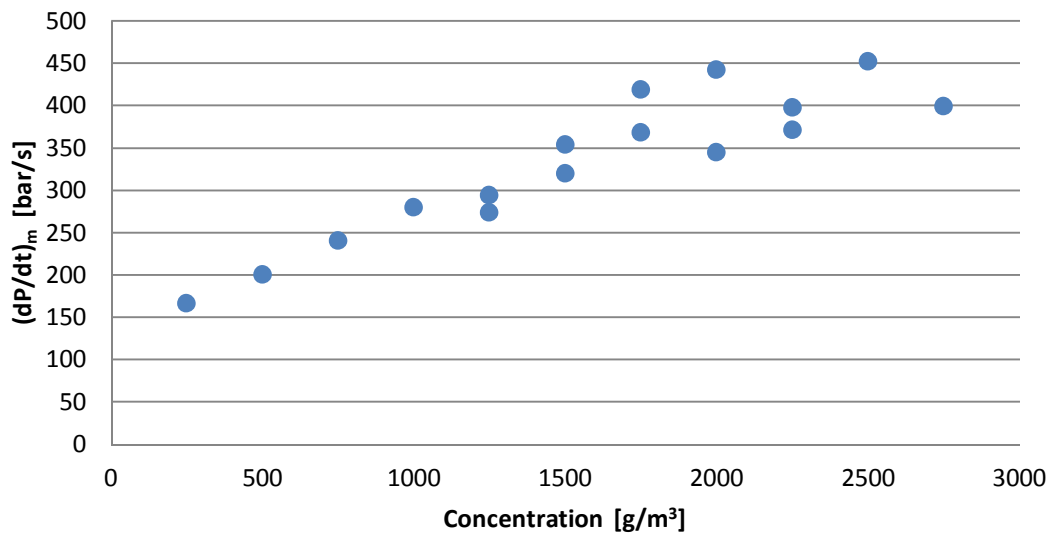
Figure 5.4   Effect of concentration on maximum rate of pressure rise for -325 mesh titanium
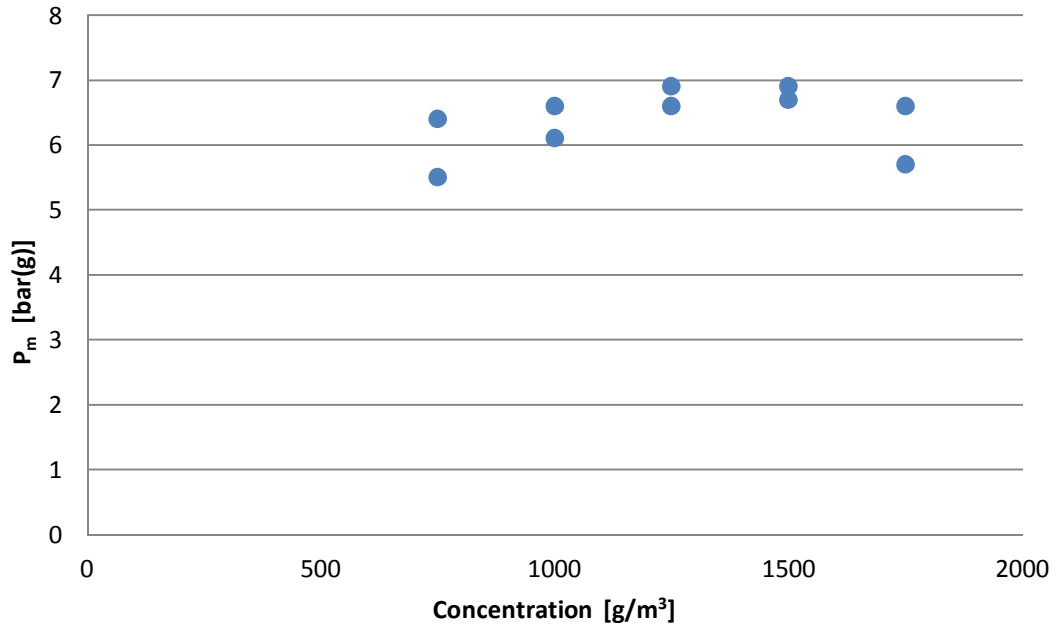
Figure 5.5 Effect of concentration on maximum pressure for ≤20 µm titanium
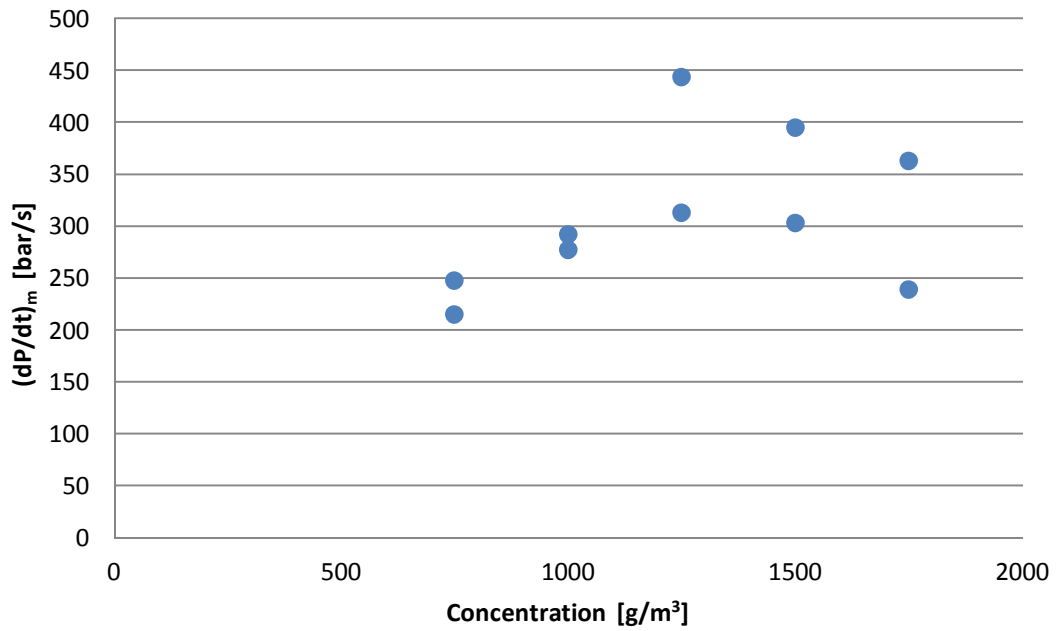
Figure 5.6 Effect of concentration on maximum rate of pressure rise for ≤20 µm titanium
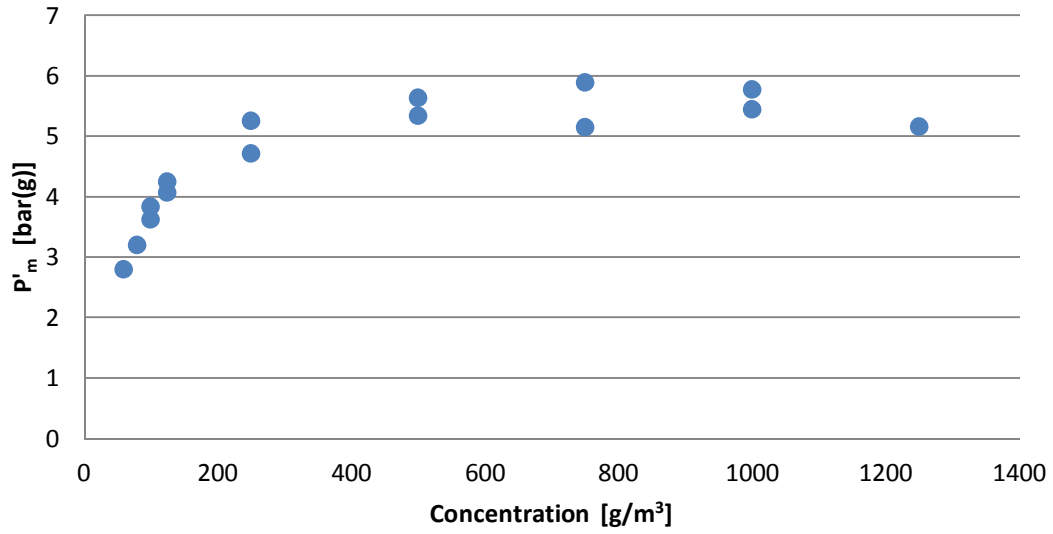
Figure 5.7   Effect of concentration on pseudo maximum pressure for 150 nm titanium
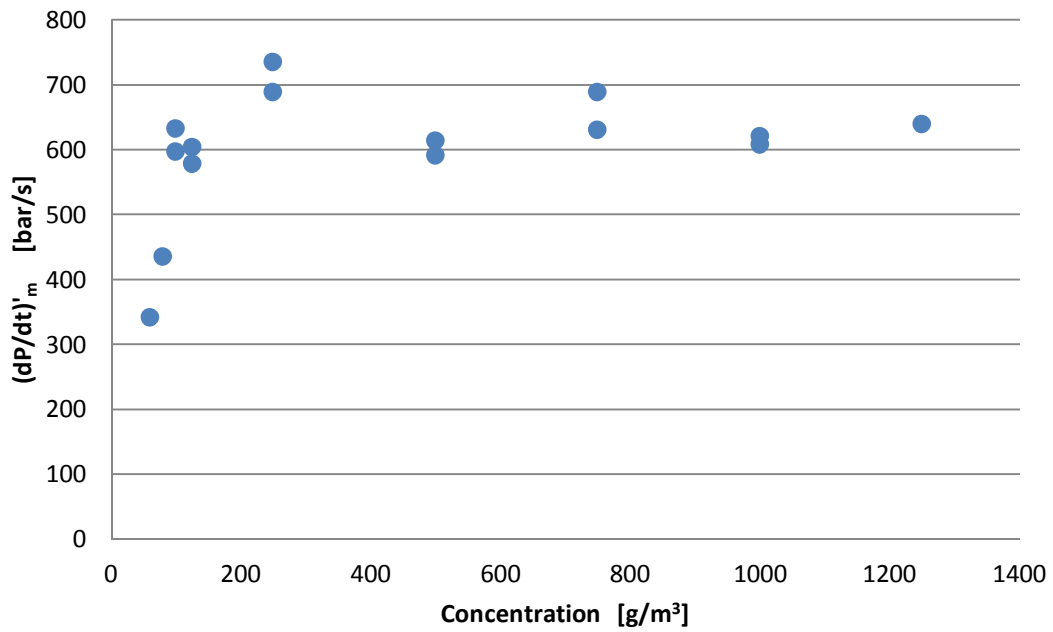
Figure 5.8   Effect of concentration on pseudo maximum rate of pressure rise for 150 nm titanium
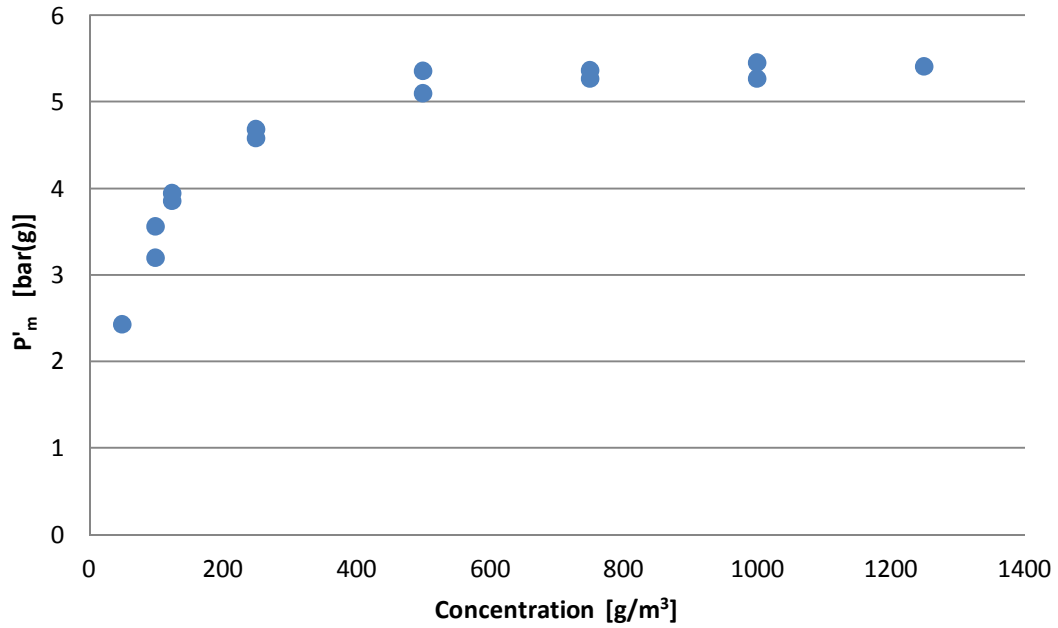
Figure 5.9   Effect of concentration on pseudo maximum pressure for 60-80 nm titanium
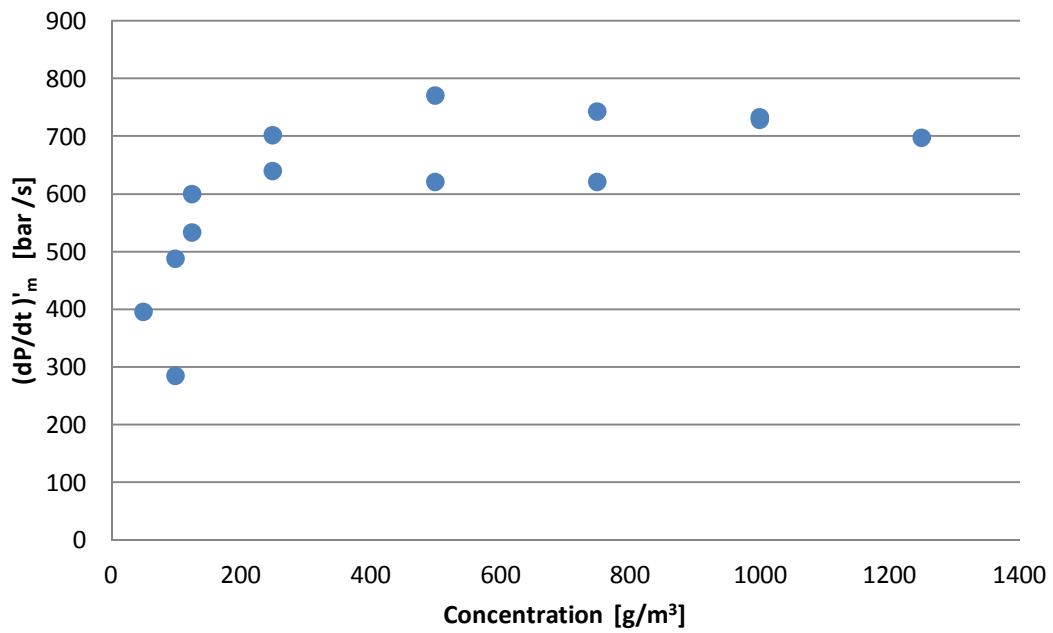
Figure 5.10   Effect of concentration on pseudo maximum rate of pressure rise for 60-80 nm titanium
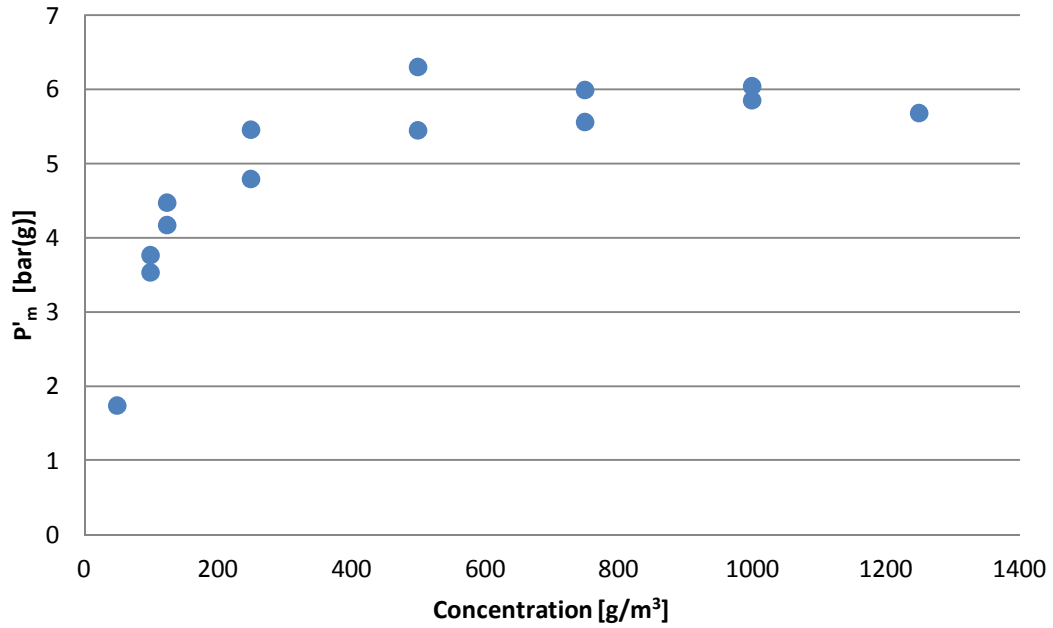
Figure 5.11　　Effect of concentration on pseudo maximum pressure for 40-60 nm titanium
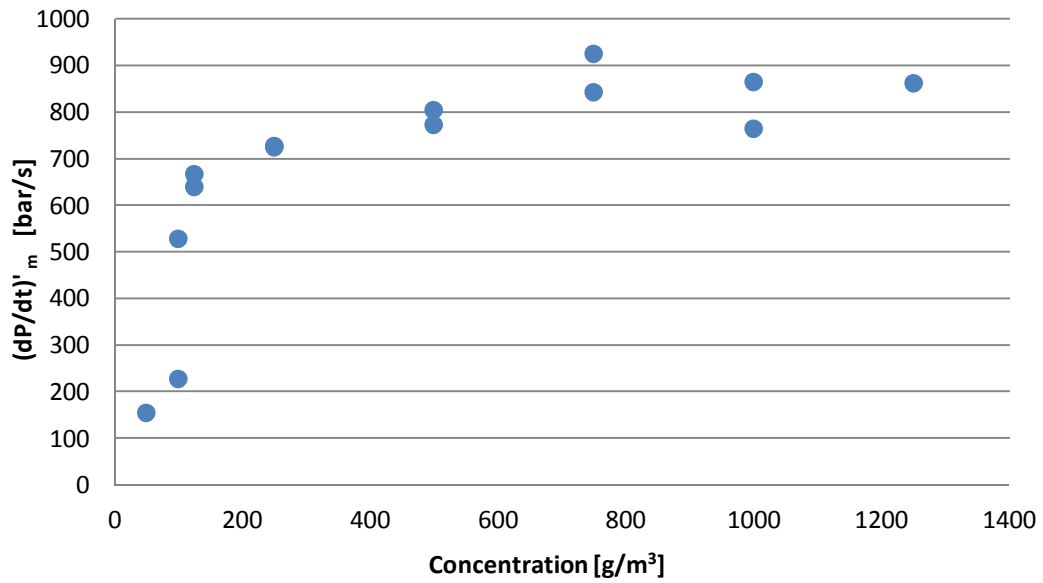
Figure 5.12　　Effect of concentration on pseudo maximum rate of pressure rise for 40-60 nm titanium

Table 5.1 Results for maximum pressure and maximum rate of pressure rise for micron-titanium samples

Titanium Sample	P_{max} [bar(g)]	$(dP/dt)_{max}$ [bar/s]
-100 Mesh	5.5	84
-325 Mesh	7.7	436
$\leq 20\ \mu m$	6.9	420

Table 5.2 Results for maximum pressure and maximum rate of pressure rise for nano-titanium samples

Titanium Sample	P'_{max} [bar(g)]	$(dP/dt)'_{max}$ [bar/s]
150 nm	5.7	713
60-80 nm	5.4	752
40-60 nm	6.1	884

5.2 Explosion Likelihood

The explosion likelihood of a dust is found using various experiments including minimum ignition energy (MIE), minimum explosible concentration (MEC), and minimum ignition temperature (MIT). MIE is seen for both micron- and nano-titanium in Figures 5.13 to 5.18. The ignition energy is plotted as a function of dust loading in mg. MEC is seen in Figures 5.19 to 5.24. Note the explosion criteria for both micron- and nano-titanium explosions previously described within this work. As explained in section 4.2.1.1 and 4.2.1.2, the explosion criteria are used to determine the lowest concentration at which an explosion occurs. MIE, MEC and MIT results are all included in Table 5.3.
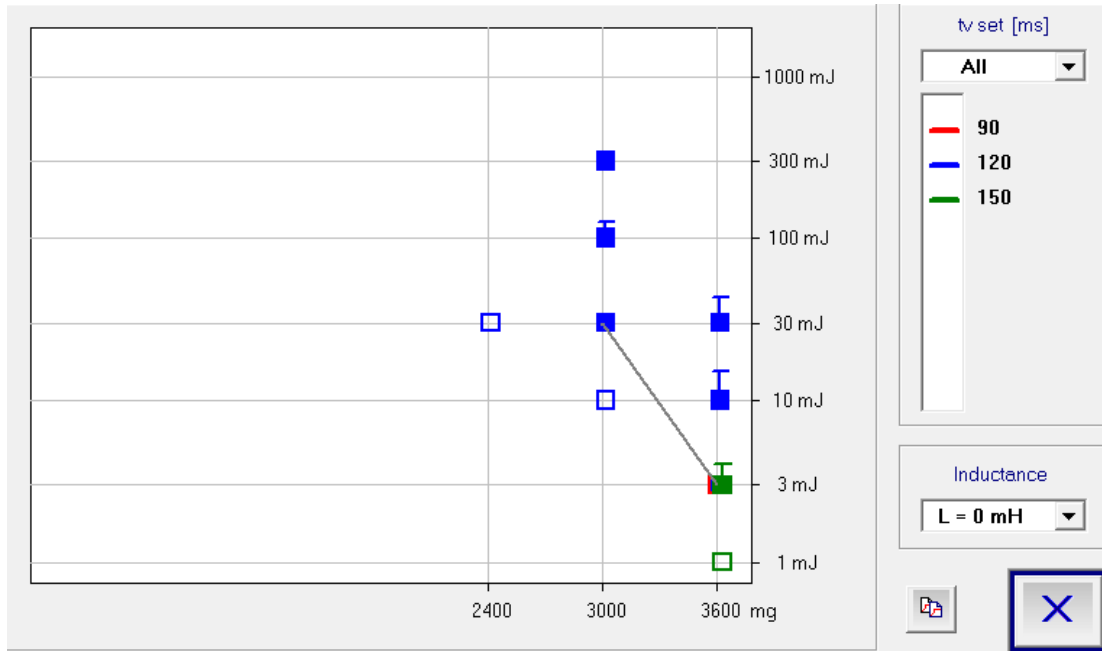
Figure 5.13   Influence of concentration on ignition energy of -100 mesh titanium
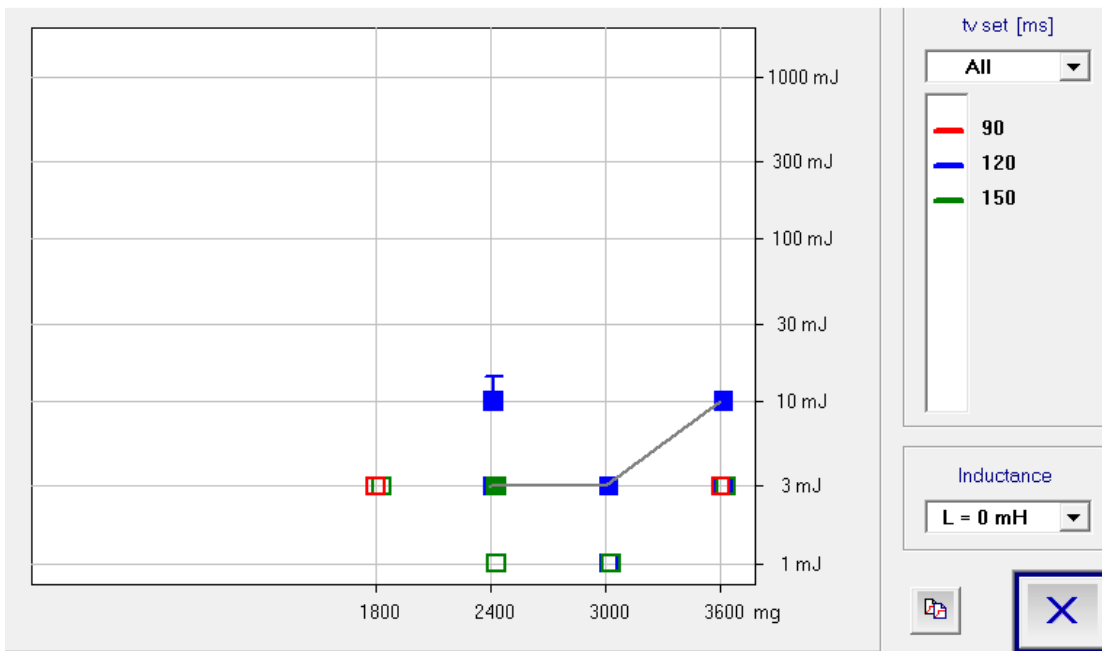
Figure 5.14   Influence of concentration on ignition energy of -325 mesh titanium
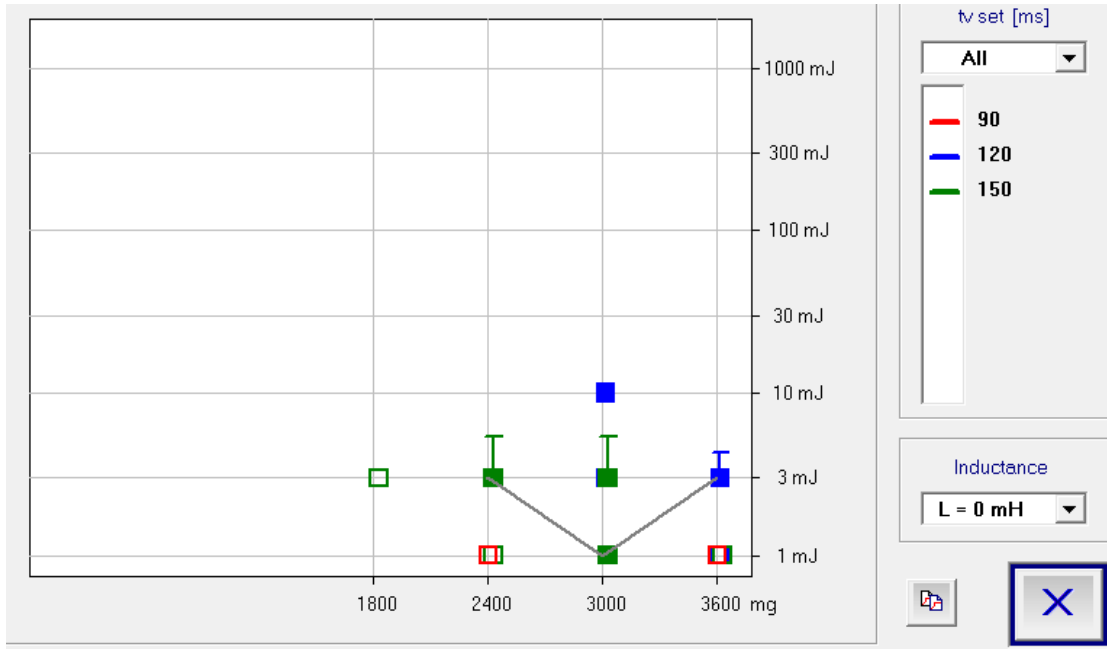
Figure 5.15   Influence of concentration on ignition energy of ≤20 µm titanium
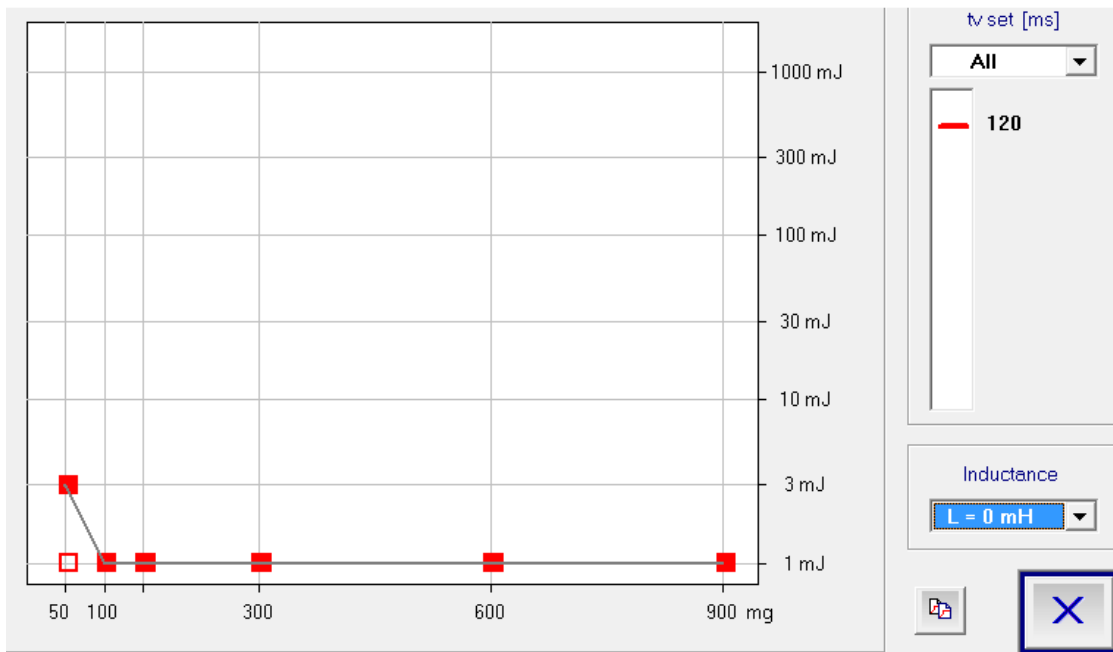
Figure 5.16   Influence of concentration on ignition energy of 150 nm titanium
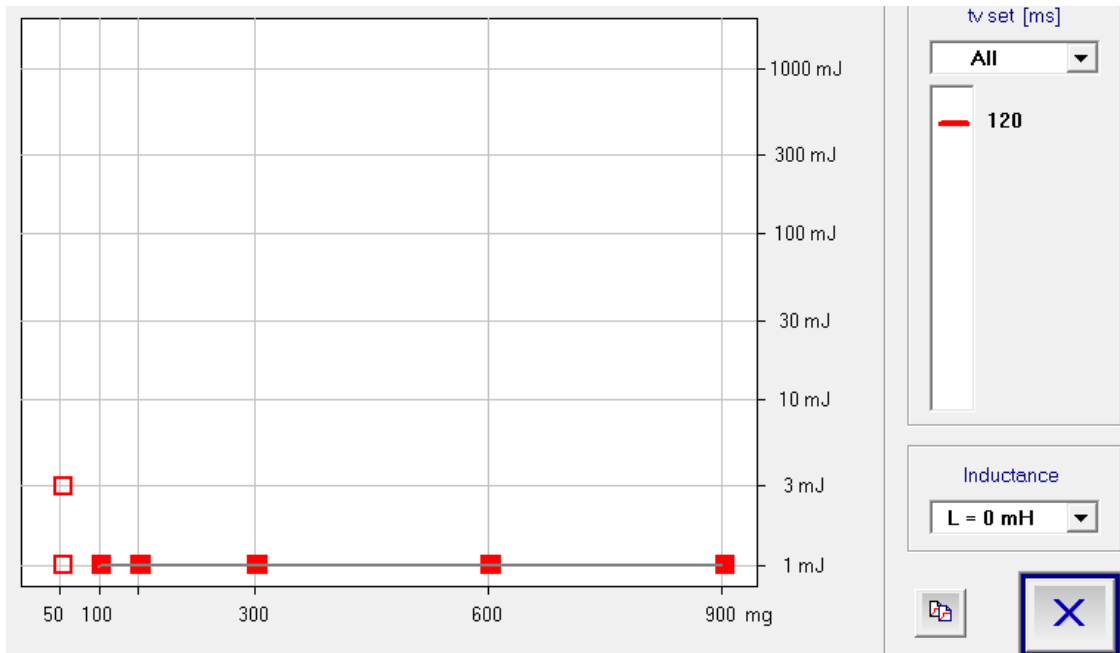
Figure 5.17   Influence of concentration on ignition energy of 60-80 nm titanium
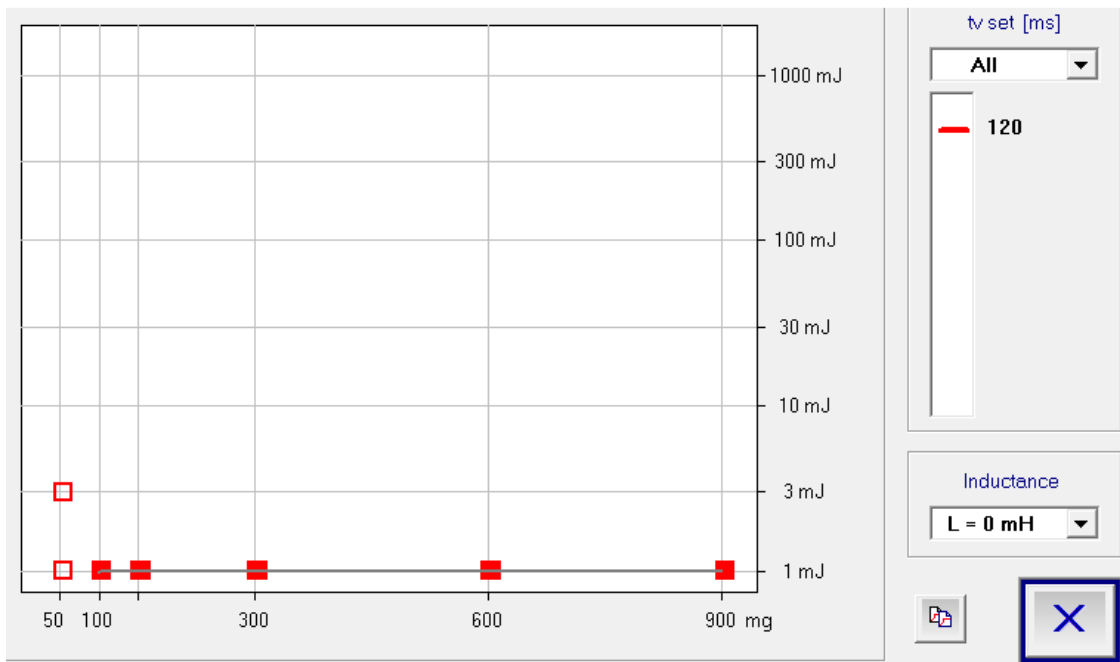
Figure 5.18   Influence of concentration on ignition energy of 40-60 nm titanium
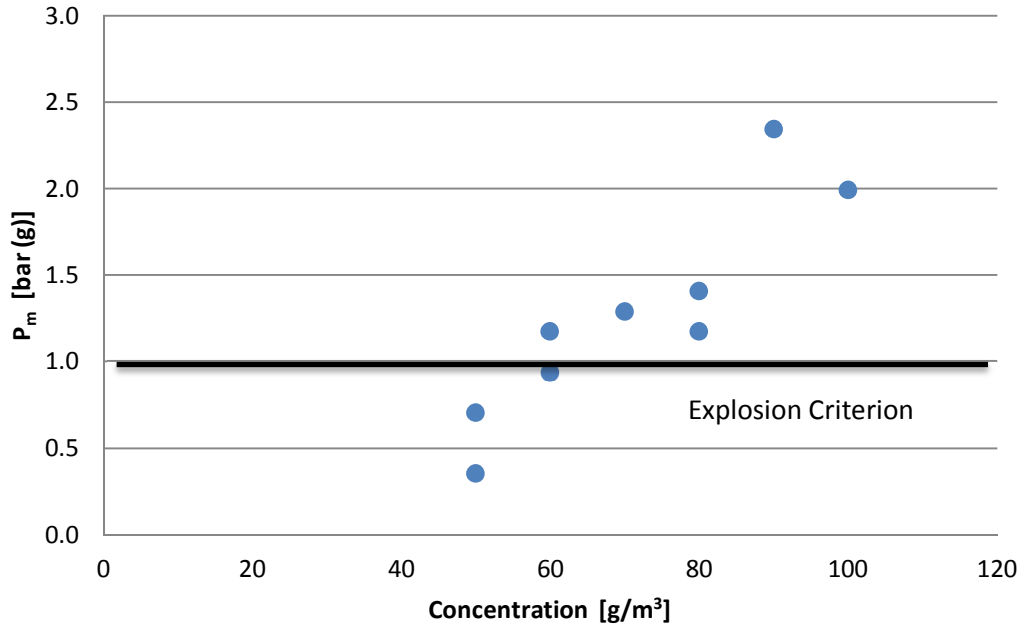
Figure 5.19   Minimum explosible concentration data for -100 mesh titanium
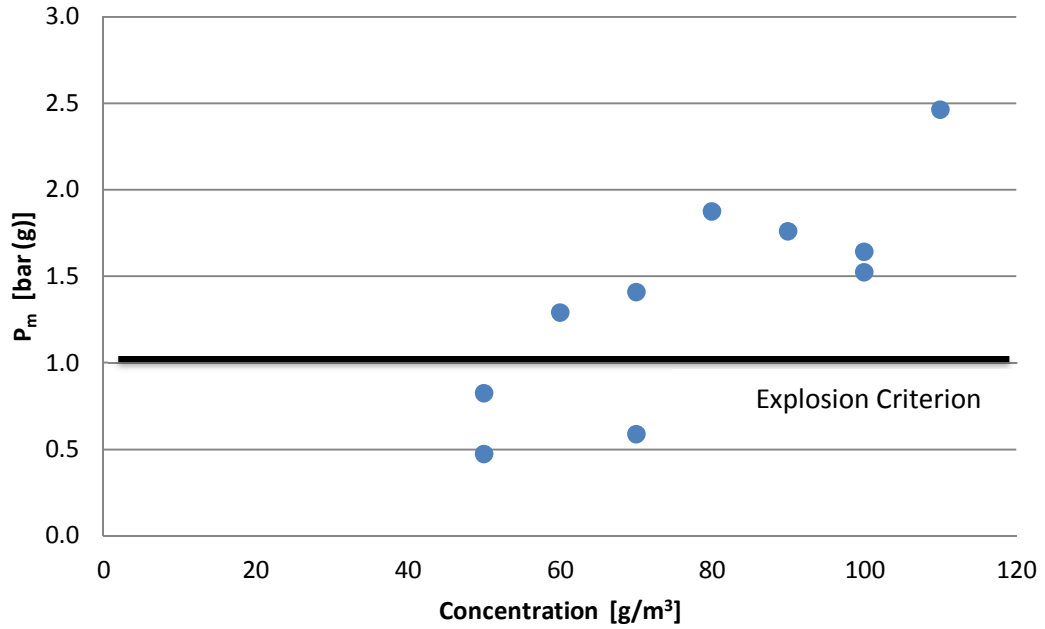
Figure 5.20   Minimum explosible concentration data for -325 mesh titanium
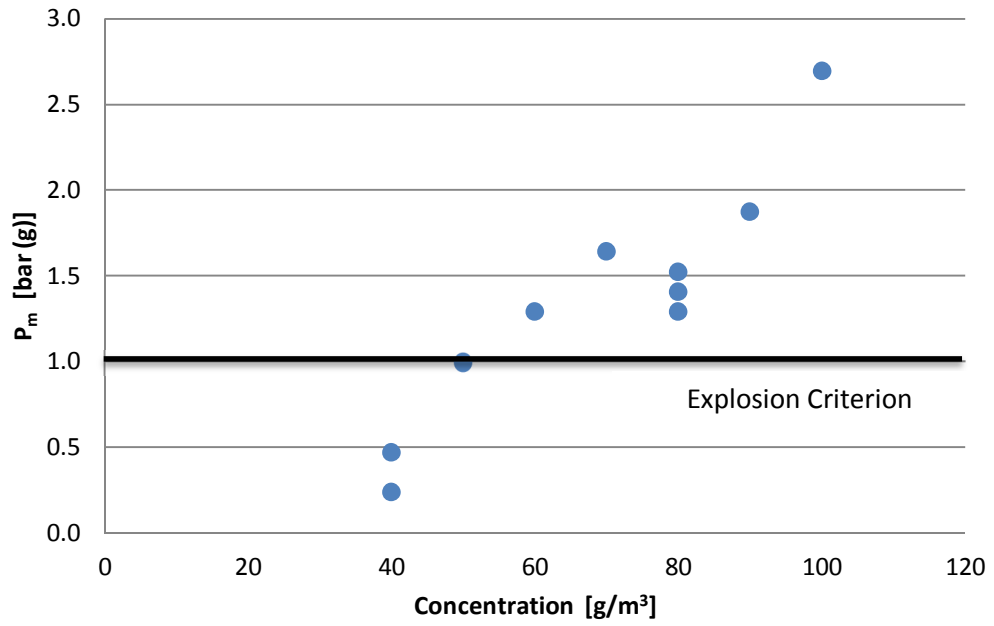
Figure 5.21   Minimum explosible concentration data for ≤20 µm titanium
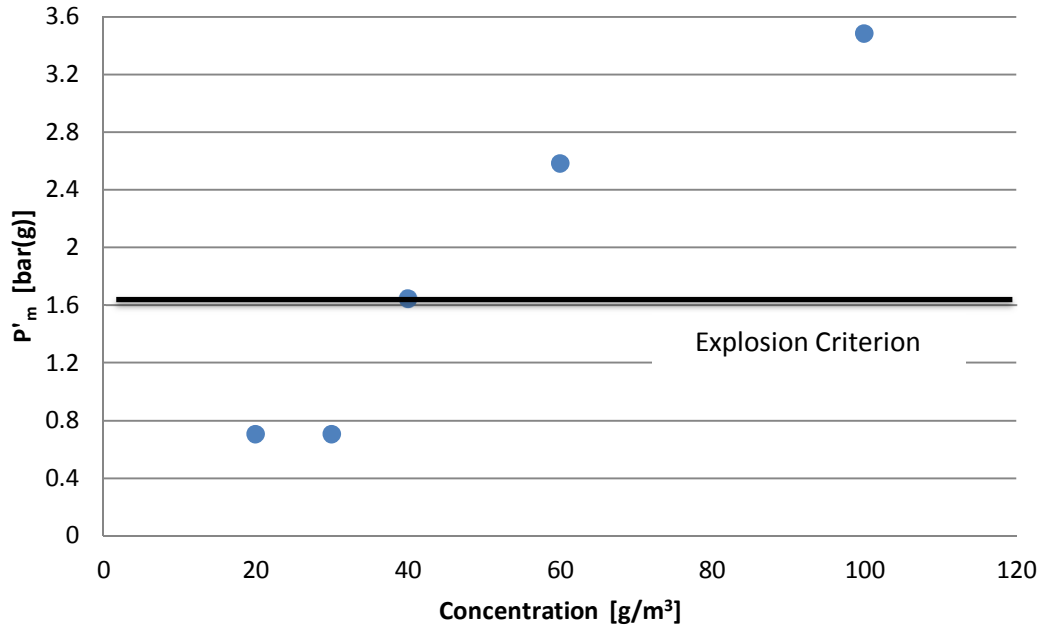
Figure 5.22   Minimum explosible concentration data for 150 nm titanium
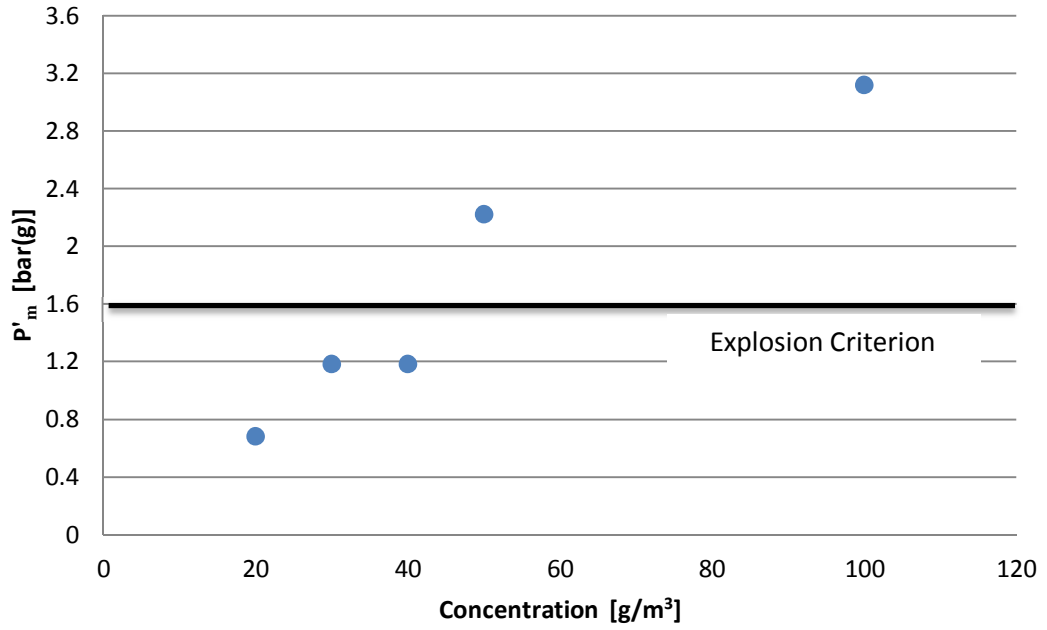
Figure 5.23   Minimum explosible concentration data for 60-80 nm titanium
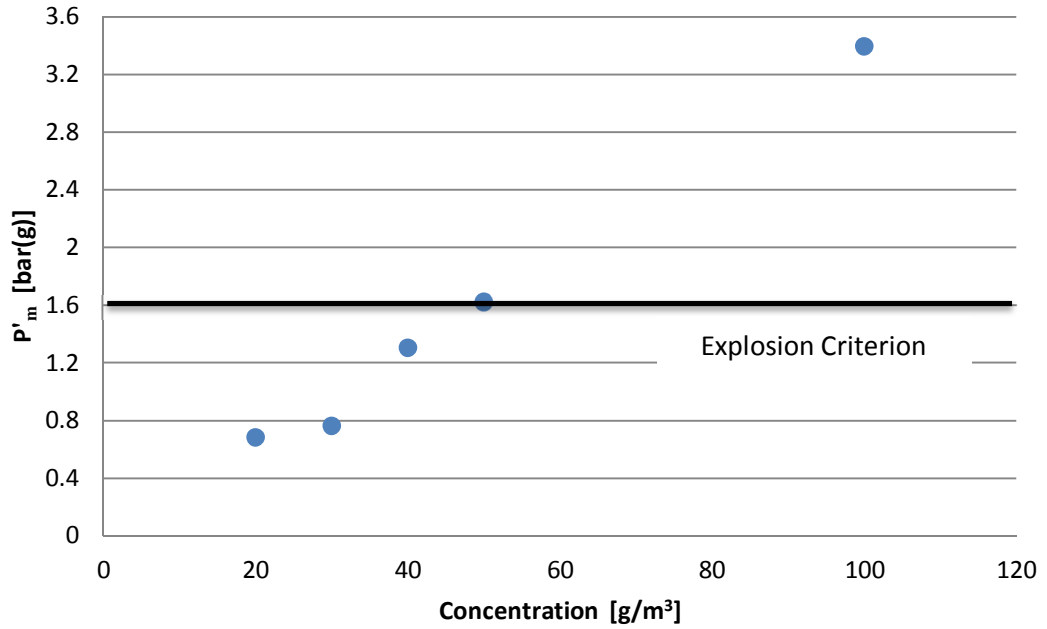
Figure 5.24   Minimum explosible concentration data for 40-60 nm titanium

Table 5.3   Explosion likelihood of micron- and nano-titanium

Titanium Sample	MIE [mJ]	MEC [g/m^3]	MIT [°C]	Comment
-100 Mesh	1-3	60	>590	MEC performed with 5kJ ignitor.
-325 Mesh	1-3	60	460	MEC performed with 5kJ ignitor.
$\leq 20\,\mu m$	<1	50	460	MEC performed with 5kJ ignitor. MIE less than 1mJ only at very high conc.
150 nm	<1	40	250	MEC performed without any energy source. MIE less than 1mJ at all conc.
60-80 nm	<1	50	240	MEC performed without any energy source. MIE less than 1mJ at all conc.
40-60 nm	<1	50	250	MEC performed without any energy source. MIE less than 1mJ at all conc.

5.3   Dust Inerting

Varied percentages of nano-titanium dioxide (TiO$_2$) are used in combination with nano-titanium to determine the dust inerting potential and the percentage of TiO$_2$ that works to suppress an explosion. Figures 5.25 to 5.30 show the inerting potential of nano-titanium dioxide with nano-titanium. Similar to an MEC test, the explosion pressure must be below the explosion criterion to be deemed inert. Figures 5.25, 5.27 and 5.29 show the explosion pressure for varying percentages of TiO$_2$. The corresponding values for the rate of pressure rise of the explosions are shown in Figures 5.26, 5.28 and 5.30 for the different percentages of TiO$_2$.
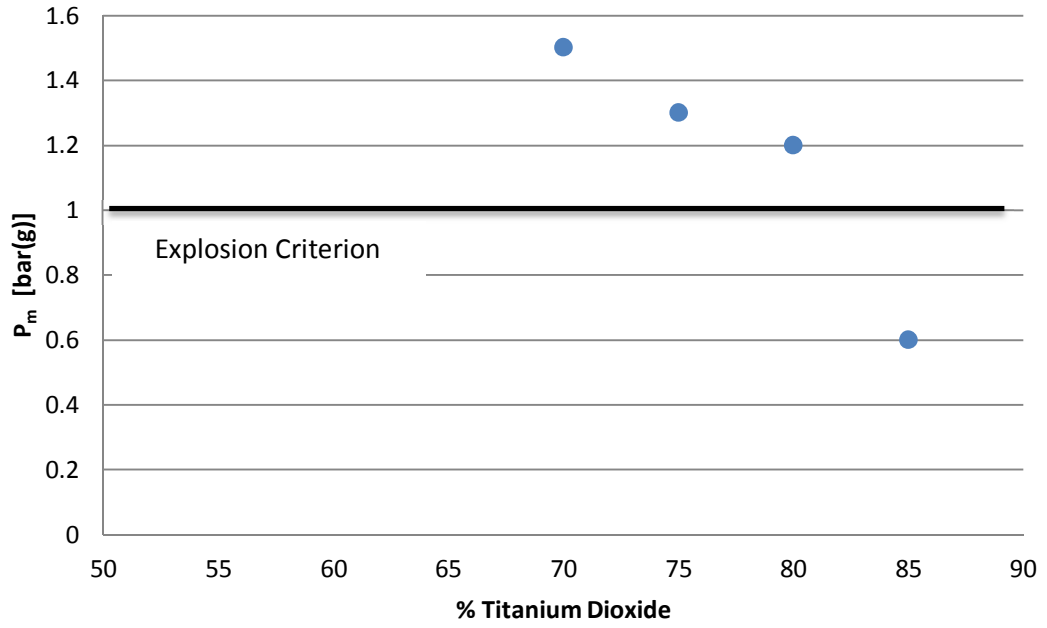
Figure 5.25   Influence of TiO$_2$ on the maximum pressure of 150 nm titanium
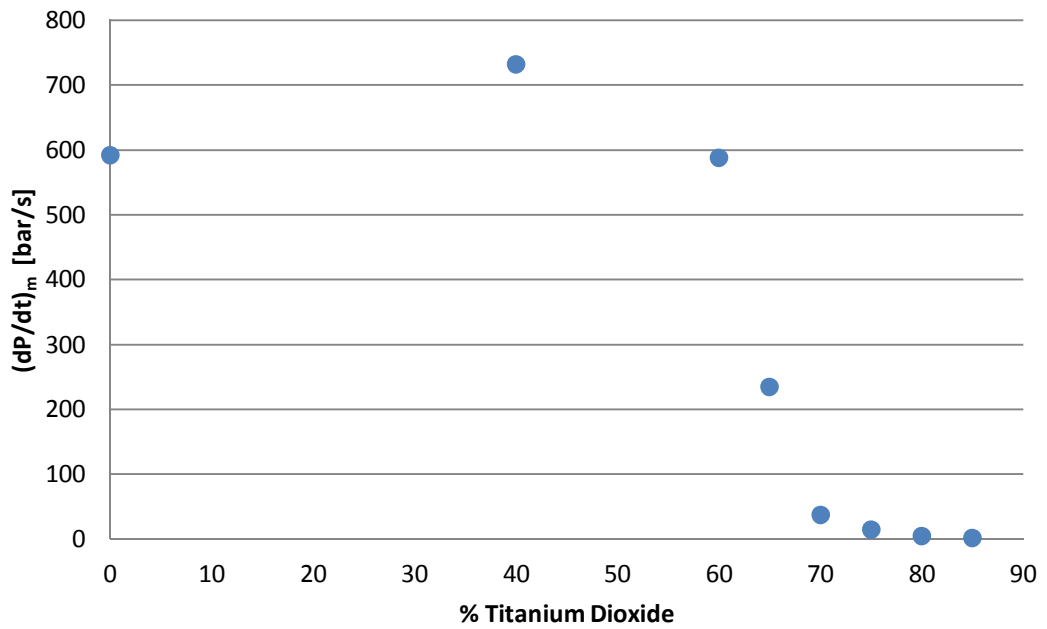
Figure 5.26   Influence of TiO$_2$ on the maximum rate of pressure rise for 150 nm titanium
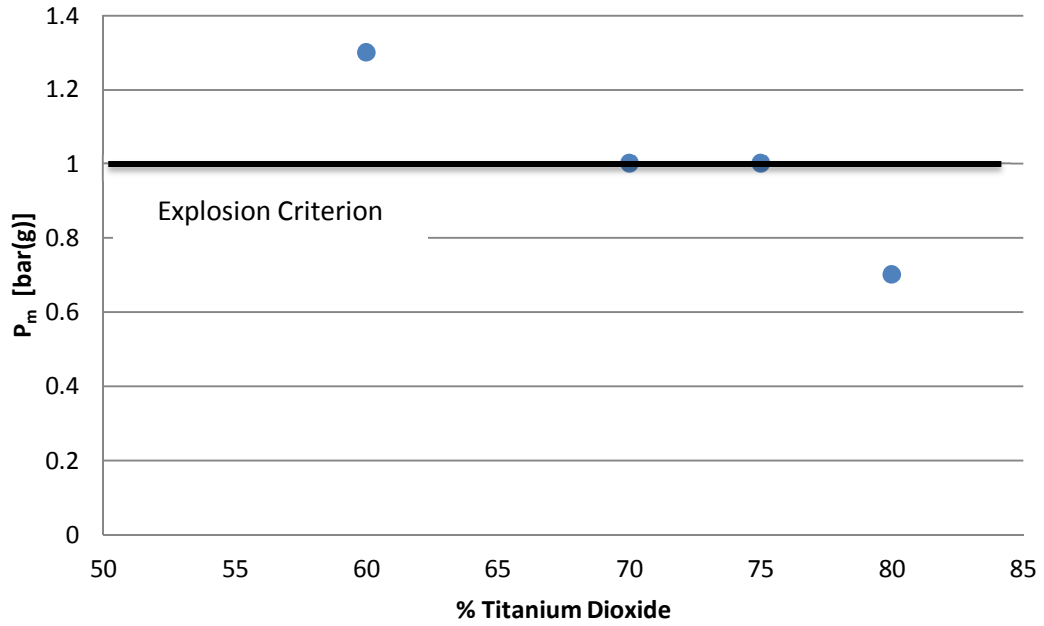
Figure 5.27   Influence of TiO₂ on the maximum pressure of 60-80 nm titanium
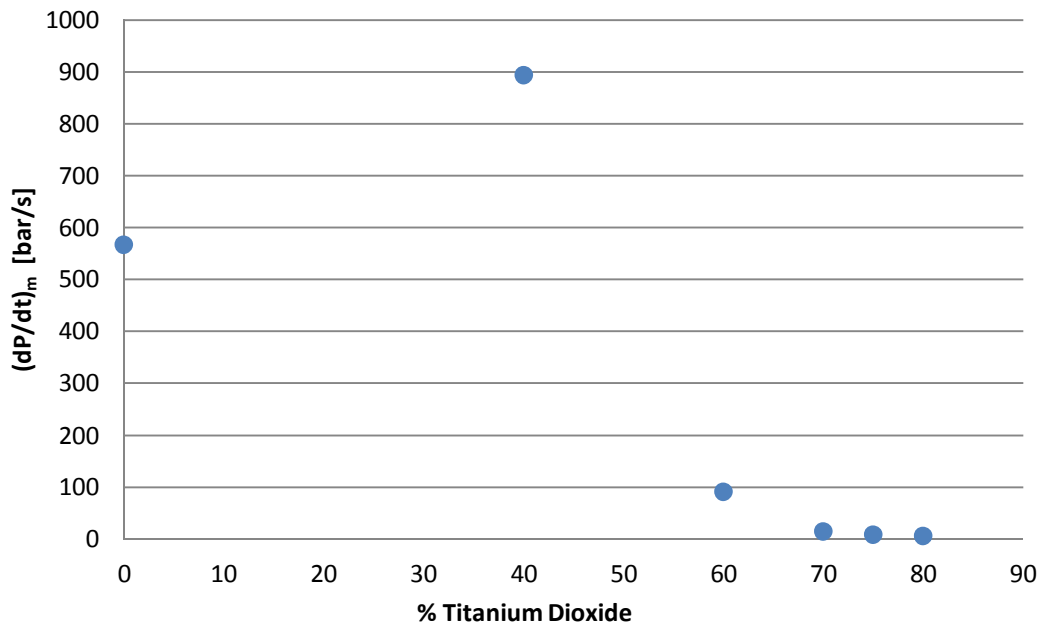
Figure 5.28   Influence of TiO₂ on the maximum rate of pressure rise for 60-80 nm titanium
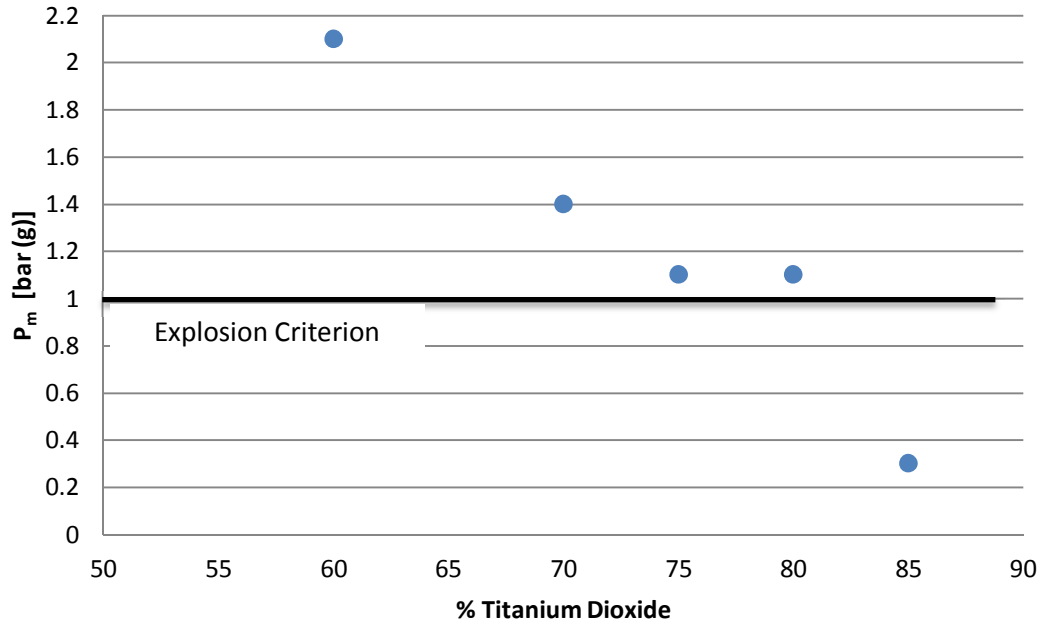
Figure 5.29   Influence of TiO$_2$ on the maximum pressure of 40-60 nm titanium
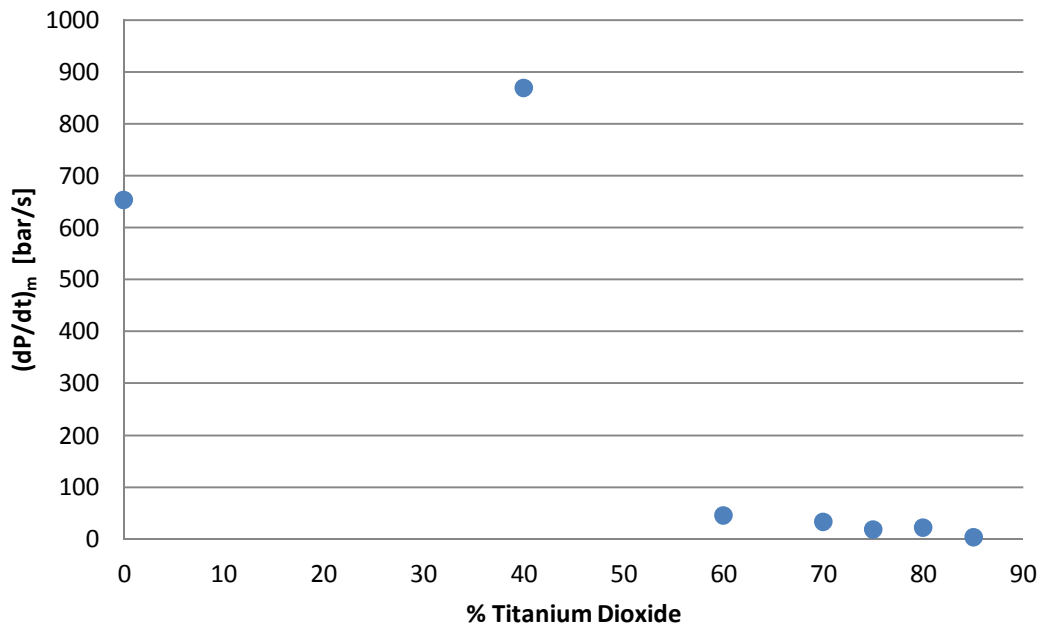
Figure 5.30   Influence of TiO$_2$ on the maximum rate of pressure rise for 40-60 nm titanium

CHAPTER 6: DISCUSSION

This chapter discusses and compares the results obtained during the experimental testing of micron- and nano-titanium dust. The explosion severity, explosion likelihood and dust inerting results, as well as the experimental challenges, are discussed for the experimental work.

6.1   Explosion Severity

The effects of explosion severity for micron- and nano-titanium are investigated using the Siwek 20-L chamber. Maximum pressure and maximum rate of pressure rise are compared between the different micron sizes and again between the different nano-sizes. The reactions and products resulting from the explosions are also discussed.

6.1.1   Micron-Titanium

Titanium results demonstrated strong overpressure and rate of pressure rise at the micron level between 150 µm and 1 µm. Three different micron-titanium samples are tested with their particle size as follows: -100 mesh (<150 µm), -325 mesh (<45 µm) and ≤20 µm.

The overpressure (P_m) and rate of pressure rise $(dP/dt)_m$ for the micron-titanium can be seen in Figures 6.1 and 6.2. The -100 mesh sample contains the largest particle sizes and, as a result, P_m and $(dP/dt)_m$ have the lowest value. As the particle size decreases to -325 mesh, there is a substantial increase in both P_m and $(dP/dt)_m$. However, when the particle size is further reduced to ≤20 µm, a slight decrease is seen in P_m and $(dP/dt)_m$. P_{max} and $(dP/dt)_{max}$ values are shown in Table 5.1. The decrease in severity between the ≤20 µm and -325 mesh titanium may be limited by particle agglomeration effects (recall the earlier discussion on sample particle size distributions, section 1.1.3).
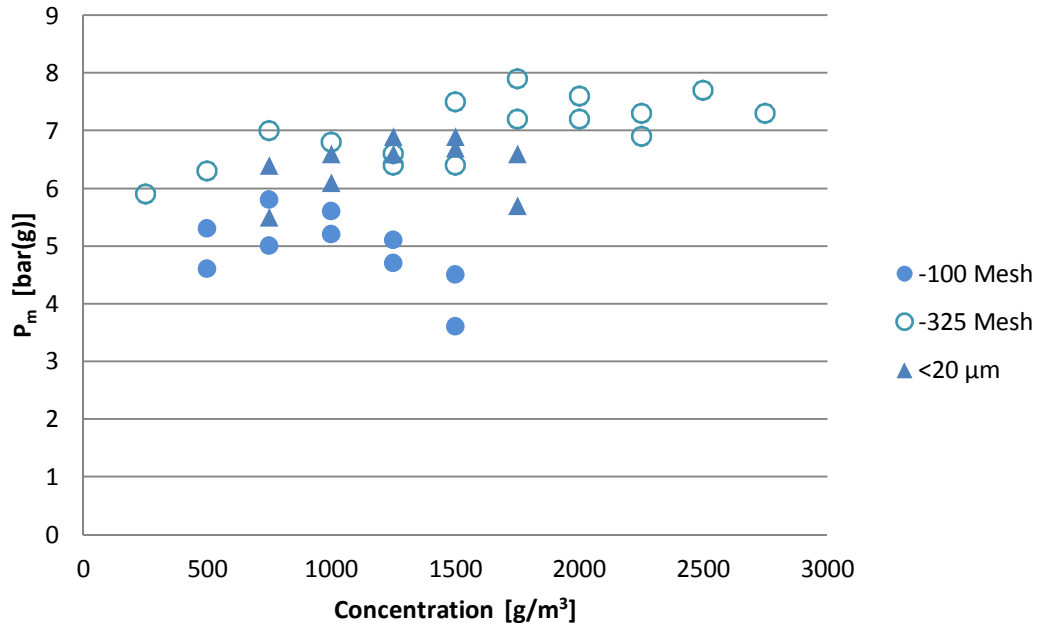
Figure 6.1   Influence of concentration on maximum pressure for micron-titanium
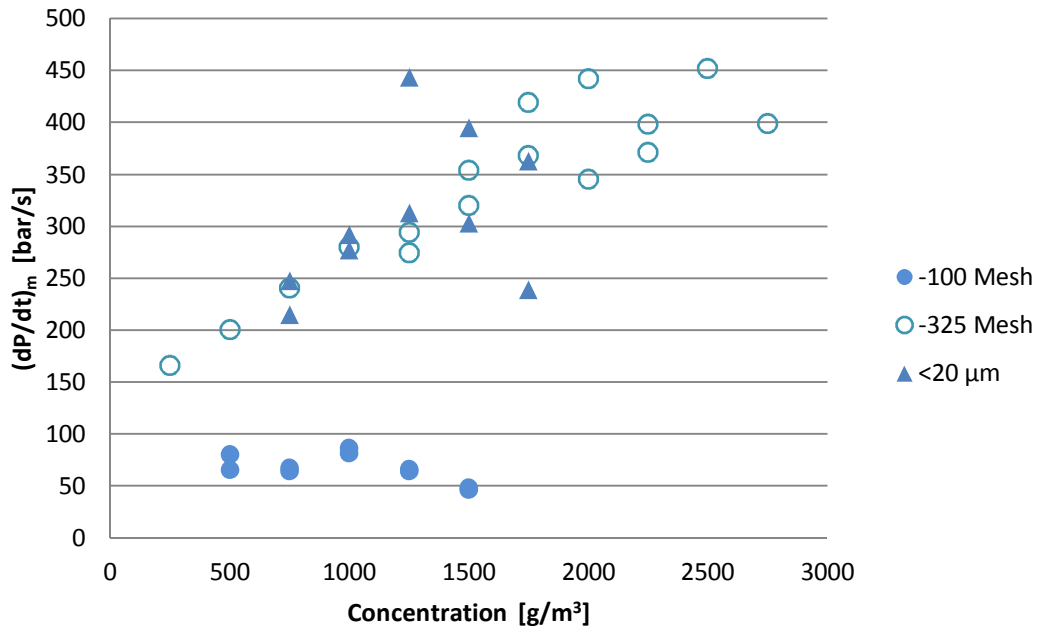
Figure 6.2   Influence of concentration on maximum rate of pressure rise for micron-titanium

67

6.1.2 Nano-Titanium

It is difficult to provide a direct comparison of explosion severity between the micron- and nano-titanium due to the pre-ignition of nano-dust. Frictional or static sparking during the dispersion sequence ignites the dust before the chemical ignitors are fired. As previously described, nitrogen is used as the dispersing gas to prevent an explosion in the external dispersion reservoir; however, when the nano-titanium/nitrogen mixture encounters the elevated oxygen concentration in the 20-L chamber (see earlier discussion on this point), immediate ignition of the dust occurs.

Consistent with the above discussion, Figure 6.3 shows a 40-60 nm titanium explosion at a dust concentration of 100 g/m^3. Here, one sees an overlap of the dust dispersion and explosion steps, with the ignitors firing after the dust has exploded. The pressure values in Figure 6.3 must be interpreted in light of the fact that piezoelectric pressure transducers are used and hence, only measure dynamic pressure changes, not static values.
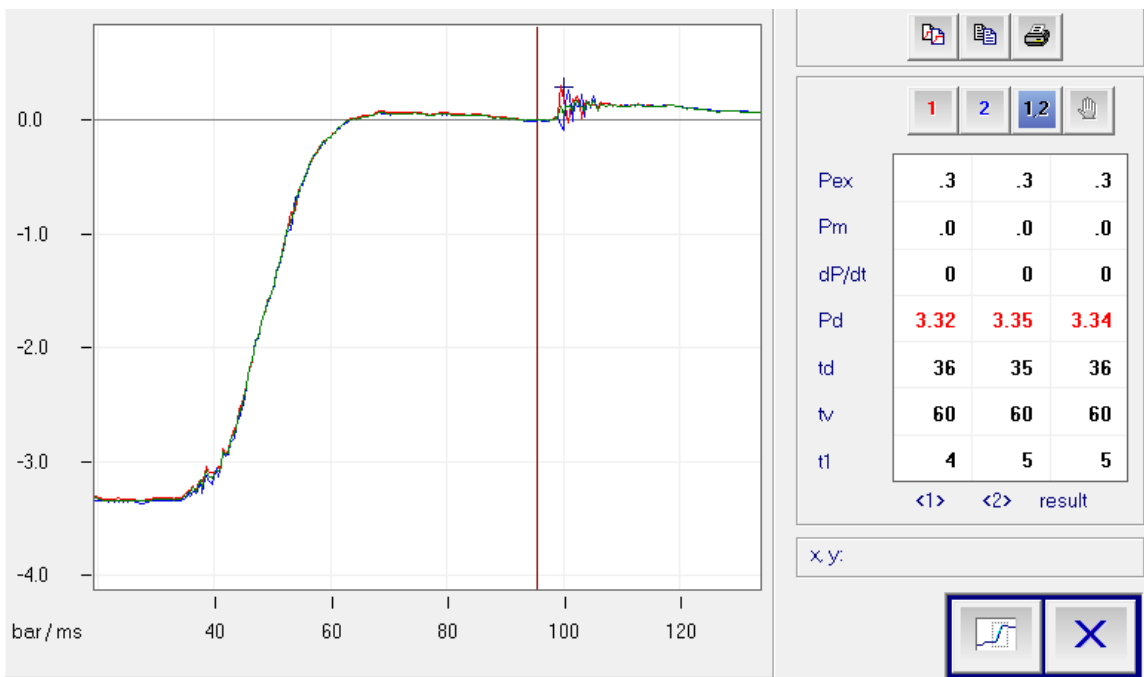
Figure 6.3   Explosion curve given by Kühner software for 150 nm titanium

The pre-ignition of the nano-titanium causes all the dust to be consumed and prevents a proper evaluation of the maximum explosion pressure. The maximum rate of pressure rise is estimated by a manual evaluation of the pressure/time trace. The explosion is violent and causes complete combustion – again, even before the chemical ignitors are activated.

All subsequent trials of this type involving nano-titanium are performed without ignitors; results similar to those shown in Figure 6.3 are obtained. Because of the pre-ignition phenomenon, typical $P_{max}/(dP/dt)_{max}$ testing is simply not possible with nano-titanium. Estimates of the maximum explosion pressure and maximum rate of pressure rise are obtained from the pre-ignition phase of the pressure/time trace (the region to the left of the vertical line at 96 ms in Figure 6.3). It is particularly noteworthy that these explosibility parameters arise from an explosion scenario *with no external ignition source* (i.e., no chemical ignitors as per typical Siwek 20-L chamber testing).

Figure 6.4 gives the maximum rate of pressure rise data acquired. For all nano-sizes, a quasi-plateau in the rate of pressure rise occurred at low concentrations. At approximately 125 g/m^3, the maximum rate of pressure rise for all three nano-sizes is between 600 - 700 bar/s. The maximum rate of pressure rise occurs at concentrations near 500 - 750 g/m^3. Micron-size titanium did not reach its maximum rate of pressure rise until concentrations in the vicinity of 1500 g/m^3. Consequently, very severe explosions with nano-titanium are seen with lower concentrations than the typical micron-titanium powders.

The maximum rate of pressure rise is obtained using two different methods. First, a manual trace is done using the Kühner software, KSEP 6.0f. This method can give a wide variation of results and is very user dependent. Another method is to use KSEP 7.0 and export the data into tabular form. The data is then imported into a program such as Microsoft Excel and the maximum rate of pressure rise is illustrated graphically. Results seen in Figure 6.4 are given by KSEP 7.0 through the use of Microsoft Excel.
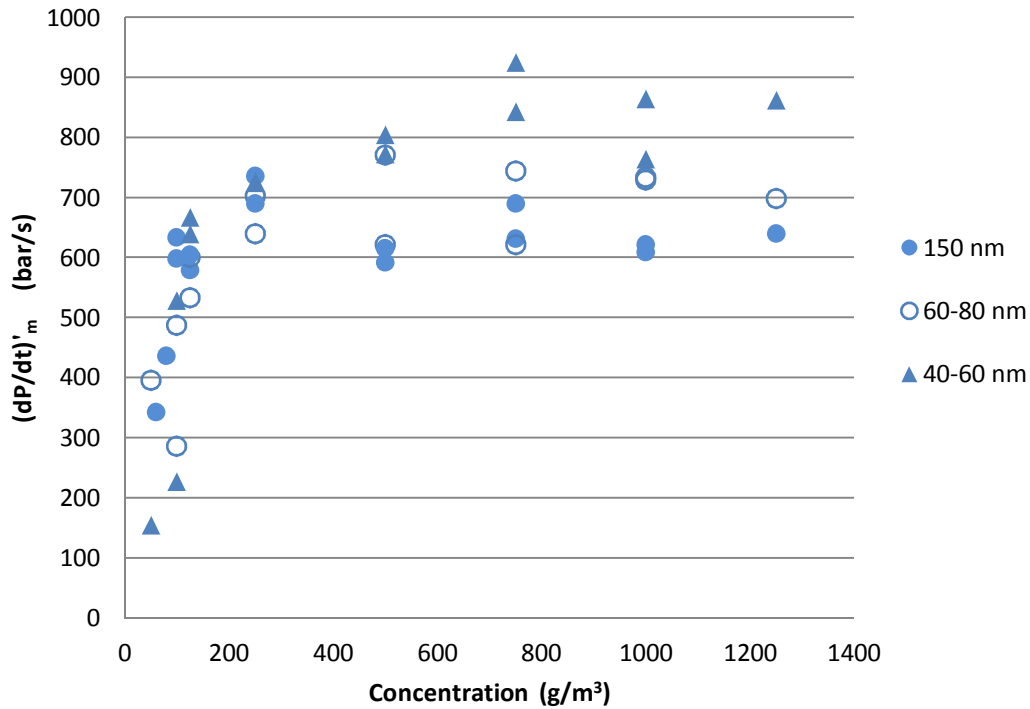
Figure 6.4   Pseudo rate of pressure rise for nano-sized titanium

Maximum explosion pressure can be estimated for the nano-titanium samples using two different methods. The first is to use the P_d value as an estimate by the Kühner KSEP 6.0f software. As per the usual 20-L chamber procedures, the chamber is partially evacuated to 0.4 bar(a) so the resulting chamber pressure upon dust dispersion and at the time of ignition (chemical ignitor firing) is at approximately 1 bar(a). The parameter P_d in the Kühner software reports the rise in pressure in the 20-L chamber due to dust dispersion. Acceptable values of P_d are in the range of 0.55 – 0.7 bar. This means that when the value of P_d is added to the initial chamber pressure of 0.4 bar, the sum is approximately 1 bar.

Recalling that the piezoelectric pressure transducers measure only dynamic pressure changes (i.e., not static pressures), P_d values as shown in Figure 6.3 are a combination of the pressure rise due to dust dispersion and the explosion itself. The nano-size P_d results are therefore not directly comparable to the micon-size P_{max} results. They are, however, self-consistent as a data set, shown in Figure 6.5. Using the P_d to report P_m does not include values that exceed the 0 bar horizontal line seen in Figure 6.6. At lower

70

concentrations, the pressure trace does not exceed the 0 bar horizontal but as concentrations increase, the pressure surpasses this line.
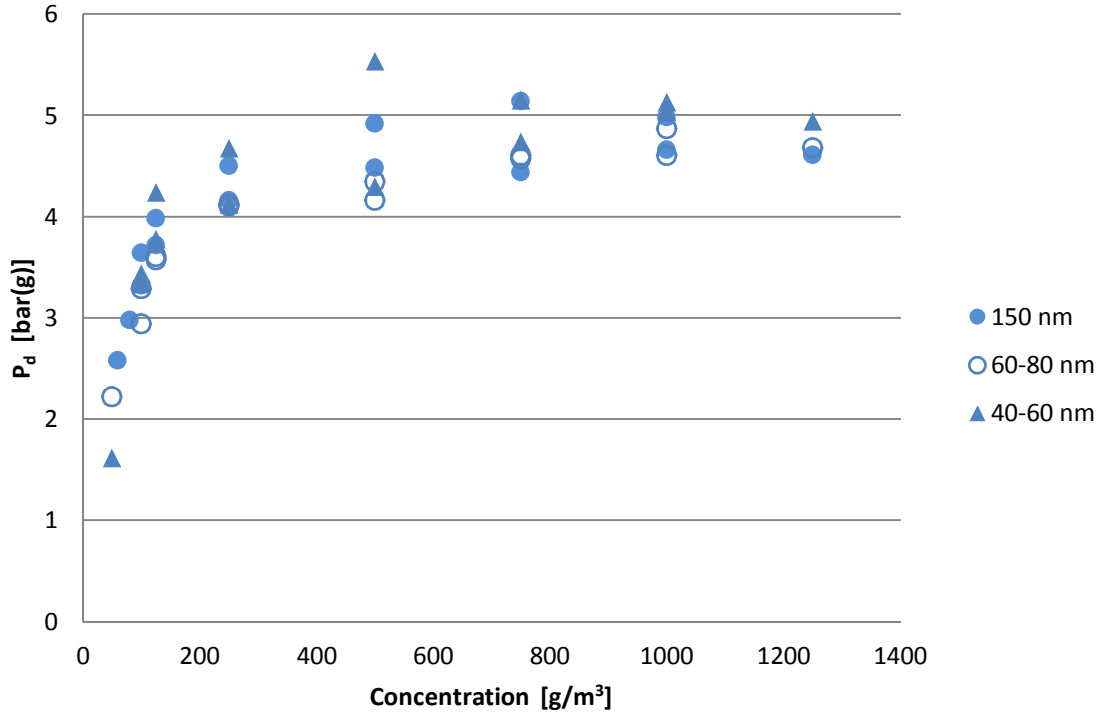
Figure 6.5   Nano-titanium pseudo maximum pressure estimation using the P_d value
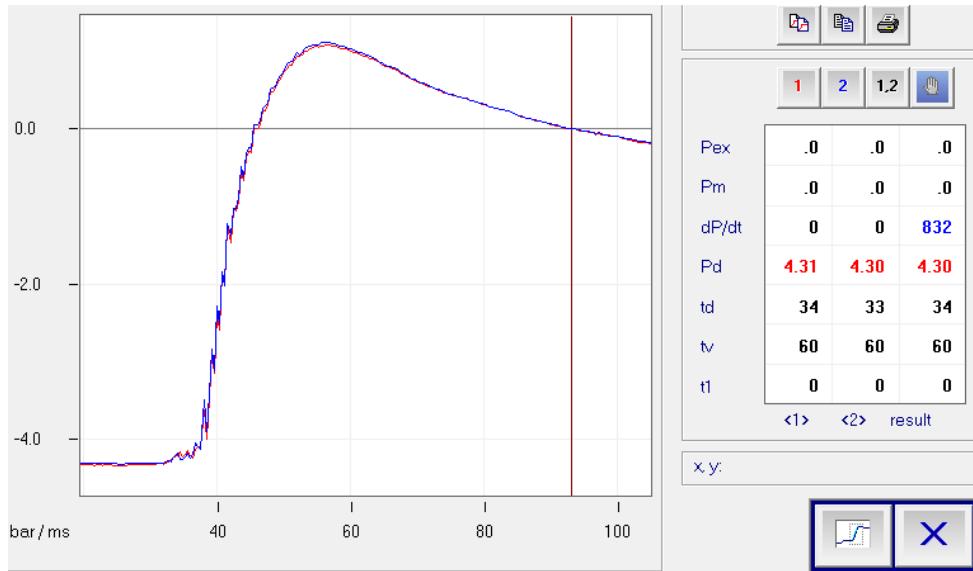
Figure 6.6   Explosion curve given by Kühner software for 40-60 nm titanium

A second method is used to determine the maximum pressure. This involves using KSEP 7.0. From this version of the software, data obtained from the Siwek 20-L chamber is transferred into tabular form with time and pressure measurements recorded from both pressure transducers. From this table, the starting P_d value (pressure before the explosion) and the maximum pressure from the explosion are found and a more precise P'_{max} can be calculated. Note that this calculated P'_{max} is more accurate than the P_d value but cannot be compared to micron-titanium P_{max} values. These results can be seen in Figure 6.7.

Similar to the case for rate of pressure rise, nano-titanium reaches its highest values of 'maximum explosion pressure' at lower concentrations than the micron-titanium, which again required dust concentrations of approximately 1500 g/m^3.
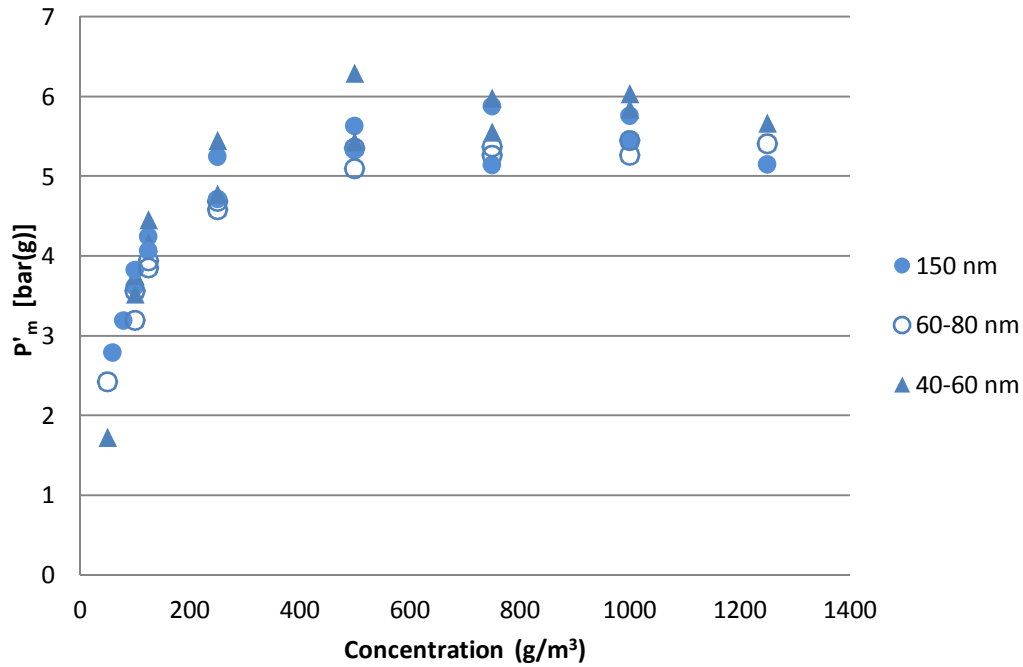
Figure 6.7   Nano-titanium pseudo maximum pressure (P'_{max})

6.1.3   Explosion Reaction

The surface area of a particle plays a major role in the combustion of different sized titanium samples studied within this work. At the micron-scale, larger amounts of dust are required to achieve the same effective surface area as a small mass of nano-titanium. For complete combustion of all the oxygen in the 20-L chamber, high concentrations of micron-size titanium are needed. In contrast, much smaller amounts of nano-titanium are required to react with the same amount of oxygen. Nano-size titanium is highly reactive at very low concentrations.

The explosion residue is examined for micro- and nano-titanium explosions. Different colours (gold, red-brown, blue, purple and white) were observed after an explosion of micron-and nano-titanium powders. For the micron-titanium, this phenomenon begins to occur at concentrations above 1250 g/m^3; however, this occurs at concentrations above 250 g/m^3 for nano-titanium. Below these specified concentrations, only a white powder is observed after the explosion which represents titanium oxidizing into titanium dioxide. At concentrations above these limits, the oxygen in the explosion chamber is mostly consumed resulting in the formation of other oxides and nitrides. Unreacted titanium reacts with non-stoichiometric amounts of oxygen to form different oxides and also reacts with nitrogen to form titanium nitride.

This phenomenon can be explained by the use of an equivalence ratio (ϕ). An equivalence ratio is the stoichiometric fuel/air mixture divided by the actual fuel/air mixture and determines whether the mixture is fuel rich or fuel lean. If $\phi = 1$, then stoichiometric amounts of fuel are present for the amount of air. The stoichiometric amount for titanium in the 20-L chamber is equivalent to 420 g/m^3, thus, for concentrations below 420 g/m^3, the fuel air mixture is lean. Concentrations above 420 g/m^3 are fuel rich. For micron-titanium to reach its maximum explosion severity, the fuel/air mixture has to be very rich while the nano-titanium reaches its maximum severity only slightly above stoichiometric.

Titanium is one of few elements that reacts and combusts within a nitrogen rich atmosphere, a reaction that occurs at temperatures above 800 ℃.[17] According to Cashdollar,[47] titanium explosions can occur well above 2000 ℃ with the maximum explosion temperature occurring at 2600 ℃ for concentrations near stoichiometric. These explosion temperatures exceed the temperature needed for nitrogen to react and therefore allow for the formation of titanium nitrides. Similar titanium colours have also been seen for titanium oxides and nitrides by Roquiny et al.[48] and Hashizume et al.[49]

X-ray diffraction is performed on the gold, red-brown, blue and purple colours observed in the titanium explosion residues. A high-speed Bruker D8 Advance XRD system isa used for the analysis. The XRD system used Cu-Ka radiation with a wave length of 1.54 A˚, tube voltage of 40 kV, and tube current of 40 mA. The results are seen in Figure 6.8 and show the presence of titanium nitrides and oxides within the explosion residues. This analysis does not include the titanium dioxide that is present after all explosions.

6.2   Explosion Likelihood

The likelihood of an explosion is measured using three different experiments: minimum ignition energy, minimum explosible concentration and minimum ignition temperature. Each test is performed and the results for the micron- and nano-titanium are compared.

6.2.1   Minimum Ignition Energy

Micron-size titanium has been previously shown to ignite at very low spark energies. Randeberg et al.[37] demonstrated that 3 μm and 9 μm titanium can ignite at energies as low as 0.012 mJ and 0.36 mJ, respectively. The MIE of titanium is very low for small micron sized particles. Low MIE values for titanium are also measured in the current work as shown in Table 5.3 (1 mJ being the lowest spark energy attainable with the MIKE 3 apparatus).
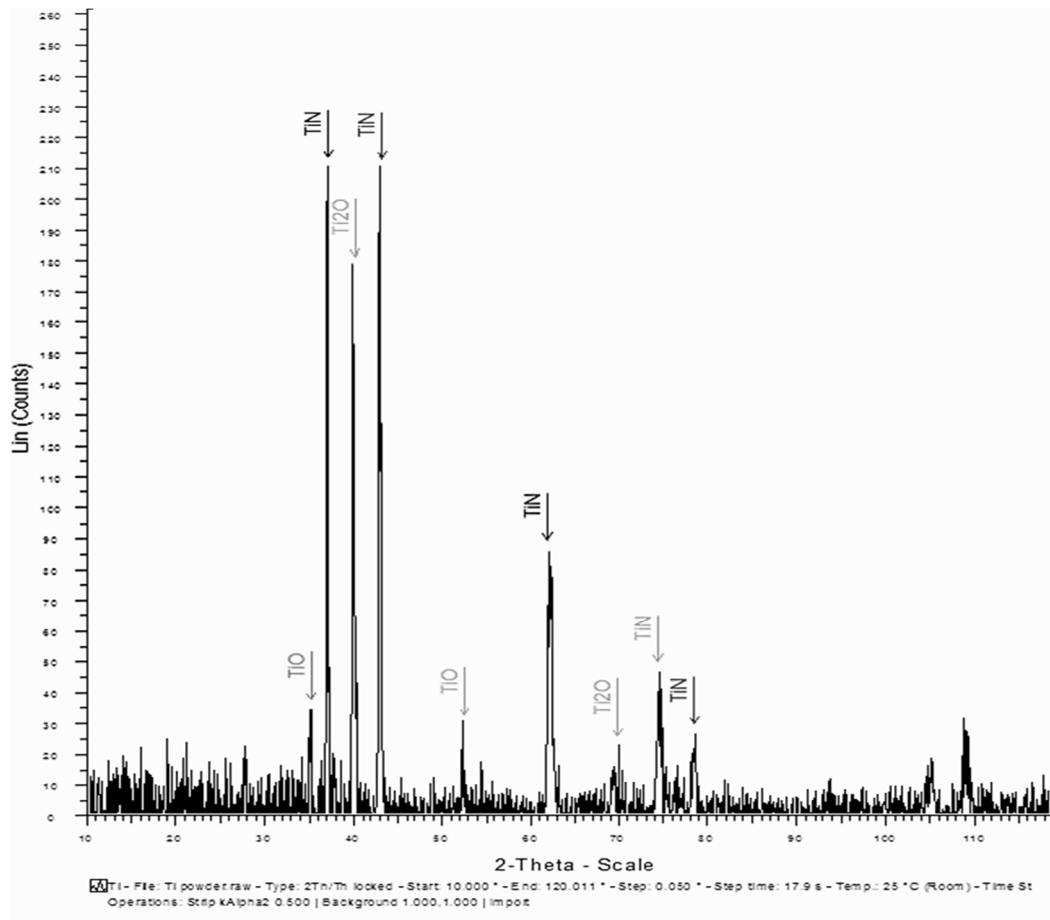
Figure 6.8   X-ray diffraction analysis for the coloured explosion residue

There is, however, a fundamental difference between the MIEs of the micron- and nano-size samples. As shown in Figure 5.15 for the ≤20 µm sample, ignition at 1 mJ occurs only at a high dust loading of 3000 mg. Figure 5.16, a MIKE 3 ignition graph for the 150 nm titanium, illustrates the significantly lower dust loadings (as low as 100 mg) required for ignition at 1 mJ.

MIE tests with dust loadings >900 mg were not attempted for the nano-titanium samples. Even at low dust loadings with these materials, the explosion in the MIKE 3 glass tube (modified Hartmann tube) was violent and produced an audible 'boom'.

6.2.2 Minimum Explosible Concentration

MEC determination for the micron-size samples in the Siwek 20-L chamber is relatively straightforward, however, the nano-size samples again posed experimental challenges due to the pre-ignition of the powder during the dispersion sequence. Using the 150 nm titanium as an example, pre-ignition did not occur at lower concentrations of 20 g/m^3 and 30 g/m^3; these concentrations can therefore be tested with nitrogen dispersion and with the chemical ignitor (5 kJ) in place. No explosions in the 20-L chamber are recorded at these conditions, meaning that the MEC of the 150 nm sample is >30 g/m^3.

Using a dust concentration of 40 g/m^3, dispersion with nitrogen caused pre-ignition of the dust; evidence being a resulting P_d value of 1.64 bar. Given that approximately 0.6 bar of the P_d value is associated with dust dispersal, and a 1 bar overpressure is the accepted explosion criterion for MEC testing, it can be argued that a P_d value >1.6 bar indicates an explosion. As a result, the MEC of nano-titanium is measured without the use of ignitors and with a 1.6 bar(g) explosion criterion.

Similar results are found with the 60-80 nm and 40-60 nm titanium. No ignition is observed at 20 g/m^3. At 30 and 40 g/m^3 some activity is present during the dispersal sequence but the P_d value remains lower than 1.6 bar and is therefore not considered an explosion. At 50 g/m^3, for both 40-60 nm and the 60-80 nm titanium, P_d surpasses the 1.6 bar limit. These results can be seen in Table 6.1.

Table 6.1   Minimum explosible concentration of nano-titanium

150 nm		60-80 nm		40-60 nm	
Concentration	P_d	Concentration	P_d	Concentration	P_d
60	2.58	50	2.22	50	1.62
40	1.64	40	1.18	40	1.3
30	0.7	30	1.18	30	0.76
20	0.7	20	0.68	20	0.68
MEC	40 g/m3	MEC	50 g/m3	MEC	50 g/m3

6.2.3 *Minimum Ignition Temperature*

A significant increase in explosion likelihood occurs with MIT as the particle size decreases. These results can be seen in Table 5.3. Larger, -100 mesh particles cannot be ignited in the BAM oven at 590 ºC (which is the highest temperature attainable with our apparatus). Smaller, micron-size particles, -325 mesh and ≤20 µm, ignite at 460 ºC. The minimum ignition temperature of all three nano-titanium was in the range of 240 - 250 ºC. These temperatures are very low, demonstrating the enhanced potential for nano-titanium ignition by hot surfaces.

The sudden decrease in MIT for nano-titanium can be related to the number of particles present within the BAM oven. For the same volume of micron- or nano-titanium injected within the BAM oven, there are ~10^7 times more nano-titanium particles than micron-titanium particles. Therefore, particle interaction for micron-titanium is much more difficult. If a nano-titanium particle ignites, heat will be transferred to a nearby particle. Micron-titanium may not have the same degree of particle interaction and a particle ignition may not transfer heat to another particle. This results in a higher temperature required for micron-titanium to cause an ignition by hot surfaces.

It is difficult to determine the minimum ignition temperature of the nano-sizes due to the unique nature of the powder. Titanium ignition within the BAM oven produces a flame that is very bright and burns quickly. With temperatures exceeding 350 ºC, the nano-titanium flashes-off rapidly. In these tests, a 'hissing' sound can be heard as the powder enters the BAM oven. Visual observation of the flames exiting the oven is more apparent at temperatures below 300 ºC.

6.3   Explosion Inerting

Explosion inerting tests are performed for all three nano-titanium samples using nano-size titanium dioxide (10-30 nm). The TiO_2 is first tested independently with two 5-kJ

ignitors in the 20-L chamber and is determined, as expected, to be chemically inert. Varied percentages of TiO_2 are admixed while the nano-titanium concentration is held constant at 125 g/m^3. Similar to all other nano-titanium tests, nitrogen gas is used as the dust carrier during dispersal.

Figure 6.9 shows the rate of pressure rise for the nano-titanium with admixed amounts of TiO_2. As the percentage of TiO_2 increases from 0 to 40%, the explosion severity actually increases within the 20-L chamber. The additional TiO_2 is not sufficient to alter the explosion severity. Added TiO_2 allows for better dispersion of the dust by distancing the nano-titanium particles. Enhanced dust dispersion increases the rate of pressure rise of the resulting explosion.

For admixed TiO_2 up to 60% of the total dust mixture, pre-ignition still occurs for all three nano-titanium sizes. At 70% TiO_2, the 150 nm titanium showed some pre-ignition activity with a P_d of 0.81 bar (just above the normally acceptable upper-end P_d value of 0.7 bar). The two smallest nano-titanium samples have no pre-ignition activity at 70% TiO_2. At 75% TiO_2, all three size mixtures are successfully dispersed with no pre-ignition activity, but the resulting dust cloud is ignitable using a 5-kJ ignitor (recall for non-ignition, P_m must be less than 1 bar(g)). For the 60-80 nano-titanium sample, 80% TiO_2 successfully suppresses an explosion; however, 85% TiO_2 is required to render the 150 nm and the 40-60 nm titanium samples inert from pre-ignition and from the external 5-kJ ignition source. These results can be seen in Figures 6.9 and 6.10, drawn for the maximum rate of pressure rise and maximum explosion pressure, respectively.

Similar effects are seen with coal dust inerting using limestone. Limestone is inert and acts as a heat sink to absorb the heat from the reacting coal dust. As the percentage of limestone is increased to 40%, the coal dust explosion increases in severity. As the percentage is further increased to 80% limestone, the coal dust explosion can be completely suppressed.[50] Comparatively, nano-titanium dioxide acts as a heat sink and prevents the nano-titanium from igniting in a similar fashion as the above example.
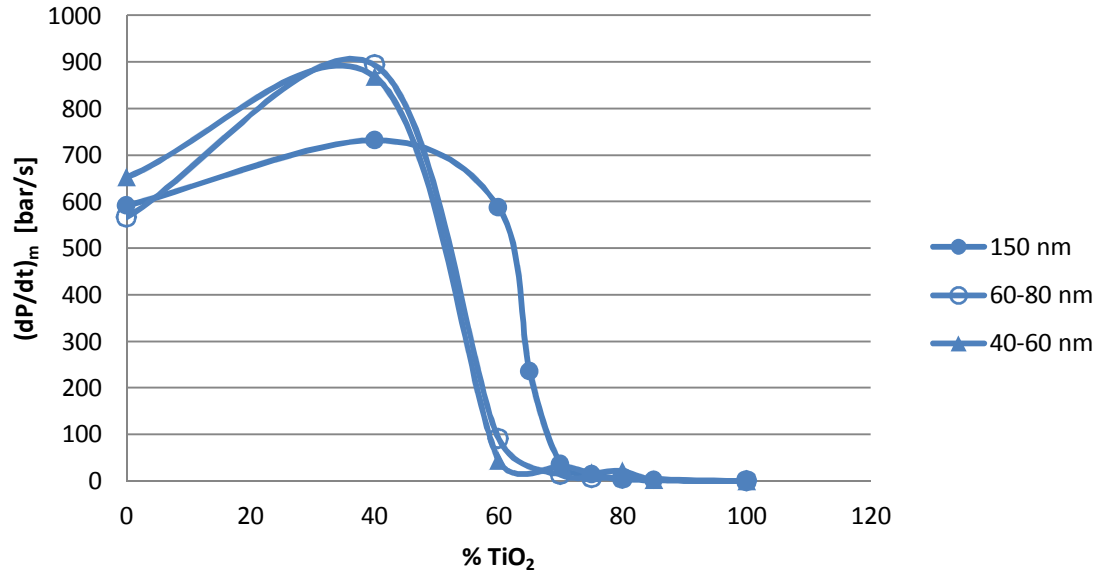
Figure 6.9   Influence of TiO$_2$ on nano-titanium rate of pressure rise
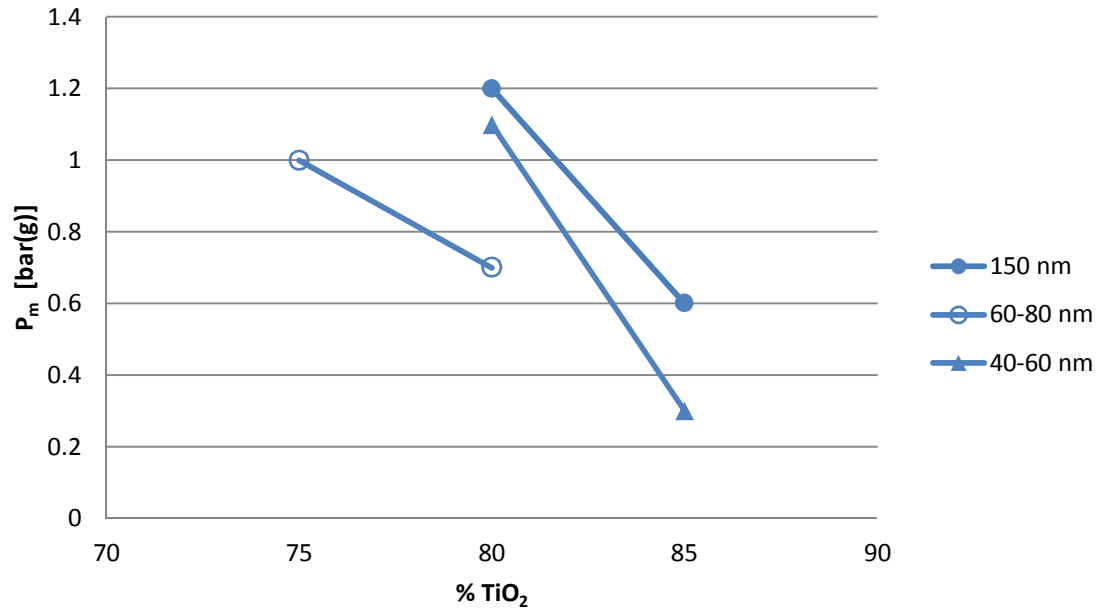
Figure 6.10   Percentages of TiO$_2$ required to suppress nano-titanium explosion

6.4   Experimental Challenges

There are many experimental challenges that arise when performing dust explosion research with micron- and nano-titanium. These include challenges related to the experimental methods, material handling, waste disposal and laboratory safety. These challenges were especially apparent when testing the nano-materials.

6.4.1   Experimental Methods

Issues with titanium powder are first noticed during the 20-L chamber $P_{max}/(dP/dt)_{max}$ testing of the -325 mesh and ≤20 µm samples. Ignition at high concentrations causes explosion residue to become lodged beneath the solenoid valve (Figure 3.1, item 2) and disrupt subsequent trials. The dense titanium cannot be completely dispersed, leaving a few grams beneath the solenoid valve. This remaining powder is then ignited by the intense heat of the explosion occurring in the 20-L chamber.

For nano-titanium, the typical dispersion sequence is not possible due to the pre-ignition of the nano-titanium powder. Table 6.2 illustrates that no combination of experimental conditions can be identified in order to disperse the dust into the 20-L chamber and achieve a pressure/time trace similar to the type shown in Figure 4.3. Numerous attempts are made by varying: (i) dust concentration, (ii) dispersion gas (nitrogen or air), (iii) dispersion gas pressure and ignition delay time (both of which affect dust cloud turbulence intensity), (iv) location of the dust prior to dispersion (placed in either the external dust storage container or the 20-L chamber itself), and (v) expected oxygen concentration in the 20-L chamber once dispersion was complete. Although no external ignition source (i.e., chemical ignitors) is used in these tests, the result is an explosion similar to those shown in Figure 6.3 and 6.6.

Table 6.2 Trials with various experimental conditions for 150 nm titanium (no ignitors)

Dust Concentration [g/m^3]	Dispersion Gas	Dispersion Pressure [bar(g)]	Ignition Delay Time [ms]	Dust Placement (Figure 3.1)	Final O$_2$ % in 20-L Chamber	Explosion During Dispersion?
125	N$_2$	20	60	In Item 3	21.0	YES
125	N$_2$	20	60	In Item 3	19.5	YES
125	N$_2$	20	60	In Item 3	17.6	YES
125	N$_2$	20	60	In Item 3	15.0	YES
125	N$_2$	20	60	In Item 3	9.0	YES
500	Air	20	60	Under Item 8	21.0	YES
500	Air	20	60	On Item 8	21.0	YES
500	Air	10	60	On Item 8	21.0	YES
500	Air	10	120	On Item 8	21.0	YES
500	Air	5	120	On Item 8	21.0	YES
500	N$_2$	20	60	On Item 8	9.0	YES
250	N$_2$	10	60	On Item 8	9.0	YES

6.4.2 Material Handling

Titanium has been shown to react with water at elevated temperatures of approximately 700 ℃. The metal has a high affinity for oxygen, stripping the oxygen from water to form titanium dioxide and hydrogen gas.[17] Hydrogen explosions have occurred in the past when cooling water unintentionally came in contact with molten titanium.[22] At ambient temperatures, micron-size titanium does not pose a hazard, however, nano-size titanium can have the same effect as molten titanium as it reacts with moisture in the air to create hydrogen gas. Hydrogen co-existing with easily ignitable nano-dust causes many concerns for the handling of the nano-titanium, therefore, nano-titanium should have limited exposure to air or moisture and needs to be kept under dry nitrogen or argon. A

nitrogen-filled glove bag is an essential feature of the safety precautions taken for the handling of nano-titanium in this research. This precaution reduces the potential of nano-titanium to come in contact with moisture in the air.

6.4.3 Waste Disposal

Disposal of unused nano-titanium powder is important to minimize the need to store the material for extended periods of inactivity. The nano-titanium needs to be deactivated and stored in a fume hood. Small quantities of nano-titanium are mixed with water or dilute nitric acid. Mixing the titanium with water creates stable titanium dioxide while forming hydrogen gas within a vented and controlled environment. Adding nitric acid to the mixture promotes the deactivation of the nano-titanium.

6.4.4 Laboratory Safety

Before any experimentation begins, the laboratory is assessed for proper ventilation equipment and personal protective equipment (PPE). An improved ventilation extraction arm is installed and the vacuum exhaust is sent through the ventilation system. Appropriate PPE includes: a filtered mask, safety glasses, face shield (when working with chemical ignitors), lab coat, and double layered nitrile gloves.

Air quality measurements for airborne nano-particles are performed during normal operation of the 20-L chamber. Two types of particle counters are used: a FLUKE 983 particle counter for particles within the range of 300 nm to 10 µm, and a KANOMAX handheld CPC model 3800 for particles within the range of 15 nm to 1 µm. It is determined that no excess particles become airborne when using nano-materials.

The application of the principles of inherently safer design when handling and working with nano-titanium and nano-materials in general is also of great importance. Principles of minimization, substitution, moderation and simplification should all be applied in

order to reduce the risk involved with nano-titanium.[12] Examples of these principles include:

MINIMIZATION – Nano-titanium is received from the manufacturer in packages of 100 g each, thus reducing the amount of material handled at any given time.

SUBSTITUTION – Nitrogen is used in place of air for nano-dust dispersion in an attempt to prevent pre-ignition during the 20-L chamber tests.

MODERATION – Unused nano-titanium is deactivated in 0.1M nitric acid, eliminating the potential risk of storing an already opened package of material.

SIMPLIFICATION – Clear and straightforward procedures are developed and implemented.

CHAPTER 7: CONCLUSION

7.1   Concluding Remarks

Many conclusions can be drawn regarding the experimental results for micron- and nano-titanium powders. Explosibility experiments were carried out on six titanium samples with varying particle size: three of these samples being micron-titanium particles and three samples being nano-titanium particles.

Micron-sized titanium is known to have severe explosion characteristics as seen in section 6.1.1. As the particle size decreased, the explosion severity increased to reach a quasi-plateau affected by the agglomeration of particles. For the nano-titanium, the objective was to directly compare the explosion severity between micron- and nano-titanium. However, direct comparison was not possible due to the pre-ignition of the nano-titanium. This resulted in different explosion conditions when comparing the micron- and nano-titanium. Nano-titanium generated different explosion curves that had to be interpreted from the generated graphs. Nano-results demonstrated significant overpressures and very high rates of pressure rise, even though no external ignition source was required to produce an explosion.

The minimum ignition energy (MIE), minimum explosible concentration (MEC) and minimum ignition temperature (MIT) are tests measuring the likelihood of an explosion as the particle size of titanium was decreased.

The MIE of micron-titanium decreased as the particle size was decreased until reaching the lowest generated energy by the MIKE 3 apparatus of 1 mJ. The MIE of micron-titanium occurred at high concentrations while the MIE of nano-titanium (ignition at 1 mJ) occurred at much leaner concentrations. Due to the MIKE 3 apparatus limitation of 1 mJ, it was difficult to conclude whether the MIE dropped as particle size was decreased from micron- and nano-sizes. The nano-titanium ignited at a much wider and leaner

concentration range, which suggests that the MIE of nano-titanium is much lower than 1 mJ and, consequently, lower than the micron-titanium samples.

MEC decreased slightly as the particle size decreased from micron to nano-sized titanium. A major difference between the micron and nano-titanium was the explosion conditions. Even at very low concentrations, the pre-ignition of nano-titanium still occurred. As a result, the nano-titanium MEC was determined by the pre-ignition phenomena while the micron-titanium MEC was determined by the use of an ignitor.

A significant reduction in MIT was observed as the micron titanium particle sizes were decreased. A substantial drop in MIT occurred between the micron and nano-sized titanium. It can be concluded that nano-titanium is very sensitive to ignition by hot surfaces.

Safety concerns were a major issue before any experimental work was initiated. Nano-titanium causes hydrogen formation when exposed to moisture. This phenomenon typically occurs at higher temperatures with micron size titanium; however, nano-titanium forms hydrogen gas (in the presence of air and moisture) at room temperature. Hydrogen gas has a very low MIE, which increases the potential of an ignition and an explosion involving nano-titanium.

Through the explosibility parameters of explosion severity (P_{max} and $(dP/dt)_{max}$) and explosion likelihood (MIE, MEC and MIT), it is clear from this study that greater dust explosion hazards are present when nano-titanium dust is involved. Dust explosion research in the field of nano-titanium should continue to evolve in order to better understand the phenomena discovered throughout this thesis.

7.2   Recommendations

There are many recommendations that can be made for future work on nano-titanium and nano-powder explosions. First, different techniques for the dispersion of the nano-

titanium should be developed and utilized. Properly dispersing the powder into the 20-L chamber is difficult and traditional methods are not sufficient.

One method that was discussed[51] was to use the perforated annular nozzle to disperse the dust into the 20-L chamber. The dust would be placed in a thin paper/plastic pouch attached onto the annular nozzle. This setup can be seen in Figure 8.1. The same procedures would be involved for a P_{max} and $(dP/dt)_{max}$ test. A vacuum would be generated and the dispersion of air would still occur. The high velocity air would be forced through the perforated nozzle and break the bag containing the nano-titanium. In theory, the nano-titanium would disperse evenly throughout the 20-L chamber and the explosion would be caused by the ignitors. It is possible that the titanium could spontaneously ignite with the jet of air bursting the bag. If this were the case, the dust would already be located in the explosion chamber and not forced through the rebound nozzle while igniting.
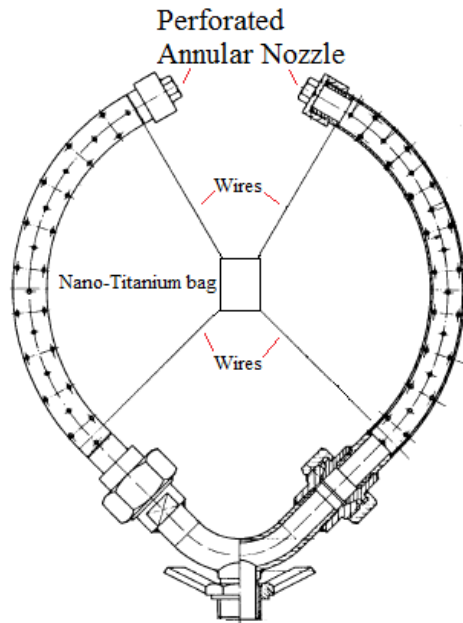
Figure 8.1   Perforated annular nozzle with suspended bag

Although the main focus of this thesis was nano-titanium, different types of nano-powders should also be further investigated for their reactivity and potential explosible properties. Nano-crystalline cellulose (NCC) is being developed for its high strength and light weight.[52] Fabricated from trees, the NCC can cause dust explosions similar to those caused by micron-crystalline cellulose (MCC). MCC has been proven to have explosible properties. Industries that use these nano-materials should be aware of the potential hazards and the proper mitigation measures in order to reduce and eliminate the risks of dust explosions.

REFERENCES

[1] Amyotte, P.R., Eckhoff, R.K. (2010): Dust Explosion Causation, Prevention and Mitigation: An Overview, Journal of Chemical Health & Safety, January/February: 15-28.

[2] NFPA (2000): NFPA 654 - Standard for the Prevention of Fire and Dust Explosions from the Manufacturing, Processing, and Handling of Combustible Particulate Solids, National Fire Protection Agency, Denver, Co, USA.

[3] Eckhoff, R.K. (2003): Dust Explosions in the Process Industries, 3rd edition, Gulf Professional Publishing/Elsevier: Boston, MA.

[4] IChemE (1993): Dust Explosion Hazards, Video Training Package 022, Institution of Chemical Engineers, Rugby, UK.

[5] Kauffman, C. W. (1982): Fuel-Air Explosions; University of Waterloo Press: Waterloo, ON, Canada: 305–347.

[6] Di Benedetto, A., Russo, P., Amyotte, P.R. and Marchand, N. (2010):Modelling the Effect of Particle Size on Dust Explosion, Chemical Engineering Science 65: 772-779.

[7] Cashdollar, K.L. (2000): Overview of Dust Explosibility Characteristics, Journal of Loss Prevention in the Process Industries 13: 183-199.

[8] OSHA (2005): Combustible Dust in Industry: Preventing and Mitigating the Effects of Fire and Explosions, U.S. Department of Labor, Retrieved from: http://www.osha.gov/dts/shib/shib073105.html [June 2012].

[9] Kletz, T.A. (1978): What you don't have, can't leak. Chemistry and Industry 6: 287–292.

[10] Amyotte, P.R., Pegg, M.J. and Khan, F.I. (2009): Application of Inherent Safety Principles to Dust Explosion Prevention and Mitigation, Process Safety and Environment Protection 87: 35-39.

[11] Morose, G. (2010): The 5 Principles of "Design for Safer Nanotechnology", Journal of Cleaner Production 18: 285-289.

[12] Amyotte, P.R. (2011): Are Classical Process Safety Concepts Relevant to Nanotechnology Application? Journal of Physics: Conference Series 304: 012071.

[13] Attar, A., Halali, M., Sobhani, M. and Ghandehari, R.T. (2011): Synthesis of Titanium Nano-Particles Via Chemcal Vapor Condensation Processing, Journal of Alloys and Compounds 509: 5825-5828.

[14] Project on Emerging Nanotechnologies (2012): A Nanotechnology Consumer Products Inventory, Retrieved from: http://www.nanotechproject.org/ [June 2012].

[15] Raab, C., Simkó, M., Fieldeler, U., Nentwich, M. and Gazsó, A. (2011): Production of Nanoparticles and Nanomaterials, Institute of Technology Assessment of the Austrian Academy of Sciences – Nano Trust Dossiers 006en.

[16] Chen, X. and Mao, S.S. (2007): Titanium Dioxide Nanomaterials: Synthesis, Properties, Modification, and Applications. American Chemical Society 107: 2891-2959.

[17] Patnaik, P. (2003): Handbook of Inorganic Chemicals, McGraw-Hill: New York, NY.

[18] Pierre, A.C. and Pajonk, G.M. (2002): Chemistry of Aerogels and Their Applications, American Chemical Society 102: 4243-4265.

[19] Kwon, Y.S., Jung, Y.H., Yavorovsky, N.A., Ilyin, A.P. and Kim, J.S. (2001): Ultra-Fine Powder by Wire Explosion Method, Scripta Materialia 44: 2247-2251.

[20] Nazarenko, O.B. and Ilyin, A.P. (2008): Nanopowders Production by Electrical Explosion of Wires: Environmental Applications, Proceeding of the 3rd Environment Physics Conference, Aswan, Egypt: 19-23 February.

[21] Kwon, Y.S., Ilyin, A.P., Nazarenko, O.B., Root, L.O., Tikhonov, D.V. and Startseva, E.V. (2011): Characterization of Nanopowders Produced by Electrical Explosion of Titanium Wires, The 6th International Forum on Strategic Technology: 52-54.

[22] Poulsen, E. (2000): Safety-Related Problems in the Titanium Industry in the Last 50 Years. JOM 52: 13-17.

[23] Victor, D., Oppenheimer, J. and Reach, L.K. (2005): Titanium Fire Rages Near Downtown Wichita, Kan., RedOrbit. Retrieve from: http://www.redorbit.com/news/science/193514/titanium_fire_rages_near_downtown_wichita_kan/ [June 2012].

[24] Hazardous Material Advisory (2010): Metal Fires, Health Hazardous Materials Division Emergency Operations Section: 1-6.

[25] NIOSH Report (2010): Seven Career Fire Fighters Injured at a Metal Recycling Facility Fire, CommandSaferty.com. Retrieved from: http://commandsafety.com/2011/08/niosh-report-addresses-operational-issues-at-metal-recycling-facility-fire/ [June 2012].

[26] NIOSH Report (2010): Tactics Factored into LA Metal Fire Explosion Injuring 7 Firefighters, VolunteerFD.org. Retrieved from: http://www.volunteerfd.org/sogs/articles/1107704 [June 2012].

[27] CSB (2010): CSB Deploys Fatal Accident in New Cumberland West Virginia, U.S. Chemical Safety Board. Retrieved from: http://www.csb.gov/newsroom/detail.aspx?nid=355 [June 2012].

[28] Ono, R. and Oda, T. (2008): Spark Ignition of Hydrogen-Air Mixture, Journal of Physics: Conference Series 142: 012003.

[29] The Chemical Safety Mechanism (2012): Lessons Learned: A Titanium Metal Fire, University of Wisconsin-Madison Office of Chemical Safety.

[30] Pritchard, D.K. (2004): Literature Review – Explosion Hazards Associated with Nanopowders, UK Health and Safety Executive. EC/04/03.

[31] Eckhoff, R.K. (2012): Personal communication.

[32] Holbrow, P., Wall, M., Sanderson, E., Bennett, D., Rattigan, W., Bettis, R., and Gregory, D. (2010): Fire and Explosion Properties of Nanopowders. UK Health and Safety Executive: RR782.

[33] Vignes, A., Traoré, M., Dufaud, O., Perrin, L., Bouillard, J. and Thomas, D. (2009): Assessing Explosion Severity of Nanopowders with the 20 L Sphere, 8th World Congress of Chemical Engineering, Montréal, Canada, 23-27 August.

[34] Dufaud, O., Vignes, A., Henry, F., Perrin, L. and Bouillard, J. (2011): Ignition and Explosion of Nanopowders: Something New Under the Dust. Journal of Physics: Conference Series 304: 012076.

[35] Wu, H.C., Ou, H.J., Peng, D.J., Hsiao, H.C., Gau, C.Y. and Shih, T.S. (2010): Dust Explosion Characteristics of Agglomerated 35 nm and 100 nm Aluminum Particles, International Journal of Chemical Engineering: 941349.

[36] Wu, H.-C., Chang, R.C. and Hsiao, H.-C. (2009): Research of Minimum Ignition Energy for Nano Titanium Powder and Nano Iron Powder. Journal of Loss Prevention in the Process Industries 22: 21-24.

[37] Randeberg, E. and Eckhoff, R.K. (2007): Measurement of Minimum Ignition Energies of Dust Clouds in the <1 mJ Region. Journal of Hazardous Materials 140: 237-244.

[38] Wu, H.-C., Kuo, Y.-C., Wang, Y.-H., Wu, C.-W. and Hsiao, H.-C. (2010): Study on Safe Air Transporting Velocity of Nanograde Aluminum, Iron, and Titanium. Journal of Loss Prevention in the Process Industries 23: 308-311.

[39] Kuhner (2011): Operating Instructions 20-l-Apparatus 6.0. Retrieved from: http://safety.kuhner.com/en/product/apparatuses/safety-testing-devices/id-20-l-apparatus.html [May 2011].

[40] Kuhner (2010): MIKE 3 Minimum Ignition Energy. Retrieved from: http://safety.kuhner.com/en/product/apparatuses/safety-testing-devices/mike-3.html [May 2011].

[41] ASTM (2006): Standard Test Method for Minimum Autoignition Temperature of Dust Clouds, E1491. West Conshohocken, PA: ASTM International.

[42] ASTM (2010): Standard Test Method for Explosibility of Dust Clouds, E1226. West Conshohocken, PA: ASTM International.

[43] ASTM (2003): Standard Test Method for Minimum Ignition Energy of a Dust Cloud in Air, E2019. West Conshohocken, PA: ASTM International.

[44] ASTM (2007): Standard Test Method for Minimum Explosible Concentration of Combustible Dusts, E1515. West Conshohocken, PA: ASTM International.

[45] Kuhner (2009): 20-l-Apparatus Annex. Retrieved from: http://safety.kuhner.com/en/product/apparatuses/safety-testing-devices/id-20-l-apparatus.html [May 2011].

[46] Kuhner (2011): Cleaning Procedure KSEP-20L. Retrieved from: http://safety.kuhner.com/en/product/apparatuses/safety-testing-devices/id-20-l-apparatus.html [May 2011].

[47] Cashdollar, K. L. and Zlochower I. A. (2007): Explosion Temperatures and Pressures of Metals and Other Elemental Dust Clouds. Journal of Loss Prevention in the Process Industries 20: 337–348.

[48] Roquiny, P., Bodart, F. and Terwagne, G. (1999): Colour Control of Titanium Nitride Coating Produced by Reactive Magnetron Sputtering at Temperature less than 100 ºC, Surface and Coatings Technology 116-119: 278-283.

[49] Hashizume, Y., Kobayashi, S. and Hanibuchi, M. (1998): Coloured Titanium Flaskes, Process for their Preparation and Resin Composition Containing Colored Titanium Flaskes, United States Patent: 5,766,334.

[50] Dastidar, A.G., Amyotte, P.R. and Pegg, M.J. (1997): Factors Influencing the Suppression of Coal Dust Explosions. Fuel 76: 663-670.

[51] Pegg, M.J. (2012): Personal communication.

[52] Hoag, H. (2011): Think Small, Canadian Chemical News Vol 63, No 4: 12-16

APPENDIX A:

Particle Size Distribution for Micron-Titanium Powders

```
Malvern Instruments  MASTER Particle Sizer M3.1 Date 04-01-12 Time 13-06
```

Size microns	% under	% in band	Size microns	% under	% in band	Result source=Sample
188.0	100.0	0.1	17.7	13.7	3.9	Record No. = 0
162.0	99.9	0.3	15.3	9.8	4.0	Focal length = 100 mm.
140.0	99.6	0.4	13.2	5.9	2.9	Experiment type pil
121.0	99.2	0.4	11.4	3.0	1.3	Volume distribution
104.0	98.7	0.3	9.8	1.6	0.7	Beam length = 2.0 mm.
89.9	98.4	0.8	8.5	1.0	0.6	Obscuration =0.2039
77.5	97.6	2.3	7.3	0.4	0.3	Volume Conc. = 0.1068 %
66.9	95.2	4.3	6.3	0.1	0.0	Log. Diff. =5.71
57.7	90.9	6.7	5.4	0.1	0.1	Model indp
49.8	84.2	9.6	4.7	0.0	0.0	
42.9	74.6	12.4	4.1	0.0	0.0	$D(v,0.5)$ = 32.9 μm
37.1	62.1	15.1	3.5	0.0	0.0	$D(v,0.9)$ = 56.4 μm
32.0	47.1	13.8	3.0	0.0	0.0	$D(v,0.1)$ = 15.4 μm
27.6	33.3	9.6	2.6	0.0	0.0	$D(4,3)$ = 35.8 μm
23.8	23.7	6.0	2.2	0.0	0.0	$D(3,2)$ = 27.5 μm
20.5	17.7	4.0	1.9	0.0	0.0	Span = 1.2

Spec. surf. area
    0.10 sq.m./cc.

Sample details:-Amyotte - <20um Titanium Powder

```
Result source    Sample       Record No.  0
BS 410:1976, ASTM B11:81
```

Mesh	Aperture	% under	% in sieve	Mesh	Aperture	% under	% in sieve
10	2000.0 μm	100.0	0.0	60	250.0 μm	100.0	0.0
12	1700.0 μm	100.0	0.0	70	212.0 μm	100.0	0.0
14	1400.0 μm	100.0	0.0	80	180.0 μm	100.0	0.0
16	1180.0 μm	100.0	0.0	100	150.0 μm	99.7	0.3
18	1000.0 μm	100.0	0.0	120	125.0 μm	99.3	0.5
20	850.0 μm	100.0	0.0	140	106.0 μm	98.8	0.5
25	710.0 μm	100.0	0.0	170	90.0 μm	98.4	0.4
30	600.0 μm	100.0	0.0	200	75.0 μm	97.2	1.2
35	500.0 μm	100.0	0.0	230	63.0 μm	93.7	3.5
40	425.0 μm	100.0	0.0	270	53.0 μm	87.3	6.4
45	355.0 μm	100.0	0.0	325	45.0 μm	78.0	9.4
50	300.0 μm	100.0	0.0	400	38.0 μm	64.4	13.6

Sample details:-Amyotte - <20um Titanium Powder

Malvern Instruments MASTER Particle Sizer M3.1 Date 04-01-12 Time 13-01

Size microns	under	% in band	Size microns	under	% in band	Result source=Sample
198.0	100.0	0.1	17.7	15.2	4.3	Record No. = 0
162.0	99.9	0.3	15.3	10.8	4.4	Focal length = 100 mm.
140.0	99.5	0.4	13.2	6.4	3.0	Experiment type pil
121.0	99.1	0.5	11.4	3.4	1.3	Volume distribution
104.0	98.6	0.4	9.8	2.1	0.7	Beam length = 2.0 mm.
89.9	98.3	0.9	8.5	1.4	0.7	Obscuration =0.2020
77.5	97.4	2.5	7.3	0.6	0.5	Volume Conc. = 0.1044 %
66.9	94.9	4.6	6.3	0.2	0.0	Log. Diff. =5.73
57.7	90.3	7.1	5.4	0.2	0.2	Model indp
49.8	83.1	10.1	4.7	0.0	0.0	
42.9	73.0	12.6	4.1	0.0	0.0	D(v,0.5) = 33.4 µm
37.1	60.5	14.7	3.5	0.0	0.0	D(v,0.9) = 57.3 µm
32.0	45.7	12.9	3.0	0.0	0.0	D(v,0.1) = 14.9 µm
27.6	32.8	8.4	2.6	0.0	0.0	D(4,3) = 36.1 µm
23.8	24.4	5.3	2.2	0.0	0.0	D(3,2) = 27.2 µm
20.5	19.1	4.0	1.9	0.0	0.0	Span = 1.3

D(3,2)   =   27.2 µm
Span   = 1.3
Spec. surf. area
0.10 sq.m./cc.

Sample details:-Amyotte - -325 mesh Titanium Powder

Malvern Instruments MASTER Particle Sizer M3.1 Date 04-01-12 Time 13-01

Result source   Sample   Record No.   0
BS 410:1976, ASTM E11:81

Mesh	Aperture	% under	% in sieve	Mesh	Aperture	% under	% in sieve
10	2000.0 µm	100.0	0.0	60	250.0 µm	100.0	0.0
12	1700.0 µm	100.0	0.0	70	212.0 µm	100.0	0.0
14	1400.0 µm	100.0	0.0	80	180.0 µm	100.0	0.0
16	1180.0 µm	100.0	0.0	100	150.0 µm	99.7	0.3
18	1000.0 µm	100.0	0.0	120	125.0 µm	99.2	0.5
20	850.0 µm	100.0	0.0	140	106.0 µm	98.7	0.5
25	710.0 µm	100.0	0.0	170	90.0 µm	98.3	0.4
30	600.0 µm	100.0	0.0	200	75.0 µm	97.0	1.3
35	500.0 µm	100.0	0.0	230	63.0 µm	93.3	3.7
40	425.0 µm	100.0	0.0	270	53.0 µm	86.5	6.8
45	355.0 µm	100.0	0.0	325	45.0 µm	76.6	9.9
50	300.0 µm	100.0	0.0	400	38.0 µm	62.7	13.9

Sample details:-Amyotte - -325 mesh Titanium Powder

Malvern Instruments MASTER Particle Sizer M3.1 Date 04-01-12 Time 13-32

Size microns	under	% in band	Size microns	under	% in band	Result source=Sample
564.0	100.0	0.0	53.1	9.2	3.4	Record No. = 0
487.0	100.0	0.0	45.8	5.9	2.0	Focal length = 300 mm.
420.0	100.0	0.0	39.5	3.8	1.0	Experiment type pil
362.0	100.0	0.6	34.1	2.9	0.9	Volume distribution
312.0	99.4	1.2	29.4	2.0	0.5	Beam length = 2.0 mm.
270.0	98.2	2.1	25.4	1.4	0.4	Obscuration =0.1061
233.0	96.1	3.8	21.9	1.0	0.4	Volume Conc. = 0.1744 %
201.0	92.3	6.6	18.9	0.6	0.3	Log. Diff. =3.52
173.0	85.6	10.3	16.3	0.3	0.1	Model indp
149.0	75.3	12.9	14.1	0.2	0.1	
129.0	62.4	14.2	12.1	0.2	0.1	D(v,0.5) = 113.2 μm
111.0	48.1	12.5	10.5	0.1	0.1	D(v,0.9) = 189.3 μm
95.9	35.6	10.1	9.0	0.0	0.0	D(v,0.1) = 54.7 μm
82.7	25.5	6.9	7.8	0.0	0.0	D(4,3) = 113.9 μm
71.4	18.6	5.1	6.7	0.0	0.0	D(3,2) = 81.8 μm
61.6	13.5	4.3	5.8	0.0	0.0	Span = 1.2
						Spec. surf. area
						0.03 sq.m./cc.

Sample details:-Amyotte - <100 mesh Titanium Powder

.

Malvern Instruments MASTER Particle Sizer M3.1 Date 04-01-12 Time 13-32

Result source   Sample   Record No. 0
BS 410:1976, ASTM E11:81

Mesh	Aperture	% under	% in sieve	Mesh	Aperture	% under	% in sieve
10	2000.0 μm	100.0	0.0	60	250.0 μm	97.3	1.9
12	1700.0 μm	100.0	0.0	70	212.0 μm	93.9	3.4
14	1400.0 μm	100.0	0.0	80	180.0 μm	87.7	6.2
16	1180.0 μm	100.0	0.0	100	150.0 μm	75.8	11.9
18	1000.0 μm	100.0	0.0	120	125.0 μm	59.4	16.4
20	850.0 μm	100.0	0.0	140	106.0 μm	44.0	15.4
25	710.0 μm	100.0	0.0	170	90.0 μm	30.9	13.1
30	600.0 μm	100.0	0.0	200	75.0 μm	20.7	10.2
35	500.0 μm	100.0	0.0	230	63.0 μm	14.3	6.4
40	425.0 μm	100.0	0.0	270	53.0 μm	9.2	5.1
45	355.0 μm	99.9	0.1	325	45.0 μm	5.5	3.6
50	300.0 μm	99.2	0.8	400	38.0 μm	3.6	2.0

Sample details:-Amyotte - <100 mesh Titanium Powder

APPENDIX B:

SEM Micrographs for Micron- and Nano-Titanium Powders
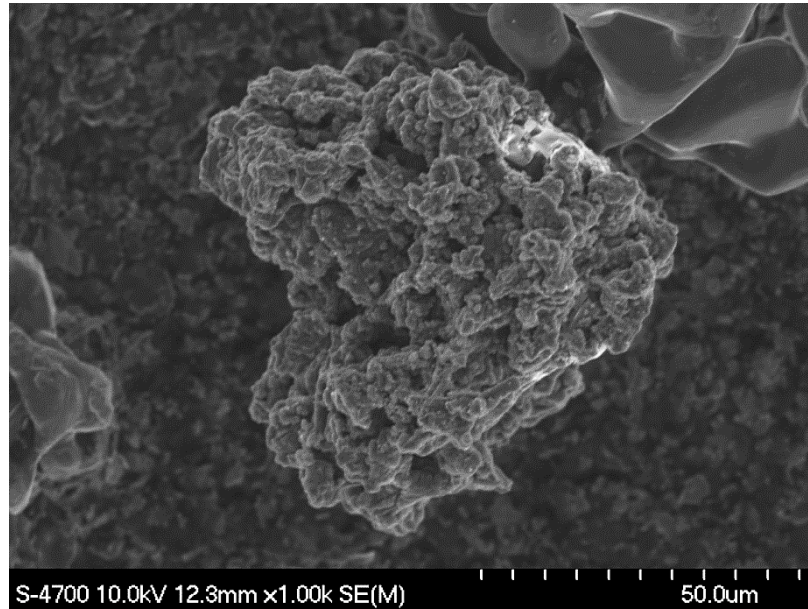
Figure B.1   -100 mesh titanium micrograph-A
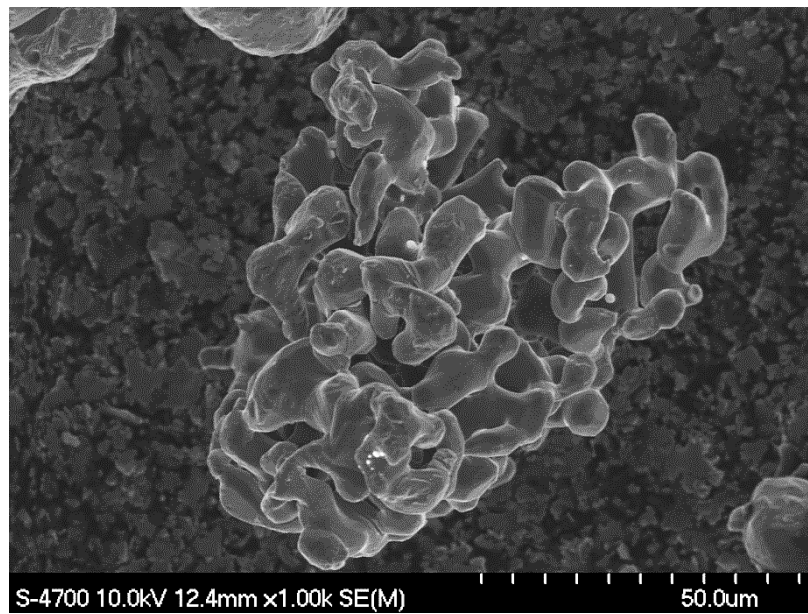
Figure B.2   -100 mesh titanium micrograph-B

Figure B.3 -100 mesh titanium micrograph-C

Figure B.4 -100 mesh titanium micrograph-D

Figure B.5   -325 mesh titanium micrograph-A

Figure B.6   -325 mesh titanium micrograph-B

Figure B.7   -325 mesh titanium micrograph-C

Figure B.8   -325 mesh titanium micrograph-D

Figure B.9   ≤20 μm titanium micrograph-A
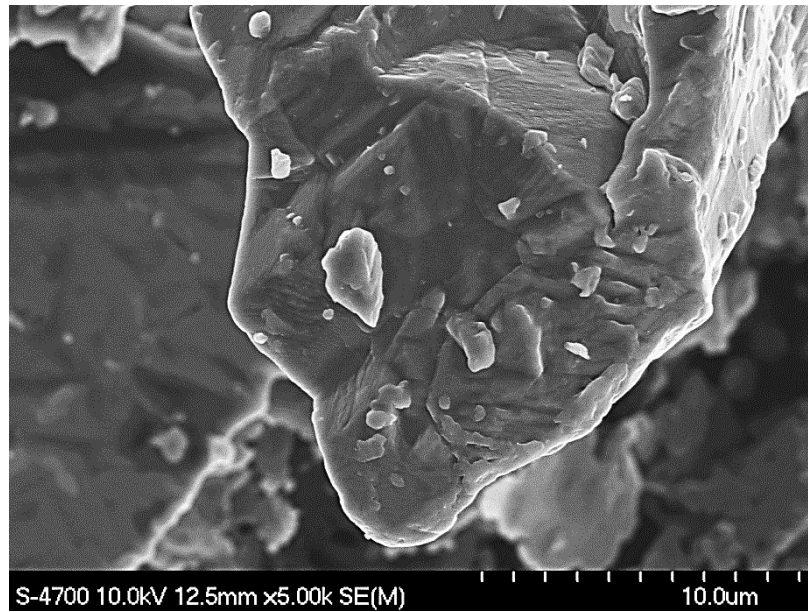
Figure B.10   ≤20 μm titanium micrograph-B
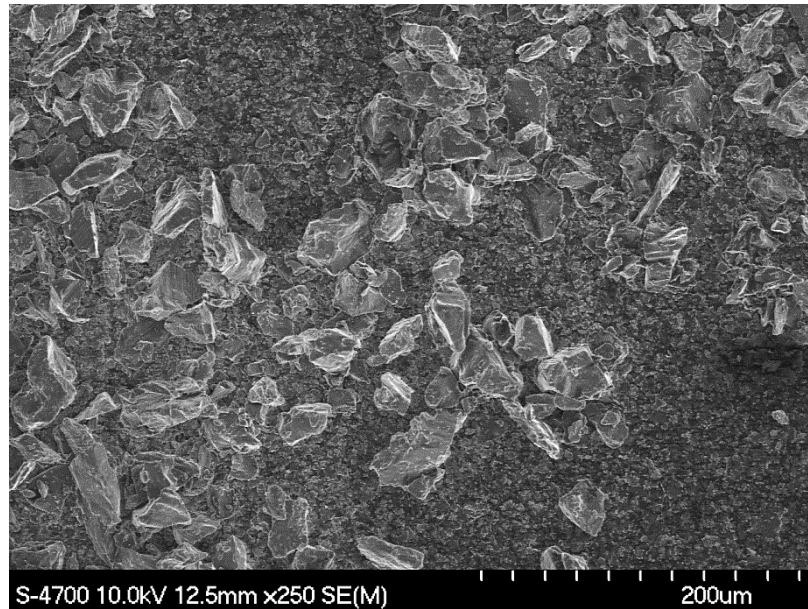
Figure B.11 ≤20 µm titanium micrograph-C
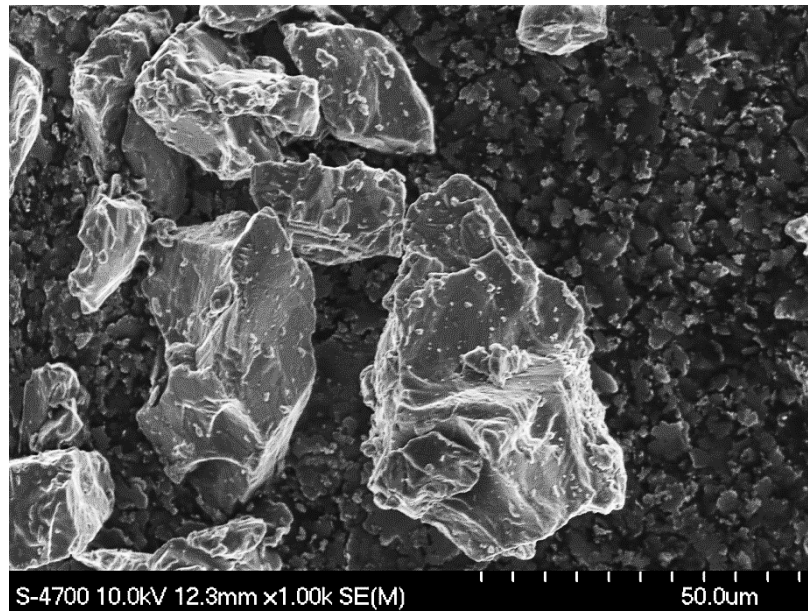
Figure B.12 ≤20 µm titanium micrograph-D
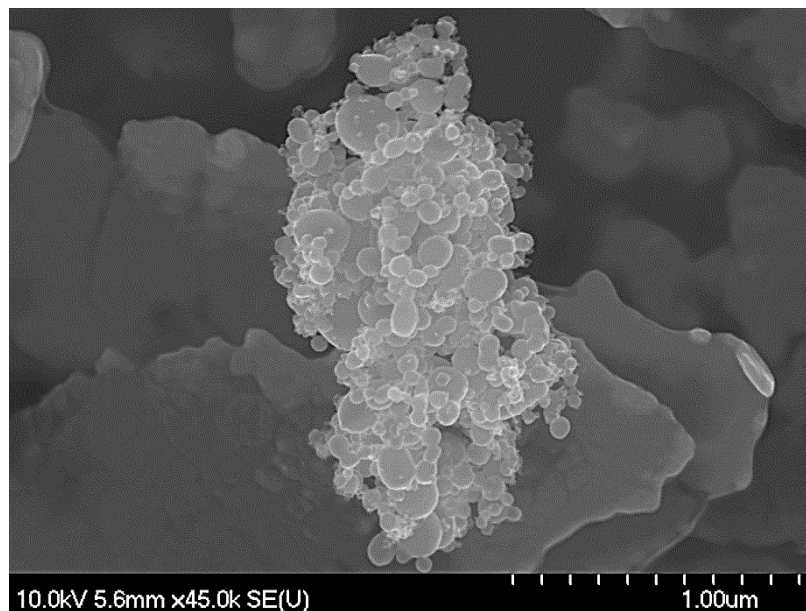
Figure B.13   150 nm titanium micrograph-A
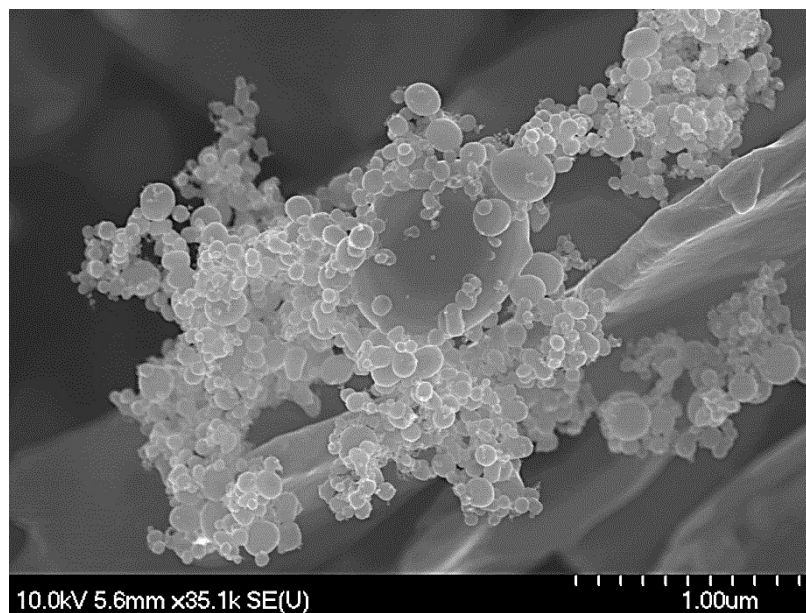
Figure B.14   150 nm titanium micrograph-B
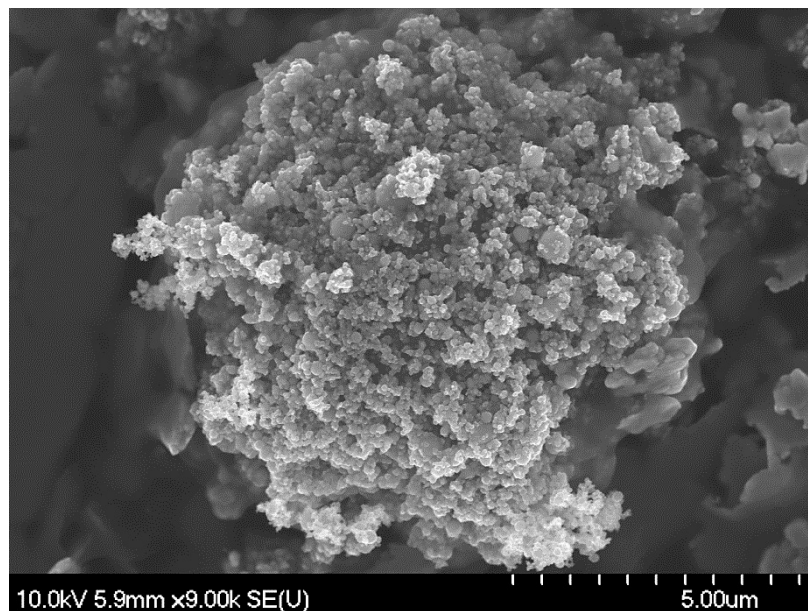
Figure B.15   150 nm titanium micrograph-C
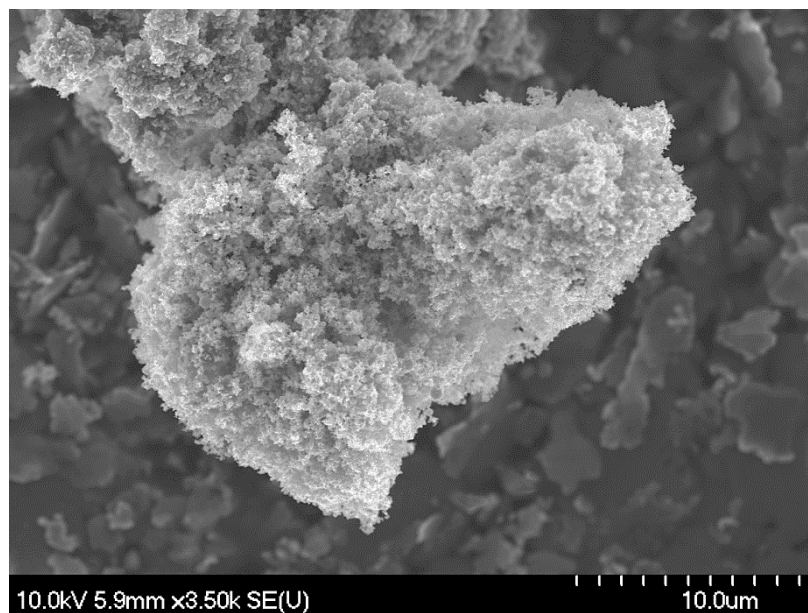
Figure B.16   150 nm titanium micrograph-D
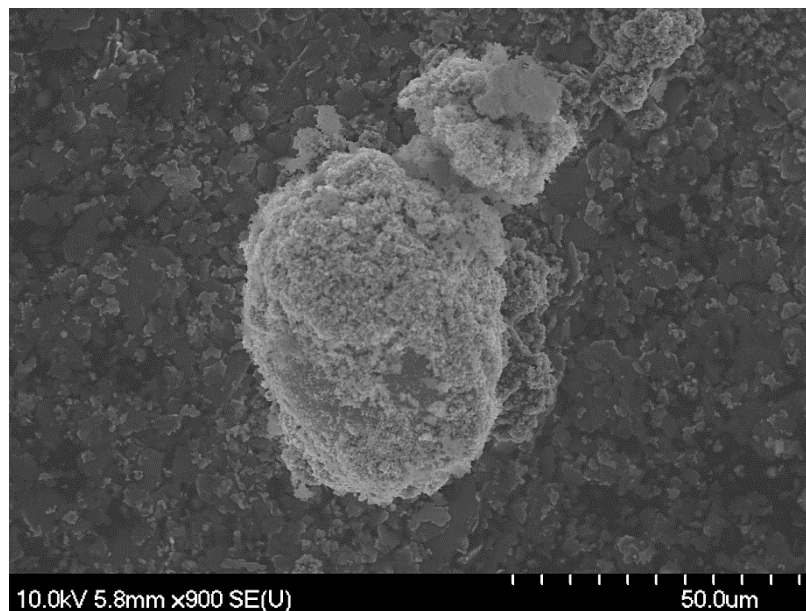
Figure B.17   60-80 nm titanium micrograph-A
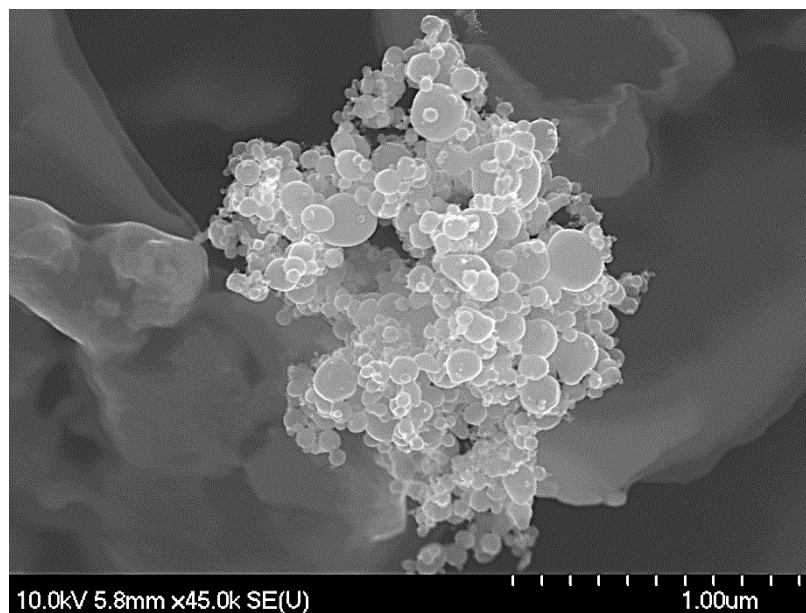
Figure B.18   60-80 nm titanium micrograph-B
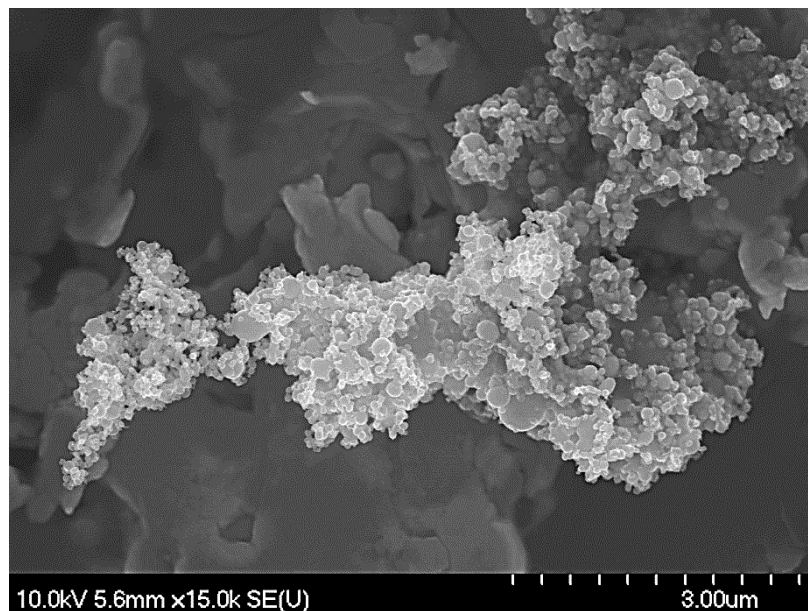
Figure B.19   60-80 nm titanium micrograph-C
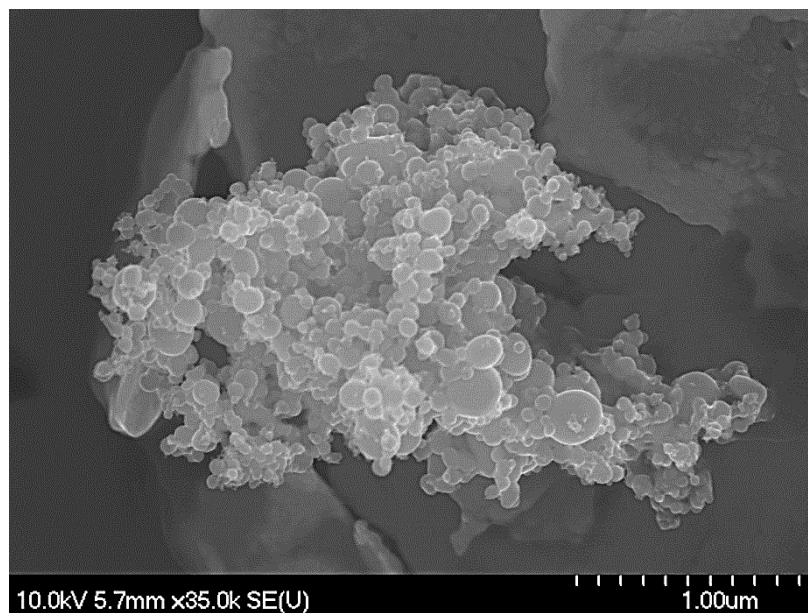
Figure B.20   60-80 nm titanium micrograph-D
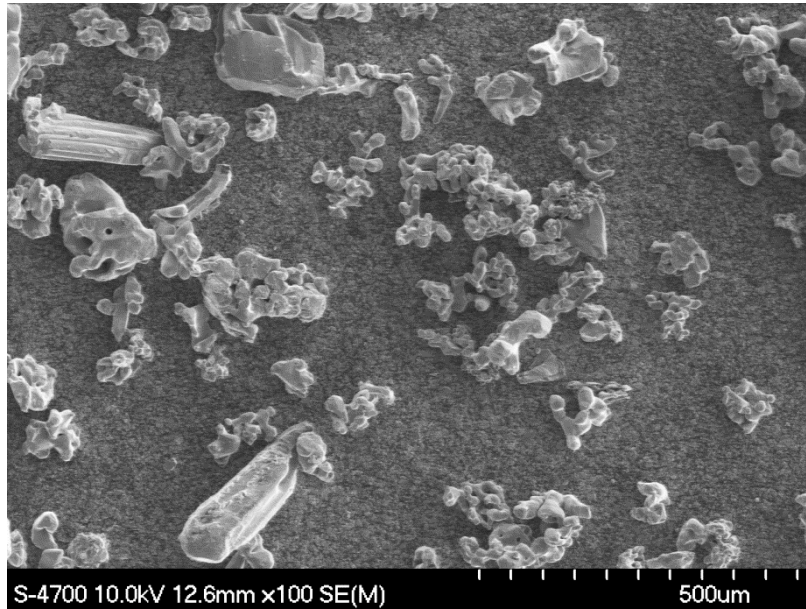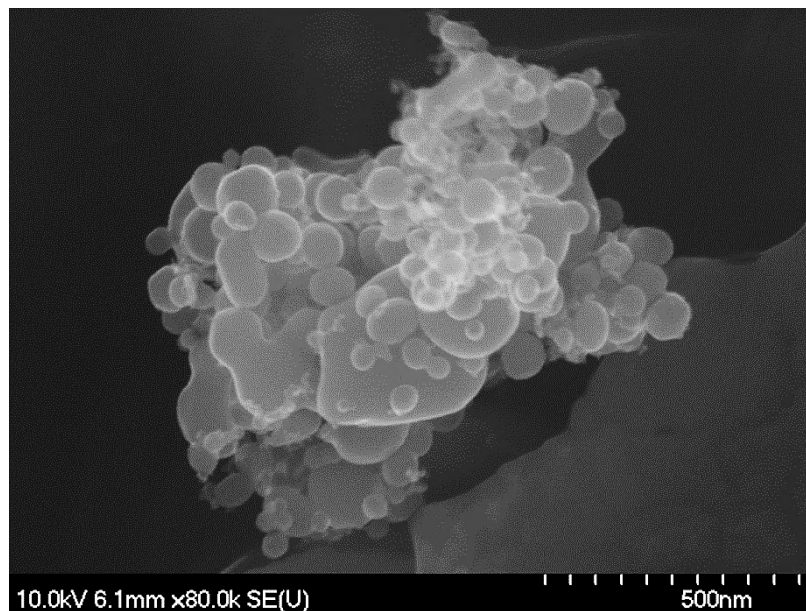
Figure B.21 40-60 nm titanium micrograph-A
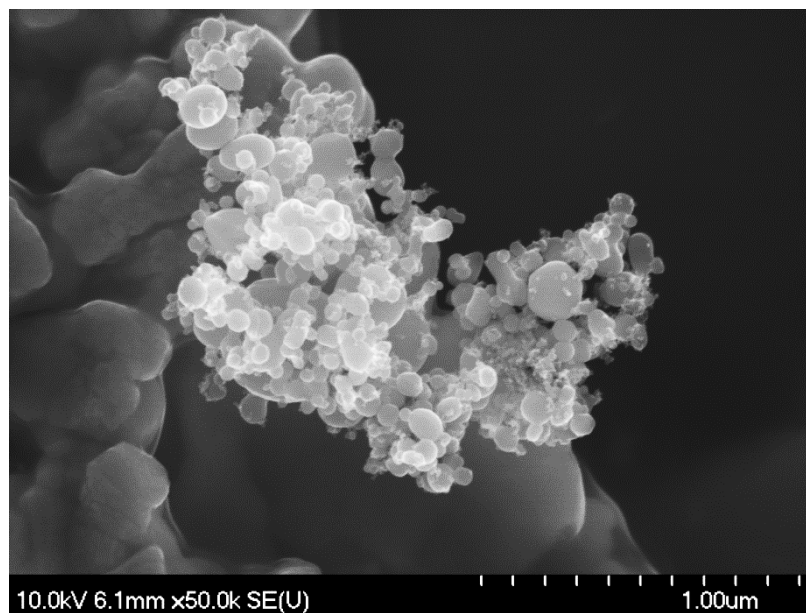
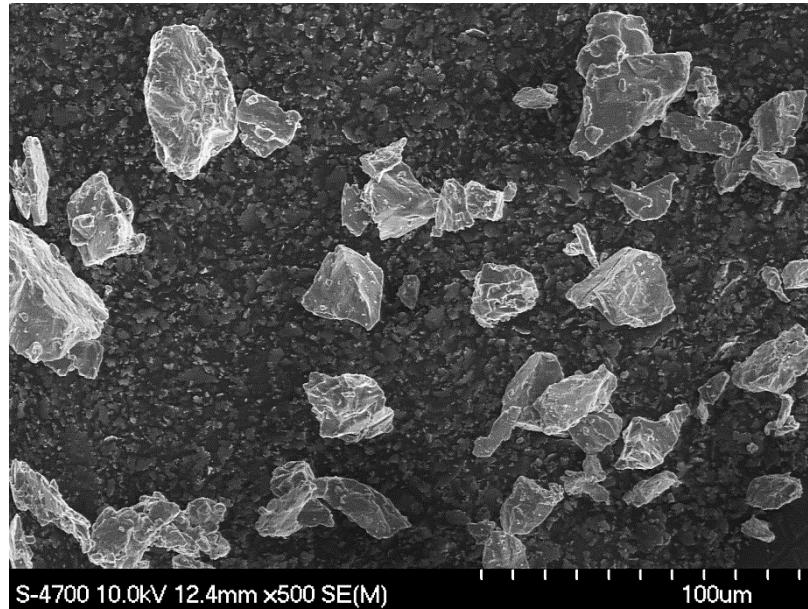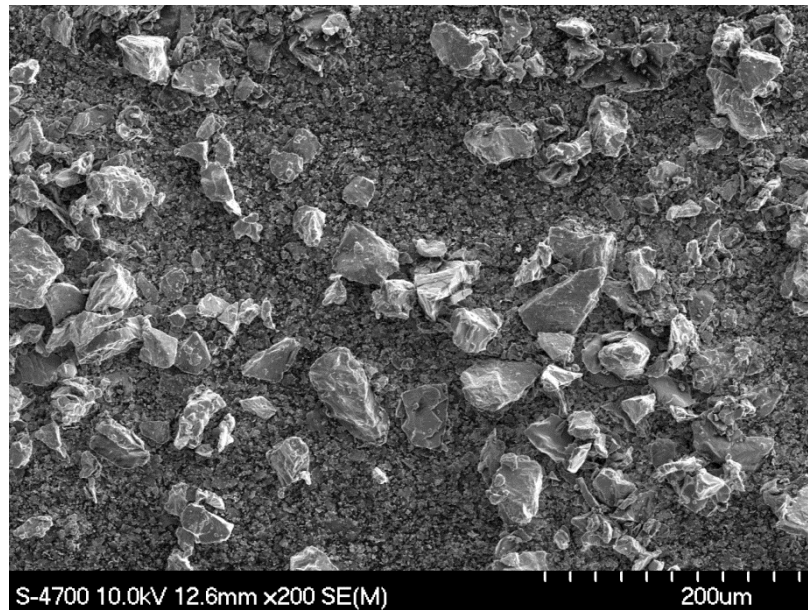**Figure B.22** 40-60 nm titanium micrograph-B
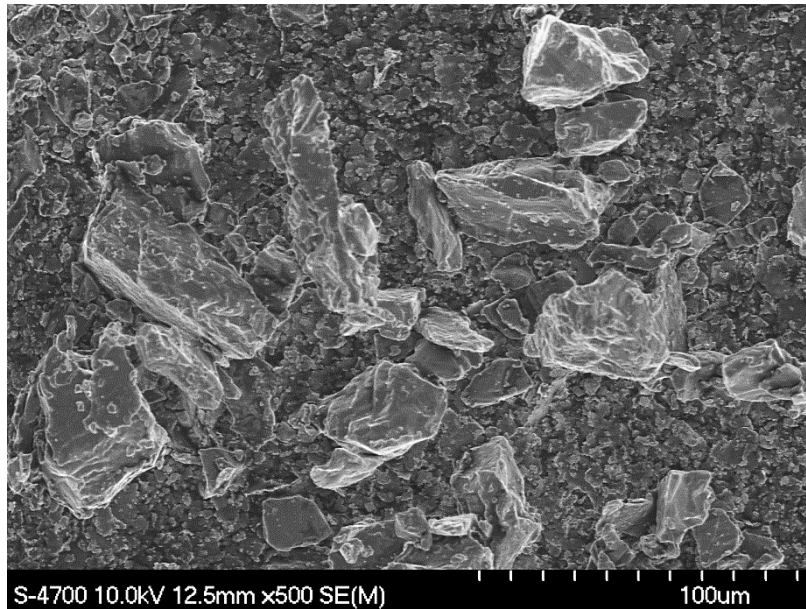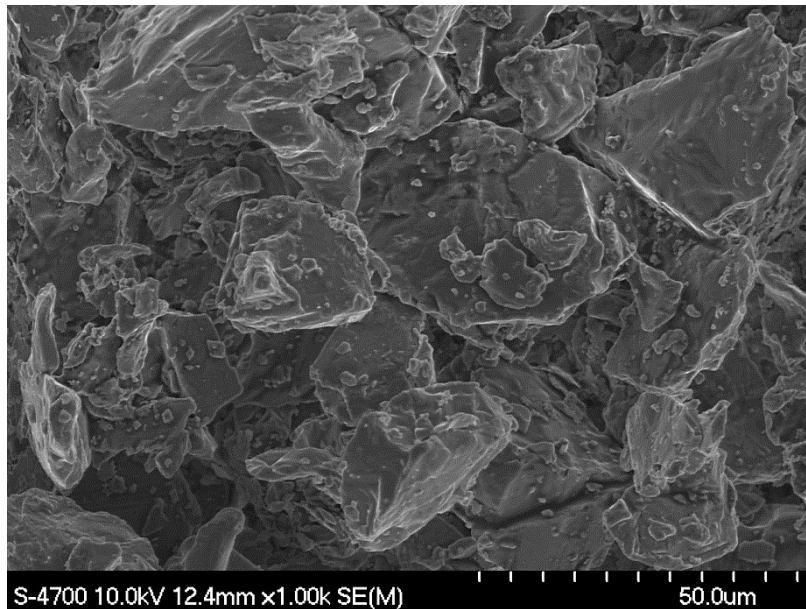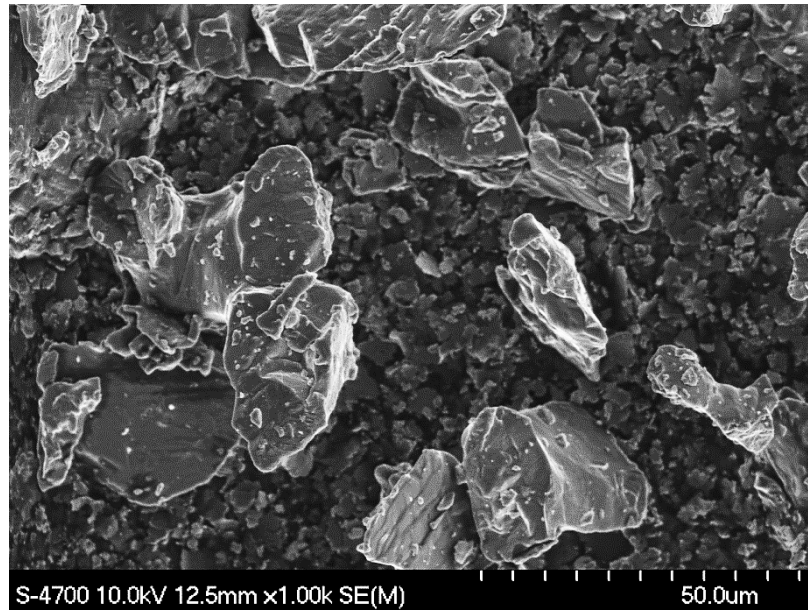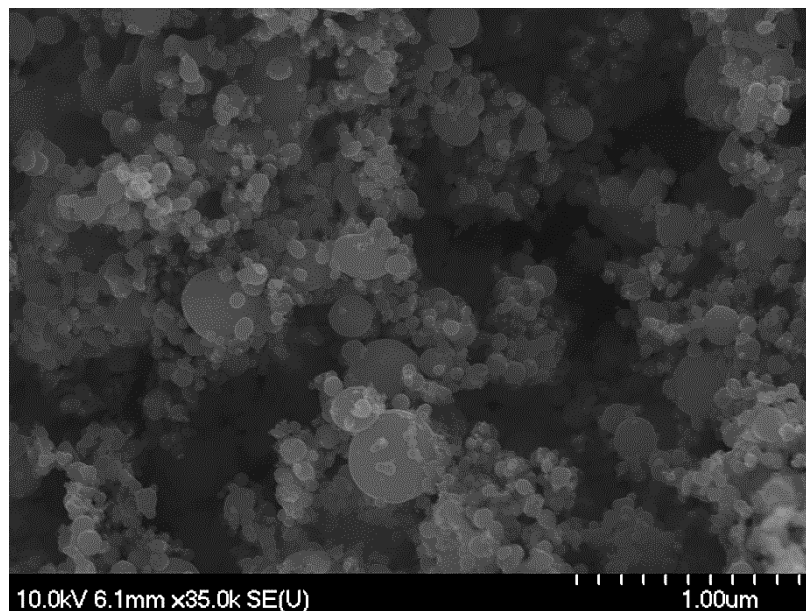
Figure B.23   40-60 nm titanium micrograph-C
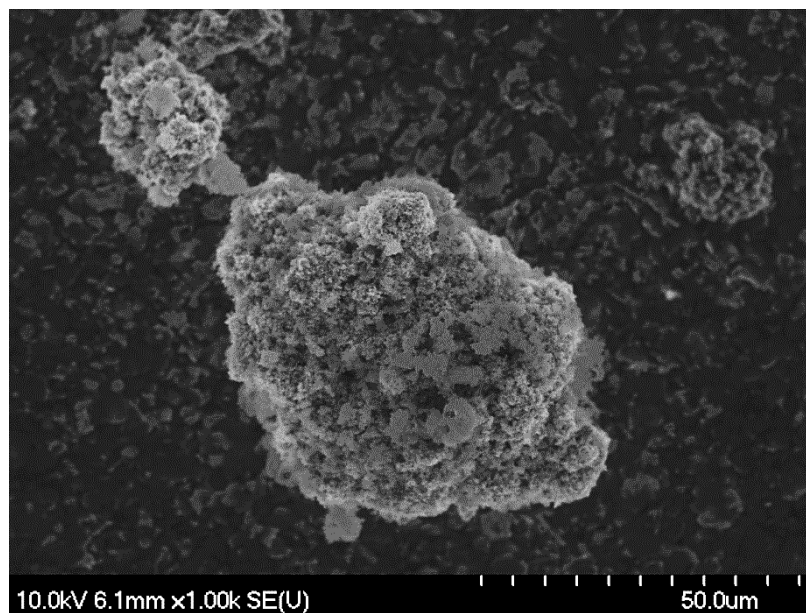
Figure B.24   40-60 nm titanium micrograph-D

APPENDIX C:

Experimental Results for Micron- and Nano-Titanium in Tabular Form

Table C.1   Explosion pressure, P_m, data for micron-titanium

Dust Concentration [g/m^3]	-100 Mesh Series-1 [bar(g)]	-100 Mesh Series-2 [bar(g)]	-325 Mesh Series-1 [bar(g)]	-325 Mesh Series-2 [bar(g)]	≤20 µm Series-1 [bar(g)]	≤20 µm Series-2 [bar(g)]
250			5.9			
500	5.3	4.6	6.3			
750	5.8	5.0	7.0		6.4	5.5
1000	5.6	5.2	6.8		6.6	6.1
1250	5.1	4.7	6.6	6.4	6.9	6.6
1500	4.5	3.6	6.4	7.5	6.7	6.9
1750			7.9	7.2	5.7	6.6
2000			7.6	7.2		
2250			7.3	6.9		
2500			7.7			
2750			7.3			

Table C.2   Rate of pressure rise, $(dP/dt)_m$, data for micron-titanium

Dust Concentration [g/m^3]	-100 Mesh Series-1 [bar/s]	-100 Mesh Series-2 [bar/s]	-325 Mesh Series-1 [bar/s]	-325 Mesh Series-2 [bar/s]	≤20 µm Series-1 [bar/s]	≤20 µm Series2 [bar/s]
250			166			
500	80	65	200			
750	67	64	240		248	215
1000	86	81	280		277	292
1250	64	66	274	294	444	313
1500	46	48	320	354	303	395
1750			368	419	239	363
2000			442	345		
2250			398	371		
2500			452			
2750			399			

Table C.3   Explosion pressure, P_m, data for nano-titanium

Dust Concentration [g/m³]	150 nm Series-1 [bar(g)]	150 nm Series-2 [bar(g)]	60-80 nm Series-1 [bar(g)]	60-80 nm Series-2 [bar(g)]	40-60 nm Series-1 [bar(g)]	40-60 Series2 [bar(g)]
50			2.4		1.7	
60	2.80					
80	3.2					
100	3.6	3.83	3.6	3.2	3.8	3.5
125	4.2	4.07	3.9	3.9	4.2	4.5
250	5.2	4.72	4.7	4.6	5.5	4.8
500	5.6	5.33	5.4	5.1	6.3	5.4
750	5.9	5.14	5.3	5.4	6.0	5.6
1000	5.8	5.44	5.3	5.5	6.0	5.9
1250		5.15		5.4		5.7

Table C.4   Rate of pressure rise, $(dP/dt)_m$, data for nano-titanium

Dust Concentration [g/m³]	150 nm Series-1 [bar/s]	150 nm Series-2 [bar/s]	60-80 nm Series-1 [bar/s]	60-80 nm Series-2 [bar/s]	40-60 nm Series-1 [bar/s]	40-60 Series2 [bar/s]
50			396		154	
60	342					
80	435					
100	633	598	285	487	529	227
125	579	604	600	533	639	667
250	735	690	702	640	727	725
500	592	615	621	771	773	805
750	631	690	621	744	843	925
1000	621	608	733	729	765	865
1250		640		698		863

Table C.5   Minimum explosible concentration, P_m, data for micron-titanium

Dust Concentration [g/m^3]	-100 Mesh [bar(g)]	-325 Mesh [bar(g)]	≤20 µm [bar(g)]
110		2.5	
100	2.0	1.5	2.7
100		1.6	
90	2.3	1.8	1.9
80	1.2	1.9	1.3
80	1.4		1.4
70	1.3	0.6	1.6
70		1.4	
60	0.9	1.3	1.3
60	1.2		
50	0.7	0.5	1.0
50	0.4	0.8	
40			0.5
40			0.2

Table C.6   Minimum explosible concentration of nano-titanium using P_d value

Dust Concentration [g/m^3]	150 nm [bar(g)]	60-80 nm [bar(g)]	40-60 nm [bar(g)]
100	3.5	3.1	3.4
80	3.0		
60	2.6		
50		2.2	1.6
40	1.6	1.2	1.3
40	1.5		
30	0.7	1.2	0.8
30		1.4	
20	0.7	0.7	0.7

Table C.7   Minimum ignition energy data for -100 mesh titanium

Ignition Energy [mJ]	Dust Amount [mg]	Ignition Delay [ms]	Inductance [mH]	Ignition or (no ignition)
1000	900	120	1	(10)
1000	1200	120	1	(10)
1000	1500	120	1	(10)
1000	1800	120	1	1
1000	2400	120	1	1
300	1800	120	1	(10)
300	2400	120	1	1
100	2400	120	1	1
30	2400	120	1	(10)
100	3000	120	1	5
100	3600	120	1	1
30	3600	120	1	(10)
30	3000	120	1	1
10	3000	120	1	(10)
10	3000	150	1	(10)
30	3600	150	1	(10)
30	2400	150	1	(10)
30	2400	90	1	(10)
10	3000	90	1	(10)
30	3600	90	1	(10)
300	3000	120	0	1
100	3000	120	0	2
30	3000	120	0	1
10	3000	120	0	(10)
30	2400	120	0	(10)
30	3600	120	0	4
10	3600	120	0	5
3	3600	120	0	(10)
3	3600	90	0	(10)
3	3600	150	0	3
1	3600	150	0	(10)

Table C.8   Minimum ignition energy data for -325 mesh titanium

Ignition Energy [mJ]	Dust Amount [mg]	Ignition Delay [ms]	Inductance [mH]	Ignition or (no ignition)
30	2400	120	1	1
10	2400	120	1	1
3	2400	120	1	(10)
3	3000	120	1	5
3	3600	120	1	(10)
10	3600	120	1	1
1	3000	120	1	(10)
1	3000	90	1	(10)
1	3000	150	1	(10)
3	3600	150	1	6
1	3600	150	1	(10)
3	2400	150	1	7
3	1800	150	1	(10)
1	2400	150	1	(10)
3	1800	90	1	(10)
10	2400	120	0	4
3	2400	120	0	(10)
3	3000	120	0	1
3	3600	120	0	(10)
10	3600	120	0	1
1	3000	120	0	(10)
3	3600	150	0	(10)
1	3000	150	0	(10)
3	2400	150	0	1
3	1800	150	0	(10)
1	2400	150	0	(10)
3	3600	90	0	(10)
3	1800	90	0	(10)

Table C.9   Minimum ignition energy data for ≤20 µm titanium

Ignition Energy [mJ]	Dust Amount [mg]	Ignition Delay [ms]	Inductance [mH]	Ignition or (no ignition)
10	2400	120	1	1
3	2400	120	1	5
3	1800	120	1	(10)
3	3000	120	1	9
3	3600	120	1	5
1	3600	120	1	3
1	3000	120	1	(10)
1	3000	150	1	(10)
1	3000	90	1	(10)
10	3000	120	0	1
3	3000	120	0	(10)
3	3600	120	0	4
1	3600	120	0	(10)
3	3000	150	0	8
3	2400	150	0	8
3	1800	150	0	(10)
1	2400	150	0	(10)
1	3000	150	0	1
1	3600	150	0	(10)
1	3600	90	0	(10)
1	2400	90	0	(10)

Table C.10   Minimum ignition energy data for 150 nm titanium

Ignition Energy [mJ]	Dust Amount [mg]	Ignition Delay [ms]	Inductance [mH]	Ignition or (no ignition)
1	300	120	0	1
1	600	120	0	1
1	900	120	0	1
1	150	120	0	1
1	100	120	0	1
1	50	120	0	(10)
3	50	120	0	1

Table C.11   Minimum ignition energy data for 60-80 nm titanium

Ignition Energy [mJ]	Dust Amount [mg]	Ignition Delay [ms]	Inductance [mH]	Ignition or (no ignition)
1	600	120	0	1
1	900	120	0	1
1	300	120	0	1
1	150	120	0	1
1	100	120	0	1
3	50	120	0	(10)
1	50	120	0	(10)

Table C.12   Minimum ignition energy data for 40-60 nm titanium

Ignition Energy [mJ]	Dust Amount [mg]	Ignition Delay [ms]	Inductance [mH]	Ignition or (no ignition)
1	50	120	0	(10)
1	100	120	0	1
3	50	120	0	(10)
1	150	120	0	1

1	300	120	0	1
1	600	120	0	1
1	900	120	0	1

Table C.13   Minimum ignition temperature data for -100 mesh

	Dust Volumes		
Temperature [ºC]	0.5 ml	1 ml	2 ml
590	No Explosion	No Explosion	No Explosion
580	No Explosion	No Explosion	No Explosion
570	No Explosion	No Explosion	No Explosion

Table C.14   Minimum ignition temperature data for -325 mesh

	Dust Volumes		
Temperature [ºC]	0.5 ml	1 ml	2 ml
590	-	Explosion	-
560	-	Explosion	-
540	-	Explosion	-
520	-	Explosion	-
500	-	Explosion	-
480	-	Explosion	-
470	-	Explosion	-
460	-	Explosion	-
450	No Explosion	No Explosion	No Explosion

Table C.15   Minimum ignition temperature data for $\leq 20\,\mu m$

	Dust Volumes		
Temperature [ºC]	0.5 ml	1 ml	2 ml
580	-	Explosion	-
560	-	Explosion	-
540	-	Explosion	-
520	-	Explosion	-
500	-	Explosion	-
480	No Explosion	Explosion	-
460	-	Explosion	No Explosion
450	-	No Explosion	-

Table C.16   Minimum ignition temperature data for 150 nm

	Dust Volumes		
Temperature [ºC]	0.5 ml	1 ml	2 ml
400	-	-	Explosion
350	-	-	Explosion
310	-	-	Explosion
290	-	-	Explosion
270	-	-	Explosion
260	-	-	Explosion
250	-	-	Explosion
240	No Explosion	No Explosion	No Explosion

Table C.17   Minimum ignition temperature data for 60-80 nm

	Dust Volumes		
Temperature [ºC]	0.5 ml	1 ml	2 ml
400	-	-	Explosion
350	-	-	Explosion
310	-	-	Explosion
290	-	-	Explosion
270	-	-	Explosion
260	-	-	Explosion
250	-	-	Explosion
240	-	-	Explosion
230	No Explosion	No Explosion	No Explosion

Table C.18   Minimum ignition temperature data for 40-60 nm

	Dust Volumes		
Temperature [ºC]	0.5 ml	1 ml	2 ml
310	-	-	Explosion
290	-	-	Explosion
270	-	-	Explosion
260	-	-	Explosion
250	-	-	Explosion
240	No Explosion	No Explosion	No Explosion